Durham E-Theses

Mechanistic studies of S-nitrosothiol reactions with reference to potential physiological activity

McAninly, John

How to cite:

McAninly, John (1994) *Mechanistic studies of S-nitrosothiol reactions with reference to potential physiological activity*, Durham theses, Durham University. Available at Durham E-Theses Online: http://etheses.dur.ac.uk/5481/

Use policy

The full-text may be used and/or reproduced, and given to third parties in any format or medium, without prior permission or charge, for personal research or study, educational, or not-for-profit purposes provided that:

- a full bibliographic reference is made to the original source
- a link is made to the metadata record in Durham E-Theses
- the full-text is not changed in any way

The full-text must not be sold in any format or medium without the formal permission of the copyright holders.

Please consult the full Durham E-Theses policy for further details.

Mechanistic Studies of S-Nitrosothiol Reactions With Reference To Potential Physiological Activity

by

John McAninly B.Sc., M.I. Biol., M.R. Pharm. S.

A thesis submitted for the degree of Doctor of Philosophy of the
University of Durham

December 1994

MECHANISTIC STUDIES OF S-NITROSOTHIOL REACTIONS WITH REFERENCE TO POTENTIAL PHYSIOLOGICAL ACTIVITY

by John McAninly

A thesis submitted for the degree of Doctor of Philosophy in the Department of Chemistry, University of Durham, December 1994

ABSTRACT

A study of the reactions of various S-nitrosothiols, particularly S-nitroso-N-acetylpenicillamine (SNAP), was undertaken. These compounds were known to produce nitric oxide (NO) when decomposing, which has important and diverse biological roles. An example of their use in physiological research was demonstrated.

The Griess method was used to determine the stoichiometry of nitrite production from S-nitrosothiol decomposition in various buffer solutions. In all cases the production was found to be almost quantitative. The kinetic measurement of SNAP decomposition in a variety of buffers and pH was undertaken. The results were complex and often erratic, conforming to first order but also half order kinetics in many cases. There was some indication that decomposition products and light could affect the reaction. The presence of disulphide (dimer) as a major reaction product was confirmed in the case of SNAP. Free-radical traps were used to probe the decomposition mechanism, as were hemin and haemoglobin as NO detectors to determine decomposition kinetics.

The true agent of S-nitrosothiol decomposition was found to be intrinsic copper in the water supply and buffer salts. S-nitrosothiols were found to be stoichiometrically decomposed by Hg^{2+} ions, but catalytically decomposed by Cu^{2+} ions. Kinetic measurement confirmed the complex nature of the catalysis. The importance of SNO and NH_2, and SNO and COO^- as binding sites was demonstrated. Some explanation was found for the differing structure/reactivity relationships observed.

It was shown that transnitrosation of a thiol could occur, involving thiolate anion attack upon the S-nitrosothiol. However, the reaction appeared to be very slow at physiological pH. The nitrosation of N-methylaniline by S-nitrosothiols was found to occur only in the presence of oxygen - direct transfer of NO did not occur, nitrosation being mediated after SNAP decomposition.

To my wife and family

MEMORANDUM

The work for this thesis has been undertaken in the Chemistry Department of the University of Durham between October 1990 and September 1993. It is the original work of the author unless otherwise stated otherwise. None of this work has been submitted for any other degree.

COPYRIGHT

ACKNOWLEDGEMENTS

Contents

Chapter Five: Transnitrosation

Chapter Six: Experimental Details

Appendix A: The Use of SNAP in Experimental Physiology

Appendix B: Research Colloquia, Seminars, Lectures and Conferences

List of Abbreviations

Chapter 1

The Biological Roles Of Nitric Oxide

1.1 Historical Perspective

The last decade has seen a remarkable increase in our understanding of the numerous biological roles of nitric oxide, this being the case even when measured against the general exponential trend in the growth of scientific information. Ironically, a wide range of pro-drugs, which are now known to generate nitric oxide *in vivo*, have been used therapeutically for the last 150 years, albeit without any real insight into their mode of action. These include glyceryl trinitrate (GTN), sodium nitroprusside (SNP) and iso-amyl nitrite (some structures are shown in Figure 1.1 below).

The first recorded therapeutic use of a nitric oxide pro-drug was as early as 1867, when Brunton used amyl nitrite to treat angina pectoris[1]. The unfortunate side-effects included flushing of the face, tachycardia and headache, due to vasodilation of arteries. Subsequently, glyceryl trinitrate was tested in 1879 and also found to be of great value[2]. These same type of compounds were to be used in the treatment of hypertension around this time and various derivatives have continued to be used as such up to the present day[3]. It was noted at the turn of the century[4] that munitions workers, who initially showed the classic effects of contact with GTN and similar compounds, developed tolerance to them over time - an obvious disadvantage for prolonged therapy. The precise mechanism of this tolerance is still unresolved[5] but is thought to depend upon the cellular depletion of thiols responsible for the conversion of GTN to nitric oxide (NO)[6]. Vasodilators such as sodium nitroprusside do not induce tolerance as they are believed to release NO spontaneously[7]. The conventional wisdom throughout 100 years had been that the vasodilatory action of these compounds was due to conversion in the bloodstream to nitrite ion (NO_2^-), which has some action in this respect. However, in the 1940s it was demonstrated[8] that a physiologically-effective dose of GTN, even if totally converted in this way, would not yield sufficient nitrite ion to account for its action. Nevertheless, the unknown mechanistic aspects of the mode of action of organic nitrates were capable of being sidelined while the data were unavailable to throw fresh light on the topic.

Class	Structure	Example
Organic nitrates	$R-O-\overset{\oplus}{N}\overset{\textstyle O}{\underset{\textstyle O^{\ominus}}{}}$	isosorbide mononitrate
Organic nitrites	$R-O-N=O$	$CH_3-\underset{\underset{\textstyle CH_3}{\textstyle \vert}}{CH}-CH_2\text{-}CH_2-ONO$ isoamyl nitrite
S-nitrosothiols	$R-S-N=O$	
Sydnonimines		
Furoxans		
Inorganic nitrite	NO_2^-	
Iron / NO complex salts	$Y[Fe(NO)X]$	$Na_2[Fe(NO)CN_5]$ sodium nitroprusside

Figure 1.1
Some classes of Nitrovasodilator

1.2 Discovery of the Physiological Role of Nitric Oxide

In the late 1970s, it was shown[9] that GTN and other organic nitrates are inactive *per se*, but produce vasodilation once metabolised to nitric oxide, **not** nitrite. Significantly, NO was found to stimulate the formation of cyclic guanosine monophosphate (cGMP), a second-messenger compound in the cell for neurotransmitters and hormones, similar to the more widely studied cyclic adenosine monophosphate (cAMP)[10]. Like cAMP, cGMP was present in virtually every cell examined. The enzyme that made cGMP from guanosine triphosphate (GTP), guanylate cyclase (GC), existed in two forms; a soluble, cytoplasmic form (sGC) and a membrane-bound, particulate form (pGC). It was discovered that sGC contained a haem group, which when bound to NO induced activation of the enzyme[11]. This explained a lot of the pharmacology of the nitrovasodilators, but was regarded as a case of NO mimicking the true cellular "first-messenger". In 1980, Furchgott and Zawadzki[12] reported that the action of acetycholine (a potent, naturally-occurring hypotensive agent) on vascular tissue was dependent on the presence of an intact vascular endothelium. They showed that a labile humoural factor was released, causing relaxation, which was later named "endothelium-derived relaxation factor" (EDRF). A variety of substances and stimuli were subsequently shown to have an endothelial requirement for their effect[13]. The following year Tannenbaum *et al* showed that nitrates were excreted by rats and humans when on low-nitrate diets and that very high excretion rates were associated with inflammatory conditions[14]. It was then demonstrated[15] that macrophages were involved in this nitrate production, explaining the increase in nitrate production during illness. Furthermore, macrophages were shown[16] to require L-arginine for the production of nitrates. It was also demonstrated by Hibbs[17] that macrophages lost their tumouricidal ability if depleted of L-arginine and that they produced citrulline as well as nitrates from arginine. Interestingly, it had been known since the 1950s that L-arginine can inhibit the growth of tumours[18]. The actual cytotoxic agent generated was nitric oxide, which was then transformed into nitrites and nitrates[19]. The enzyme involved was

named NO synthase and could be inhibited by a methyl derivative of arginine, N[G]-monomethyl-L-arginine (L-NMMA)[20]. Initial suggestions had been that EDRF might be a product of the enzyme arachidonic acid lipoxygenase[21] or of the cytochrome P_{450} multi-enzyme complex[22]. It was known that EDRF had a physiological half-life of seconds[23] and was inhibited by haemoglobin (Hb) (which has a haem moiety) and methylene blue[24]. After much speculation Furchgott suggested[25] in 1986 that EDRF might be nitric oxide or a related compound. This was a bold pronouncement given that NO previously was known best as an air pollutant! Conclusive proof came in 1987 when Moncada and Palmer[26] elegantly demonstrated that EDRF and NO are the same. They stimulated the release of EDRF from endothelial cells, using it thereafter to cause the relaxation of a vascular smooth muscle preparation. At the same time, they measured by chemical means the nitric oxide production of the endothelial cells and found it exactly sufficient to match the observed effect of the EDRF.

1.3 Formation and Mechanism of Action of NO

Confirmation of the identity of EDRF as NO (or a closely-related nitrosyl compound that captured and then released NO) came with the discovery that EDRF is produced by the oxidation of the guanidino nitrogen of arginine[27]. This can be competitively inhibited by several structural analogues of arginine e.g. N[G]-nitro-L-arginine (L-NA), N[G]-nitro-L-arginine methyl ester (L-NAME) and L-NMMA. Their structures are shown in Figure 1.2 below.

L-NA
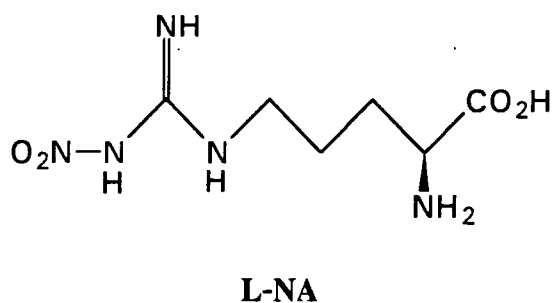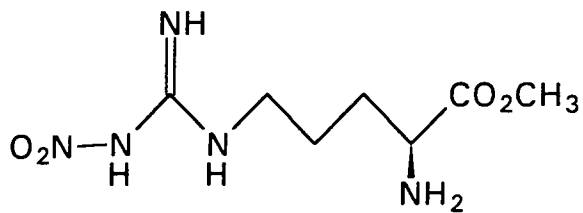
L-NAME
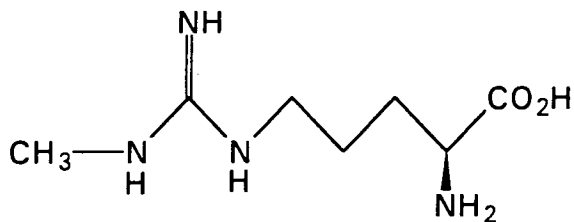
L-NMMA

Figure 1.2   Structures of Some Arginine Analogues

The reaction sequence is shown in Scheme 1.1 below.

L-Arginine   N^G-Hydroxyarginine   L-Citrulline
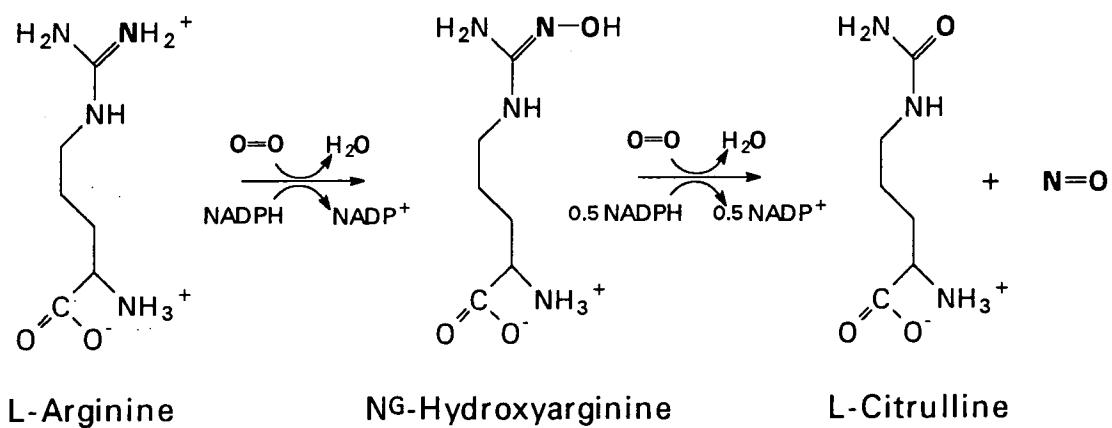
Scheme 1.1

It is carried out by NO synthase. This exists as several isozymes and bears a close relation to part of the cytochrome P_{450} enzyme complex. The two main types of the enzyme are a) constitutive and b) inducible. Both are dimeric enzymes containing two identical sub-units of 130-150 kDa and four prosthetic groups[29, 30]. The essential similarities and differences between the two main types of the enzyme[31] are shown in Table 1.1 below, modified from reference 28.

Table 1.1   Similarities and differences between the two NO-synthases

Constitutive	Inducible
Dioxygenase	Dioxygenase
NADPH dependent	NADPH dependent
Ca^{2+}/calmodulin dependent	Ca^{2+}/calmodulin independent
Picomoles NO released	Nanomoles NO released
Short-lasting release	Long-lasting release
Inhibited by L-arginine analogues	Inhibited by L-arginine analogues

The constitutive NO synthase provides a rapid-response control mechanism, allowing the endothelial cell to act as a transducer regulating blood vessel tone[28] and thus controlling local homeostatic processes. The constitutive enzyme is calmodulin dependent because it is this co-factor which actually binds Ca^{2+} cf. the role of troponin C in muscle contraction[32]. The apparent independence of the inducible enzyme to calmodulin and Ca^{2+} may derive from the enzyme being bound to calmodulin very strongly, so that the purified enzyme already possesses this co-factor. The inducible enzyme is expressed in response to endotoxin or cytokines and may be implicated in pathophysiological roles e.g. in the vascular damage seen in endotoxic shock.

An outline for the action of NO in the vasculature can now be given (see Figure 1.3). The endothelial cell responds to a hormone by increasing intracellular Ca^{2+} concentration. This activates NO synthase to generate NO. The NO diffuses to the

target (the vascular smooth muscle cell) where it binds to the iron atom in the haem prosthetic group of the sGC. This activates production of cGMP, causing a decrease in intracellular free Ca^{2+} and hence smooth muscle relaxation. (It is thought that cGMP activates a protein kinase which phosphorylates Ca^{2+} transporters, causing the sequestration of Ca^{2+} in the sarcomere[33]).
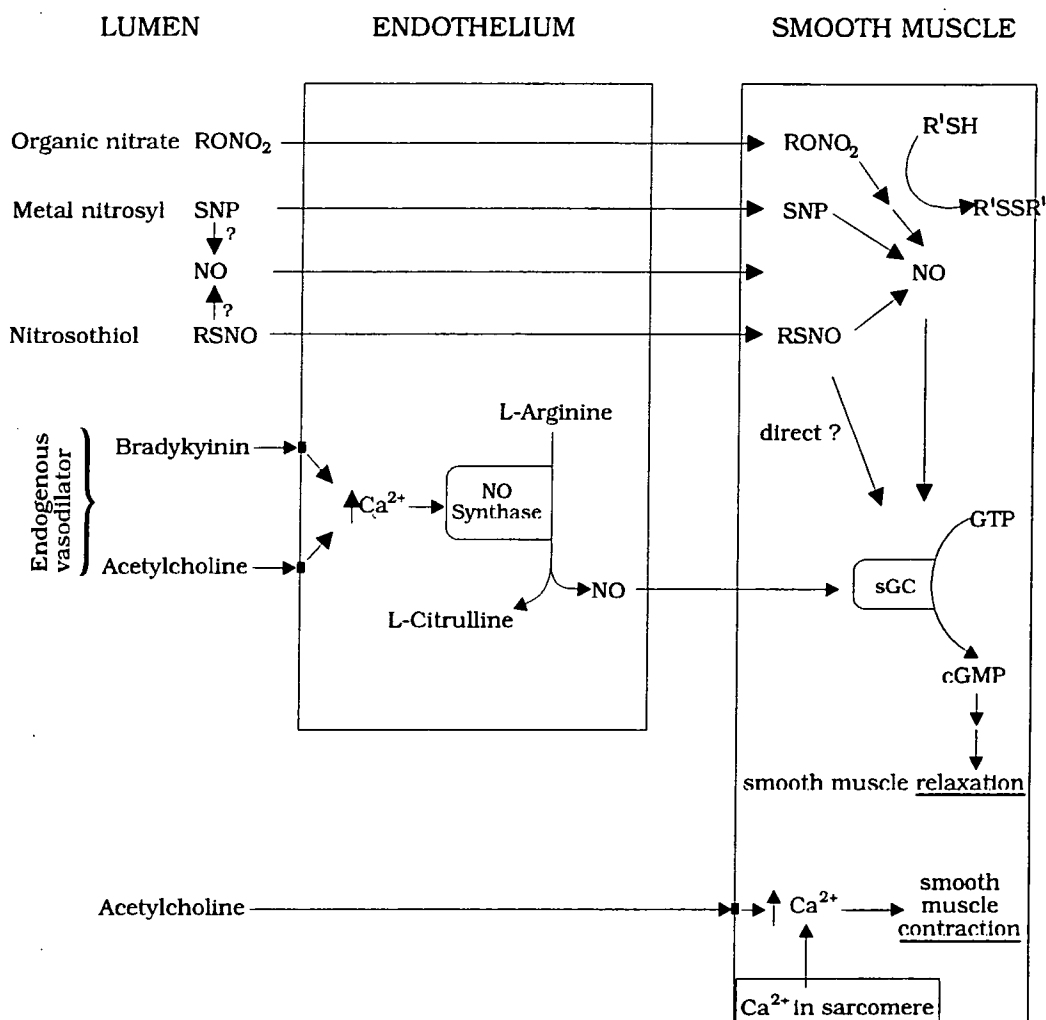
Figure 1.3 Possible mechanisms of action of exogenous and endogenous vasodilators

Variations in this scheme have been suggested. Thus Meyers[34] proposed that EDRF may actually be S-nitrosocysteine. However, this work has been criticised on several grounds e.g. possible contamination of NO with nitrite[35]. Much of the search for more complex intermediates seems to be based on a disbelief that so reactive a molecule as NO could exist for sufficient time to act as an intercellular messenger.

However, at the low concentration pertaining in the cell, it would have a half-life sufficient for this purpose. Stamler[36] has reported that nitrosated thiol groups act as a more stable vasodilator than NO itself and more recently[37] that serum albumin forms the main store of NO transport in the blood. The nitrosation of these proteins raises chemical problems however, as NO alone is incapable of nitrosating thiols[31].

1.4 Multiple Roles of NO

The physiological responses that require NO production are now known to be very extensive. Some of the more important aspects will be discussed.

1.4.1 Vasculature

Mention has already been made of the crucial importance of NO in maintaining vascular tone.

1.4.2 Platelets

EDRF had been found to inhibit platelet aggregation[38]. Later, it was shown that NO and prostacyclin act synergistically in this manner and in disaggregating platelets[39]. Only those nitrovasodilators which are believed to release NO spontaneously (such as SNP and the sydnonimines) inhibit platelet aggregation, indicating that platelets lack uptake/conversion mechanisms for organic nitrates to NO. Of late, it has become clear that platelets generate NO and that this acts as a negative feedback mechanism to regulate platelet aggregation[40]. This formation is dependent on the free Ca^{2+} concentration.

1.4.3 Nervous System
i) Central

A wide variety of brain neurotransmitter substances have been known for some time e.g. acetylcholine, serotonin, glutamate, glycine. In 1977, NO was shown to stimulate sGC in murine cerebral cortex homogenates[41]. With the discovery that L-

arginine was an endogenous activator of sGC in neuroblastoma cells[42], the way was open for an investigation of the L-arginine-NO pathway in the central nervous system. This indicated that rat brain preparations possessed NO synthase[43] and that intracellular Ca^{2+} levels controlled its activity. The indications are that NO plays a role in the extracellular matrix of the brain, as Hb acts as an inhibitor. NO appears to act as a "retrograde messenger" in the brain[44]. A postsynaptic cell, stimulated by a neurotransmitter such as glycine, forms NO which diffuses **out** of the cell to the presynaptic cell. Computer modelling has been applied to show that a complex, 3-D network could have transmission strengths controlled by a diffusible, unstable, retrograde transmitter[45]. In such a way NO could act as a means of long-term memory by forming feedback loops. It may also act as a more "normal" neurotransmitter.

ii) Peripheral

NO has a vital role in the peripheral nervous system. For decades a particular group of autonomic nerves had defied classification as noradrenergic or cholinergic nerves. They were therefore classified as NANC nerves (non-noradrenergic, non-cholinergic nerves). These are important components of smooth muscle autonomic innervation in the gastrointestine, airways etc[46]. Much work centred on the rat anococcygeus muscle, which has inhibitory NANC innervation[47]. L-NMMA was shown to inhibit NANC-mediated relaxation of this muscle without affecting the response to SNP, while the effect was reversed by L-arginine[48]. This evidence shows that at least some NANC neurotransmission is mediated by NO, and may be widespread. Certainly, in those systems tested, NO has been found.

1.4.4 Immunological Reactions

i) Macrophages

As previously mentioned, macrophages were implicated in the endogenous synthesis of nitrates in humans. It was shown that the cytotoxicity of macrophages against tumour cells depended on L-arginine and that NO was the precursor of the nitrites and

and nitrates in these cells. A striking difference between the macrophage NO synthase and that in endothelial cells, platelets and brain cells was that it required activation, with an eight hour lag phase, and once induced continued NO synthesis until substrate depletion or cell death[49]. Unlike other cell types, the macrophage NO synthase was inhibited by L-canavanine[50]. Activated macrophages can be cytotoxic against bacteria, protozoa[51] or neoplastic cells[52]. These effects are not dependent on phagocytosis and can be cytostatic or cytolytic. The specific mode of action centres on inhibition of DNA replication, mitochondrial respiration and aconitase activity. Thus inhibition of ribonucleotide reductase, which converts ribonucleotides to deoxyribonucleotides, for DNA synthesis, may be one way in which macrophages inhibit the rapid growth of tumour cells. All of the enzymes affected contain non-haem iron co-ordinated to sulphur atoms[53], which act as catalytic centres. Exposure of Fe-S groups to NO results in iron-nitrosyl complex formation[54]. The inhibition of these enzymes was accompanied by the release of intracellular iron from the target cells[55]. Thus these results seem to indicate a mechanism by which NO produces activated macrophage-induced cytotoxicity. It must be underlined that NO is cytotoxic in some cells and cytostatic in others. This variation may be due to the relative importance or susceptibility of iron-sulphur enzymes in different cells.

ii) Neutrophils

Human neutrophils have been shown to inhibit platelet aggregation, with increase of their cGMP levels, this process being inhibited by L-NMMA[56]. The presence of NO synthase in neutrophils has now been confirmed[57]. Chemoattractants enhanced the synthesis of NO by neutrophils, but at higher concentrations some of them also caused the release of superoxide anion ($\cdot O_2^-$) which interacted with the NO, decreasing its level. Treatment with superoxide dismutase (SOD, an enzyme which specifically destroys the $\cdot O_2^-$ radical) or L-arginine enhanced the biological action of NO. It has been suggested[59] that NO and $\cdot O_2^-$ react rapidly to form peroxynitrite anion (ONOO$^-$) as shown in the reaction scheme below.

$$NO + \cdot O_2^- \longrightarrow ONOO^-$$
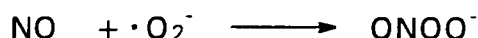
This can decompose upon protonation into $OH\cdot$ and $NO_2\cdot$, both powerful oxidants and highly destructive of DNA and cell membranes[60].

$$ONOO^- + H^+ \rightleftharpoons ONOOH$$

$$ONOOH \rightleftharpoons \cdot NO_2 + OH\cdot$$
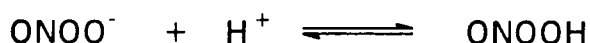
If this is the case, SOD may protect tissues against their formation. However, the occurrence of these reactions *in vivo* is not established, so the interaction between NO and $\cdot O_2^-$ may increase toxicity or act as a neutralising mechanism.

iii) Other Cells and Tissues

NO synthase has been found in both the cortex and medulla of the adrenal gland, being similar to that in the endothelium, platelets etc[61]. It may have a modulatory role in the control of synthesis and secretion of corticosteroids and catecholamines, as cGMP has been shown to be involved in both[62]. It has also been demonstrated in mast cells, appearing to modulate histamine release[63]. Elevated nitrite levels have been found in the plasma and synovial fluid of patients with rheumatoid arthritis, but the evidence is insufficient so far to implicate NO in the disease aetiology.

iv) Septic Shock

One of the most interesting and still poorly understood areas of study is the role of NO in septic (endotoxic) shock syndrome. This can be defined as the chronic, profound vasorelaxation, coupled with insensitivity to vasoconstrictors such as adrenaline, which occurs in such diverse cases as septicaemia or anti-tumour therapy. When rats were treated with lipopolysaccharide (LPS) to induce an immunological response, NO synthase activity was induced in the lung and liver (particularly the hepatocytes)[64]. *In vitro* data have suggested that NO has a cytotoxic effect on hepatocytes subjected to endotoxic challenge[65], while L-NMMA has been

induced gastrointestinal damage[66]. However, Thiernermann and Vane have shown that L-NMMA inhibits LPS-induced hypotension in rats[67]. In support of this, there is complementary evidence from studies of glucocorticoids. These are beneficial in the prevention or treatment of endotoxic shock and in the treatment of inflammatory conditions (e.g. auto-immune diseases) and stress[68]. Typical glucocorticoids such as dexamethasone and cortisol prevent the *in vivo* induction of NO synthase in liver, lung and vascular tissue of rats after treatment with LPS[69]. These apparently conflicting results require further research, but it is probable that induction of NO synthase at a low level may lead to hypotension with or without cellular damage, depending on the rate of NO release. Certainly, endogenous NO can have a double-edged role[70].

1.5 Therapeutic Possibilities of NO

In view of the ubiquitous nature of the roles of NO in human physiology, it is to be expected that therapeutic possibilities must present themselves. Essentially, these interventions could either be directed to the production of NO at a particular site, or the prevention of its production.

It has been shown that NO can act as a mutagen, in bacteria, by converting 5-methylcytosine into thymine and thus changing the DNA base-pair sequence[71]. Mutagenesis of human cell lines has also been demonstrated[72]. There is some possibility therefore of using an NO-releasing chemical, of high DNA specificity, as a possible anti-cancer drug.

The anti-bacterial action of NO extends to unicellular parasites. For example, the protozoan *Leishmania major* (responsible for the eponymous disease) can be destroyed by macrophages[73] using NO, while S-nitroso derivatives of cystine and glutathione can inhibit the growth of the virulent malarial parasite *Plasmodium falciparum*[74]. In view of the increasing resistance of these parasites to conventional drug therapy such as chloroquine, a new line of attack would be most welcome.

13

One area where present knowledge of NO functioning has already had useful therapeutic outcomes is in the treatment of septic shock syndrome. Patients who were dying because their sepsis condition was intractable to even massive doses of adrenaline have been treated with L-NMMA and have made remarkable recoveries[75].

The role played by NO in preventing platelet aggregation offers the possibility of drugs which may be useful in the prevention of embola formation and hence reduce strokes. They may also help prevent the development of atherosclerosis, in the aetiology of which platelets have been implicated. The balance to be struck is between enhancing the benefits accruing from the constitutive NO synthase effects and reducing the deleterious effects of overproduction of the inducible enzyme.

The widely publicised aspect of NO, at least in the popular press, is in penile erection. For those men suffering problems of impotence, it is now known that approximately 90% is due to NANC nerve lesions involving NO and not psychological problems. This offers hope of rational treatment.

The role of NO in the brain is still less well-defined, but if NO does act as a "retrograde messenger" then it may be possible to treat those diseases where memory loss is a particular problem e.g. senile dementia and Parkinson's disease. It is known that overproduction of NO contributes to the cellular damage occurring after a stroke and may lead to epileptic seizures[76]. A better understanding of how some brain cells protect themselves against the toxic effects of NO could result in the development of important new drugs.

NO has been used by itself recently to treat persistent pulmonary hypertension of the newborn[77]. By selectively reducing pulmonary vascular resistance, NO may prove useful in the treatment of pulmonary hypertension.

In pathological conditions associated with excess NO synthesis, it may be possible to reduce this overproduction by decreasing levels of arginine in the circulation. Giving arginase to rats suffering endotoxic shock leads to a fall in circulating arginine and a

rise in blood pressure. The corollary does not apply to cases where there is underproduction of NO - giving arginine is ineffective, as normally its supply is not rate-limiting.

Another approach to reducing the activity of the inducible enzyme e.g. in inflammatory conditions, could be the inhibition of the synthesis of co-factors for NO synthesis, e.g. tetrahydrobiopterin (BH_4).

It may also be possible to manipulate the production of endogenous NO synthase inhibitors. One was recently reported (N^G-dimethylarginine) to accumulate in patients with chronic renal failure, thus contributing to hypertension[78].

Possibly the greatest problem in the development of NO-based drugs is the size of the NO molecule itself - being so small and having such wide roles makes for poor specificity. The design of molecules that transport NO, deliver it to the precise cellular target and then release it, will be vital.

1.6 Conclusion

Our appreciation of the significance of NO has developed enormously in the last decade. We now know that NO has multifarious functions in the body and there must still be unknown areas of physiological importance to be discovered. This is no longer surprising, given that NO synthase is part of a very ancient biochemical inheritance[79]. Even those areas discovered contain many unsolved problems. The next decade promises to offer as many exciting discoveries and possibilities as the last.

References

1. T. L. Brunton, *Lancet*, 1867, **2**, 97

2. W. Murrell, *Lancet*, 1879, **1**, 80

3. Symposium (review), *Am. J. Cardiol.*, 1987, **60**, 1H

4. G. C. Laws, *J.A.M.A.*, 1898, **31**, 793

5. M. Packer, *J. Am. Coll. Cardiol.*, 1990, **16**, 932

6. J. Abrams, *Am. J. Med.*, 1991, **91**(3C), 106S

7. M. Feelisch, *J. Cardiovasc. Pharm.*, 1991, **17**(3), S25

8. J. C. Krantz, C. J. Carr, S. E. Forman, N. Cone, *J. Pharmacol. Exp. Ther.*, 1940, **70**, 323

9. S. Katsuki, W. P. Arnold, C. K. Mittal, F. Murad, *J. Cyclic Nucleotide Res.*, 1977, **3**, 23

10. K. D. Schultz, G. Schultz, *Nature* (London), 1977, **265**, 750

11. P. A. Craven, F. R. DeRubertis, *J. Biol. Chem.*, 1978, **253**, 8433

12. R. F. Furchgott, J. V. Zawadzki, *Nature* (London), 1980, **288**, 373

13. S. Moncada, R. M. J. Palmer, E. A. Higgs, in *Biology and Pathology of Platelet-Vessel Wall Interactions*, Eds. G. Jolles, J. Y. Legrand, A. Nurden, Academic (London), 1986, 289

14. L. C. Green, D. A. Wagner, K. Ruiz de Luzuriaga, N. Istfan, V. R. Young, S. R. Tannenbaum, *Proc. Natl. Acad. Sci.*, U.S.A., 1981, **78**, 7764

15. D. J. Stuehr, M. A. Marletta, *Proc. Natl. Acad. Sci.*, U.S.A., 1985, **82**, 7738

16. R. Iyengar, D. J. Stuehr, M. A. Marletta, *Proc. Natl. Acad. Sci.*, U.S.A., 1987, **84**, 6369

17. J. B. Hibbs, Z. Vavrin, R. R. Taintor, *J. Immunol.*, 1987, **138**, 550

18. H. M. Levy, M. Montanez, E. R. Feaver, E. A. Murphy, M. S. Dunn, *Cancer Res.*, 1954, **14**, 198

19. J. B. Hibbs, R. R. Taintor, Z. Vavrin, E. M. Rachlin, *Biochem. Biophys. Res. Commun.*, 1988, **157**, 87

20. J. B. Hibbs, R. R. Taintor, Z. Vavrin, *Science*, 1987, **235**, 473

21. H. A. Singer, M. J. Peach, *J. Pharmacol. Exp. Ther.*, 1883, **226**, 790

22. A. Pinto, N. G. Abraham, K. M. Mullane, *J. Pharmacol. Exp. Ther.*, 1986, **236**, 445

23. T. M. Griffith, D. H. Edwards, M. J. Lewis, A. C. Newby, A. H. Henderson, *Nature* (London), 1984, **308**, 645

24. W. Martin, G. M. Villani, D. Jothianandan, R. F. Furchgott, *J. Pharmacol. Exp. Ther.*, 1985, **232**, 708

25. R. F. Furchgott, in *Vasodilatation: Vascular Smooth Muscle, Peptides, Autonomic Nerves and Endothelium*, Ed. P. M. Vanhoutte, Raven Press, New York, 1988, 401

26. R. M. J. Palmer, A. G. Ferrige, S. Moncada, *Nature* (London), 1987, **327**, 524

27. R. M. J. Palmer, D. S. Ashton, S. Moncada, *Nature* (London), 1988, **333**, 664

28. S. Moncada, R. M. J. Palmer, E. A. Higgs, *Pharmacol. Rev.*, 1991, **43**, 109

29. S. H. Snyder, D. S. Bredt, *Sci. Am.*, 1992, **226**(5), 28

30. R. G. Knowles, S. Moncada, *T. I. B. S.*, 1992, **17**, 399

31. A. R. Butler, D. L. H. Williams, *Chem. Soc. Rev.*, 1993, 233

32. W. F. Ganong, in *Review of Medical Physiology*, Lange Medical Publications, 11th Ed., 1983, 49

33. P. L. Feldman, O. W. Griffith, D. J. Stuehr, C. & EN, 1993, 26

34. P. R. Myers, R. L. Minor, R. Guerra, J. N. Bates, D. G. Harrison, *Nature* (London), 1990, **345**, 161

35. R. F. Furchgott, M. T. Khan, D. Jothianandan, in *Endothelium-Derived Relaxation Factor*, Eds. G. M. Rubanyi, P. M. Vanhoutte, Karger, Basel, 1990, 8

36. J. S. Stamler, D. I. Simon, J. A. Osborne, M. E. Mullins, O. Jaraki, T. Michel, D. J. Singel, J. Loscalzo, *Proc. Natl. Acad. Sci.*, U.S.A., 1992, **89**, 444

37. J. S. Stamler, O. Jaraki, J. Osborne, D. I. Simon, J. Keaney, J. Vita, D. J. Singel, C. R. Valeri, J. Loscalzo, *Proc. Natl. Acad. Sci.*, U.S.A., 1992, **89**, 7674

38. B. Furlong, A. H. Henderson, M. J. Lewis, J. A. Smith, *Br. J. Pharmacol.*, 1987, **92**, 639

39. M. W. Radomski, R. M. J. Palmer, S. Moncada, *Proc. Natl. Acad. Sci.*, U.S.A., 1987, **92**, 639

40. M. J. Radomski, R. M. J. Palmer, S. Moncada, *Proc. Natl. Acad. Sci.*, U.S.A., 1990, **87**, 5193

41. N. Miki, Y. Kawabe, K. Kuriyama, *Biochem. Biophys. Res. Commun.*, 1977, **75**, 851

42. T. Deguchi, M. Yoshioka, *J. Biol. Chem.*, 1982, **257**, 10147

43. R. G. Knowles, M. Palacios, R. M. J. Palmer, S. Moncada, *Proc. Natl. Acad. Sci.*, U.S.A., 1989, **86**, 5159

44. M. Barinaga, *Science*, 1991, **254**, 1296

45. J. A. Gally, P. M. Read, G. N. Reeke, G. M. Edelman, *Proc. Natl. Acad. Sci.*, U.S.A., 1990, **87**, 3547

46. P. J. Barnes, *Arch. Int. Pharmacodyn.*, 1986, **280**, 208

47. J. S. Gillespie, *Br. J. Pharmacol.*, 1972, **45**, 404

48. C. G. Li, M. J. Rand, *Clin. Exp. Pharmacol. Physiol.*, 1989, **16**, 933

49. D. J. Stuehr, M. A. Marletta, *J. Immunol.*, 1987, **139**, 518

50. R. Iyengar, D. J. Stuehr, M. A. Marletta, *Proc. Natl. Acad. Sci.*, U.S.A., 1987, **84**, 6369

51. J. S. Remington, T. C. Merigan, *Proc. Soc. Exp. Biol. Med.*, 1969, **131**, 1184

52. L. J. Old, D. A. Clarke, B. Benacerraf, *Nature* (London), 1959, **184**, 291

53. J. B. Hibbs, R. R. Taintor, Z. Vavrin, D. L. Granger, J. C. Drapier, I. J. Amber, J. R. Lancaster, in *Nitric Oxide from L-Arginine: A Bio-regulatory System*, Eds. S. Moncada, E. A. Higgs, Elsevier, Amsterdam, 1990, 189

54. H. Beinert, *F. A. S. E. B. J.*, 1990, **4**, 2483

55. J. B. Hibbs, R. R. Taintor, Z. Vavrin, *Biochem., Biophys. Res. Commun.*, 1984, **123**, 716

56. D. Salvemini, G. DeNucci, R. J. Gryglewski, J. R. Vane, *Proc. Natl. Acad. Sci.*, U.S.A., 1989, **86**, 6328

57. T. B. McCall, M. Feelisch, R. M. J. Palmer, S. Moncada, *Br. J. Pharmacol.*, 1991, **102**, 234

58. T. B. McCall, N. K. Boughton-Smith, R. M. J. Palmer, B. J. R. Whittle, S. Moncada, *Biochem. J.*, 1989, **261**, 293

59. M. Saran, C. Michel, W. Bors, *Free Rad. Res. Commun.*, 1989, **10**, 221

60. J. S. Beckman, T. W. Beckman, J. Chen, P. A. Marshall, B. A. Freeman, *Proc. Natl. Acad. Sci.*, U.S.A., 1990, **87**, 1620

61. M. Palacios, R. G. Knowles, R. M. J. Palmer, S. Moncada, *Biochem. Biophys. Res. Commun.*, 1989, **165**, 802

62. G. Derome, R. Tseng, P. Mercier, I. Lemaire, S. Lemaire, *Biochem. Pharmacol.*, 1981, **30**, 855

63. D. Salvemini, E. Masini, E. Anggard, P. F. Mannaioni, J. Vane, *Biochem. Biophys. Res. Commun.*, 1990, **169**, 596

64. R. G. Knowles, M. Merret, M. Salter, S. Moncada, *Biochem. J.*, 1990, **270**, 833

65. R. D. Curran, T. R. Billiar, D. J. Stuehr, K. Hofmann, R. L. Simmons, *J. Exp. Med.*, 1989, **170**, 1769

66. I. R. Hutcheson, B. J. R. Whittle, N. K. Boughton-Smith, *Br. J. Pharmacol.*, 1990, **101**, 815

67. C. Thiemermann, J. Vane, *Eur. J. Pharmacol.*, 1990, 182, 591

68. *British National Formulary, B. M. A./R. Pharm. Soc. G. B.* (London), 1993, **25**, 268

69. R. G. Knowles, M. Salter, S. L. Brooks, S. Moncada, *Biochem. Biophys. Res. Commun.*, 1990, **172**, 1042

70. H. H. H. W. Schmidt, T. D. Warner, F. Murad, *Lancet*, 1992, **339**, 986

71. D. A. Wink *et al*, *Science*, 1991, **254**, 1001

72. T. Nguyen, D. Brunson, C. L. Crespi, B. W. Penman, J. S. Wishnok, S. R. Tannenbaum, *Proc. Natl. Acad. Sci.*, U.S.A., 1992, **89**, 3030

73. F. Y. Liew, S. Millott, C. Parkinson, R. M. J. Palmer, S. Moncada, *J. Immunol.*, 1990, **144**, 4794

74. K. A. Rockett, M. M. Awburn, W. B. Cowden, I. A. Clark, *Inf. Immun.*, 1991, **59**, 3280

75. A. Petros, D. Bennett, P. Vallance, *Lancet*, 1991, **338**, 1557

76. V. L. Dawson, T. M. Dawson, E. D. London, D. S. Bredt, S. H. Snyder, *Proc. Natl. Acad. Sci.*, U.S.A., 1991, **88**, 6368

77. J. D. Roberts, D. M. Polanmer, P. Lang, W. M. Zapol, *Lancet*, 1992, **340**, 818

78. P. Vallance, A. Leone, A. Calver, J. Collier, S. Moncada, *Lancet*, 1992, **339**, 572

79. M. W. Radomski, J. F. Martin, S. Moncada, *Phil. Trans. Roy. Soc.* (London), 1991, **334**, 129

Chapter 2

Aspects of the Chemistry of Nitric Oxide and some of its Compounds

2.1. The Chemistry of NO

A brief outline of the general physical and chemical properties of NO will be given before a more detailed consideration of its role in nitrosation is discussed.

Nitric oxide is a colourless gas at room temperature, with a boiling point of -151°C and a melting point of -163.6°C. It is only slightly soluble in water (1.8×10^{-3} mol dm^{-3} at 25°C, 1 atm. pressure)[1]. It is a relatively stable free-radical, whose structure is best represented by the canonical forms shown in Equation 2.1 below.

$$\overset{\oplus}{\cdot N}\!\!-\!\!\overset{\ominus}{O} \longleftrightarrow \overset{\cdot}{N}\!\!=\!\!O \longleftrightarrow \overset{\ominus}{N}\!\!=\!\!\overset{\oplus}{O}\overset{\cdot}{} \longleftrightarrow N\!\!\equiv\!\!O\cdot$$

Equation 2.1

It is paramagnetic and reacts rapidly with other free radicals and atoms. Due to its presence in the emissions from car and aircraft exhausts and in other forms of air pollution, its reactions in the gas phase have been widely studied[2] and much use has been found for NO as a free-radical trap in gas-phase reaction kinetics. One practical importance of such studies lies in the need to reduce urban air pollution, an extreme example being photochemical smog. The recent legislation with regard to catalytic converters for new cars is a (belated) government response to the greater public awareness of environmental issues.

Traditionally, NO is prepared in the laboratory by the reduction of 50% nitric acid with copper turnings (Equation 2.2) the resulting gas, collected over water, instantly turning brown on exposure to air due to the formation of nitrogen dioxide (Equation 2.3). More cleanly and conveniently it can be prepared by the reducing action of ascorbic acid on sodium nitrite (nitrous acid) solution (Equation 2.4). Industrially, its formation is a crucial step in the production of nitric acid, being formed by the oxidation of ammonia with a platinum/rhodium catalyst.

2.2 $\quad 8HNO_3 + 3Cu \longrightarrow 3Cu(NO_3)_2 + 2NO + 4H_2O$

2.3 $\quad \underset{\text{colourless}}{2NO + O_2} \longrightarrow \underset{\text{brown}}{2NO_2}$

21

2.4

HO—OH
H—
HOCH₂—CH O ═O
OH

$\xrightarrow[H^+]{2HNO_2}$

O═ ═O
H—
HOCH₂—CH O ═O
OH

+ 2NO
+ 2H₂O
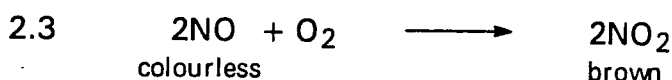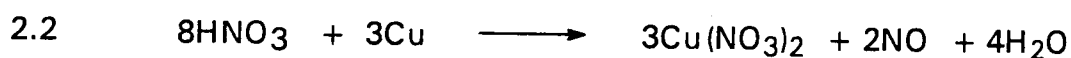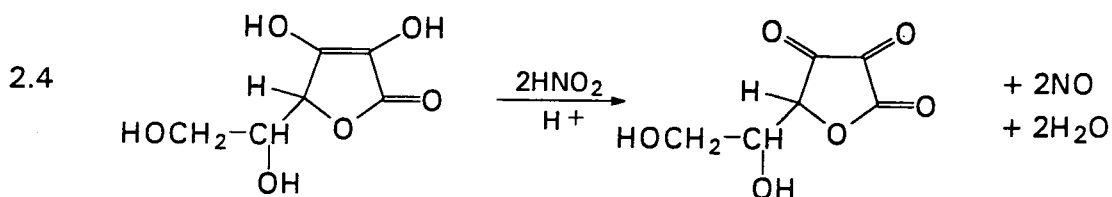
Equations 2.2, 2.3, 2.4

The reaction of NO with air is a textbook example of a third order reaction, being second order in NO (Rate = $k[NO]^2[O_2]$). It is generally thought that there is an initial formation of a dimer, which subsequently reacts with oxygen in the rate limiting step (Equation 2.5)

$$2NO \rightleftharpoons N_2O_2 \xrightarrow{oxygen} 2NO_2$$
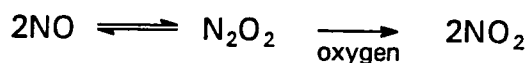
Equation 2.5

The reaction of NO with oxygen in aqueous solution is also third order[4], but no nitrate is produced when high NO purity is maintained, as might be expected from a reaction in which NO_2 is a reaction intermediate (Equation 2.6).

$$N_2O_4 + H_2O \rightarrow HNO_2 + HNO_3$$
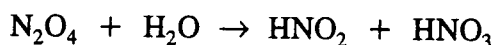
Equation 2.6

A mechanism has been proposed to explain this. It is thought that NO is oxidised in a rate-limiting step to NO_2 which reacts with further NO to give N_2O_3. This is then hydrolysed to yield nitrous acid (see Equations 2.7 below).

$$NO_2 + \tfrac{1}{2}O_2 \rightarrow NO_2$$
$$NO_2 + NO \rightarrow N_2O_3$$
$$N_2O_3 + H_2O \rightarrow 2HNO_2$$
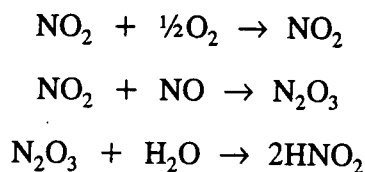
Equations 2.7

The reaction of NO_2 with NO is extremely fast[5] while its reaction with water is far slower. Some recent work[6] has questioned the presence of N_2O_3 in this reaction scheme.

Nitric oxide can act as an effective nitrosating agent in the presence of catalysts such as metals, although it has often (erroneously) been reported to act alone. These spurious reactions are probably due to oxidation of NO, by trace amounts of oxygen, to the genuine nitrosating species such as dinitrogen trioxide or dinitrogen tetroxide.

Diethylamine is nitrosated by NO in the presence of Cu(II) salts, due to the formation of a metal-nitrosyl complex as shown in Equations 2.8 below[7].

$$CuCl_2 \; + \; NO \; \rightleftharpoons \; Cu^{II} \, NO \; complex$$

$$Cu^{II} \, NO \; complex \; + R_2NH \; \longrightarrow \; Cu^{I} \; complex \; +R_2NNO \; + H^{\oplus}$$
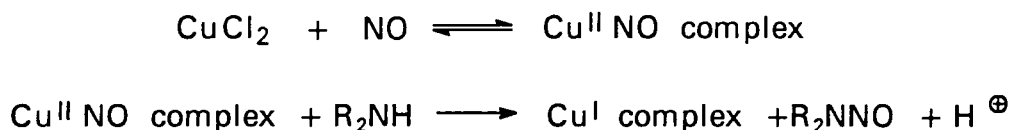
Equations 2.8

Another important aspect of NO chemistry is its ability to form complexes with a wide variety of transition metals. This is of crucial importance in the biological role(s) of NO. As has been previously mentioned, the vasodilatory and cytotoxic effects of NO are both thought to be mediated via a reaction of NO with iron. The former depends on the reaction with the haem prosthetic group in guanylate cyclase. It is thought that the Fe(II) atom is displaced out of the plane of the porphyrin ring upon combination with NO and that this configurational change activates the enzyme to produce cGMP from GMP[8].

The reaction of NO with oxyhaemoglobin is thought to be a means whereby NO is "mopped up" in the arterial system after release, with the formation of nitrate and methaemoglobin (Fe (III))[9]. This reaction forms the basis of an analytical procedure[10] for detecting NO in biological and physical systems. At a more mundane level, a similar reaction is employed by canned meat producers; the addition of sodium nitrite to meat as an anti-bacterial agent (particularly against *Clostridium botulinum*) has the useful side-effect of giving the meat a pink colour[11], which is attractive to the consumer.

Although NO/metal complexes have been known for a great many years, for example the "brown-ring" test for nitrates (due to the formation of $[Fe(H_2O)_5NO]^{2+}$) it is only

in the last twenty years or so that major research interest has focused on them, given their potential use as homogeneous catalysts and their widely understood role in biological systems[12]. A wide range of transition metal nitrosyl complexes have been prepared, by a wide variety of methods, apart from the obvious one of direct combination with NO. Their structure has been studied in detail using X-ray crystallography, electron-spin resonance spectroscopy (ESR), ^{15}N-nmr spectroscopy[13] etc. Happily for the biologist, in NO-Fe(II) haem complexes the NO still has an unpaired electron and these "spin-labelled" structures can be studied using ESR[14].

Nitrosyl complexes can act as direct electrophilic nitrosating agents (e.g. nitroprusside anion $[Fe(CN)_5NO]^{2-}$) with amines[15], while others can transfer NO^+ in reactions with amines, alcohols, ß-diketones etc. (e.g. ruthenium nitrosyls[16]). They can be treated as being sources of NO^+ or NO. The most studied metal nitrosyl is nitroprusside (pentacyanonitrosylferrate II, $[Fe(CN)_5NO]^{2-}$). It reacts readily with primary or secondary amines[17] and is useful when reactions need to be carried out in neutral or basic media (as opposed to the usual acid conditions used in nitrosation), as nitrosation will still occur[18]. It also reacts with ketones[19] to form the oxime and the aquo complex and with thiolate anion (RS$^-$) forming the disulphide[20].

Two other metal complexes with a long history are Roussin's black and red salts[21], first prepared in 1858, with definitive structural formulae being established exactly one hundred years afterwards[22, 23]. They are iron-sulphur cluster nitrosyls with the respective formulae $Fe_4S_3(NO)_7^-$ and $Fe_2S_2(NO)_4^{2-}$. Modern interest derives from the fact that they are thought to be representative of the structure of certain enzymic co-factors involved in mitochondrial electron-transport systems in cell respiration. The methyl ester of the red salt is known to nitrosate secondary amines to nitrosamines[24] and has been implicated in the aetiology of certain distinctive cancers. An interesting review[25] of these and related compounds has recently been published.

2.2 Nitrosating Reagents

The field of nitrosation is very great and therefore only a brief overview may be given before more attention is paid to specific nitrosation reactions. A large number of reagents are available to perform nitrosation. Perhaps the commonest is an acidic solution of nitrous acid. This is easily produced from the action of an aqueous mineral acid upon sodium nitrite (Equation 2.9).

$$NaNO_2 + HCl \longrightarrow NaCl + HNO_2$$
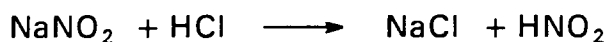
Equation 2.9

Nitrous acid exists in *cis* and *trans* forms[26], with the latter predominating, as shown in Figure 2.1
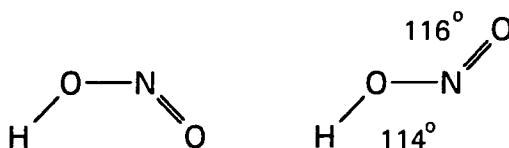
The bond lengths are   N=O 1.20Å,   N-O 1.46Å,   H-O 0.98Å

Figure 2.1

It is a weak acid[27] with a pK_a of 3.15 at 25°C so that it exists essentially in the molecular form at a pH below 2.0. When present in a very highly acid medium, nitrous acid forms the nitrosonium ion (NO^+). This is detectable by the change from the characteristic 5-peak "fingerprint" of nitrous acid[28] to the formation of a peak at 260nm, as shown in Equation 2.10

$$H_3O^+ + HNO_2 \rightleftharpoons NO^+ + 2H_2O$$

Equation 2.10

This ion is responsible for a great many nitrosation reactions. Further effective nitrosating species can be produced by the addition of halide ions. These nucleophilic species (X^-) generate nitrosyl species (XNO) in equilibrium, which can act as excellent nitrosation agents[29, 30] (Equation 2.11).

$$HNO_2 + H_3O^+ + X^- \longrightarrow XNO + 2H_2O$$

Equation 2.11

Nitrosyl thiocyanate (ONSCN) is another very effective nitrosating agent, formed in a similar situation to that above, by addition of a thiocyanate salt to an aqueous acidic solution of nitrous acid. Although less reactive than the nitrosyl halides, it is nevertheless a far better nitrosating agent due to the far larger[31] equilibrium constant favouring its formation, compared to the nitrosyl halides. Probably the most efficient catalyst of nitrosation however is thiourea. The actual nitrosating agent is the S-nitrosothiouronium ion ($(NH_2)_2CS^+NO$), formed in aqueous solution as before[32].

Other less commonly used nitrosating agents include nitrosyl acetate (sodium nitrite in glacial acetic acid, for water insoluble reactants), nitrogen oxides such as dinitrogen trioxide (N_2O_3), and dinitrogen tetroxide (N_2O_4). The reagents which undergo nitrosation are varied, so a general outline with a few examples will be given.

2.3 C-nitrosation

The products of C-nitrosation of aliphatic and alicyclic compounds depend upon experimental conditions, as the nitroso compounds formed are sensitive to acid or base catalysis and solvent/temperature. They can be nitroso monomers, nitroso dimers or oximes, the former being found when nitrogen oxides alone are used as nitrosating agents. In general the dimers and the oximes are more stable, but structural features may stabilise the monomer, which is characteristically blue or green. Their physical and chemical properties have been extensively reviewed[33, 34].

Alkanes can be nitrosated by nitrosyl chloride when irradiated with u.v./visible light. The mechanism is clearly free-radical in nature[35]. It is important industrially in the formation of caprolactam, a Nylon-6 precursor, from cyclohexane. An acid solution is used which not only catalyses the oxime formation, but also its Beckmann-type rearrangement to the cyclic amide[36, 37] (Equation 2.12).
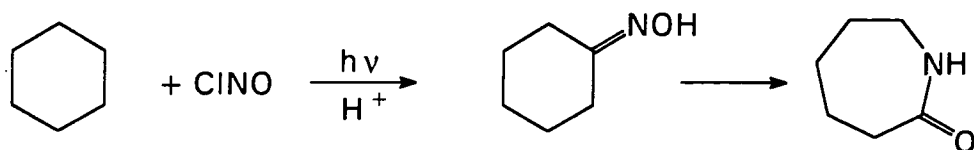
Equation 2.12

Ketones are readily nitrosated at the adjacent methyl or methylene group. Often the nitrosating agent used is aqueous acidic nitrous acid or alkyl nitites in acidified ethanol. Typical are the reactions of acetone and acetylacetone to give the corresponding oximes (Equations 2.13 and 2.14).

$$CH_3COCH_3 \xrightarrow{XNO} CH_3COCH{=}NOH$$

Equation 2.13

$$CH_3COCH_2COCH_3 \xrightarrow{XNO} CH_3CO\underset{\underset{NOH}{\|}}{C}COCH_3$$
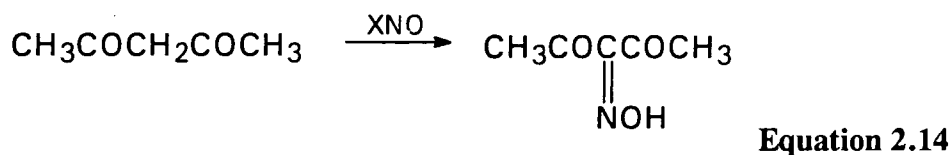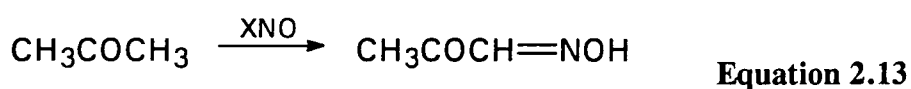
Equation 2.14

With an unsymmetrical ketone e.g. methylethylketone, the oxime usually is produced from nitrosation of the methylene rather than the methyl group[38] (Equation 2.15).

$$CH_3CH_2COCH_3 \xrightarrow{XNO} CH_3\underset{\underset{NOH}{\|}}{C}COCH_3$$
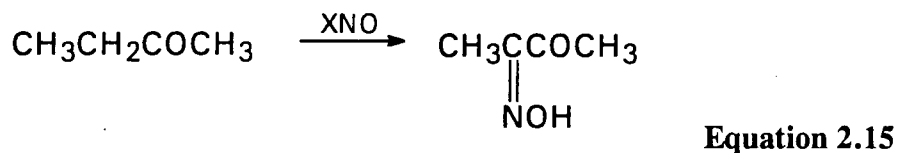
Equation 2.15

In contrast to the open-chain ketones where mono-nitrosation occurs, common cyclic ketones seem to form the α,α'-disubstituted oxime e.g. with cyclohexanone (Equation 2.16).

Equation 2.16
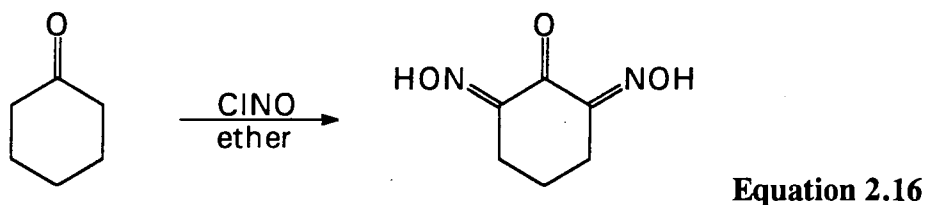
In general, any electron-withdrawing group adjacent to a methyl or methylene group will undergo these reactions e.g. nitroalkanes.

Nitrosation of aromatic systems usually involves reactants containing hydroxy, alkoxy or amine groups, as electron-releasing groups are necessary to allow nitrosation at a reasonable rate. Thus for example phenol is readily nitrosated by nitrous acid in dilute acid solution[39] to give mainly the 4-nitrosophenol, with some (10%) 2-nitrosophenol (Equation 2.17).
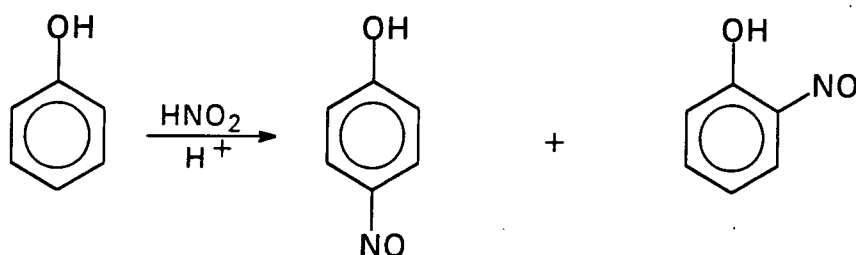
<div align="right">**Equation 2.17**</div>

The same main product is formed from phenol and acidic nitrite ion upon irradiation with u.v. light[40]. If excess nitrous acid is used, the reaction may proceed further to form the corresponding nitro compound. Secondary and tertiary aromatic amines react similarly to phenol[41], but in the latter excess nitrous acid results in dealkylation as well as nitration e.g. with N,N-dimethylaniline[42] (Equation 2.18).
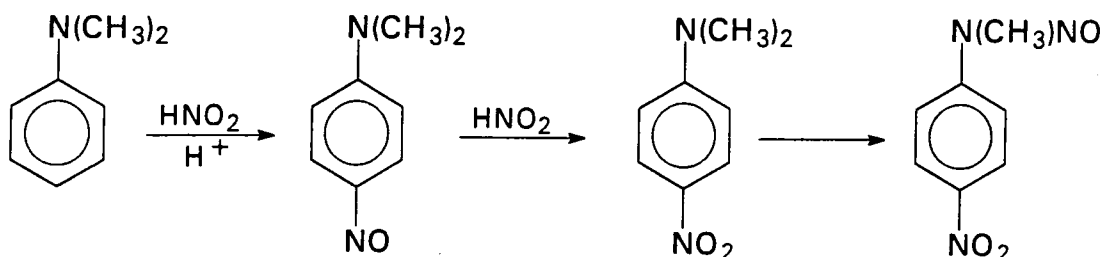
<div align="right">**Equation 2.18**</div>

Nitrosation of aromatic carbon may also occur via substitution of groups by NO e.g. 3,5-dibromo-4-hydroxybenzoic acid is readily decarboxylated by aqueous nitrous acid in acid solution[43] (Equation 2.19).

The chemical structure showing the reaction:

$$\text{(3,5-dibromo-4-hydroxybenzoic acid)} \xrightarrow[\text{H}^+]{\text{HNO}_2} \text{(nitroso product)} + CO_2 + H^+$$
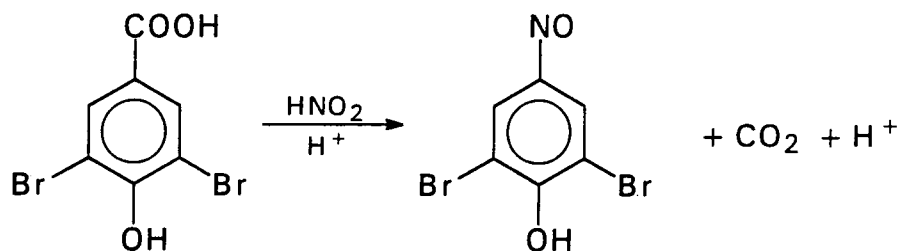
Equation 2.19

Similar reactions occur with tertiary aromatic amines, where 4-position substituents may be replaced by NO, although the final product is the nitro, rather than the nitroso derivative[44].

2.4 N-nitrosation

Primary aliphatic and aromatic amines react readily with a range of nitrosating agents to give a wide range of deamination products including phenols, alcohols, alkenes etc. The first step is thought to be the rate-limiting N-nitrosation in both cases, which is followed by a series of reactions to give a diazonium ion[45], as shown below in Scheme 2.1.

$$RNH_2 \xrightarrow[\substack{\text{electrophilic}\\\text{attack}}]{XNO} \overset{\oplus}{R}NH_2NO \xrightarrow{\text{deprotonation}} RNHNO$$

a N-nitrosamine

$$\Big\updownarrow \text{tautomerisation}$$

$$\overset{\oplus}{H_2O}N{=\!\!=}NR \underset{\text{protonation}}{\overset{H^+}{\rightleftharpoons}} RN{=\!\!=}N{-\!}OH$$

$$\Big\downarrow \substack{\text{loss of water}\\\text{as leaving group}}$$

$$H_2O + \overset{\oplus}{N_2}R$$

a diazonium ion
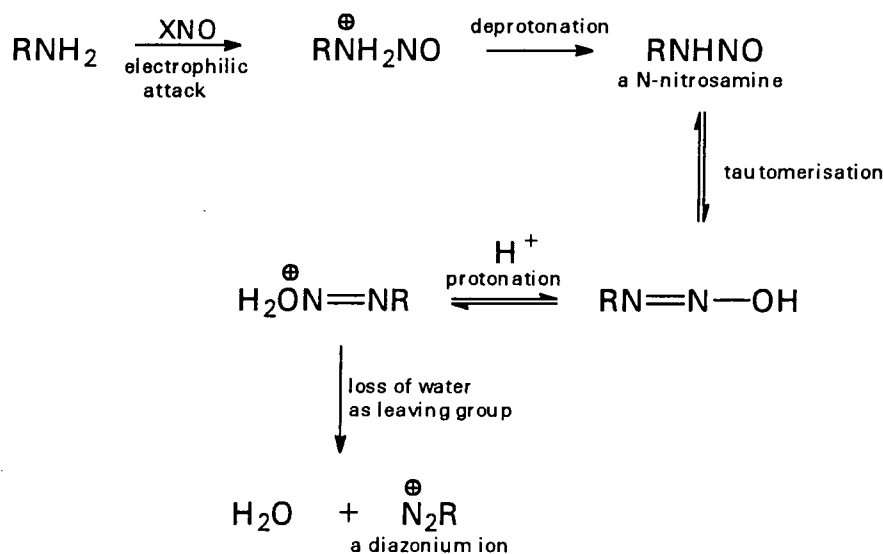
Scheme 2.1

The same outline applies to the corresponding secondary amines, but they stop at the formation of the nitrosamine (R_2NNO) as they lack the α-hydrogen necessary for proton transfer to form the diazo hydroxide. As they share a common rate-limiting

step however, the rate constants for primary and secondary amine nitrosation are often similar[46]. The main difference between aliphatic and aromatic primary amines is the stability of the diazonium ion intermediate formed during nitrosation, the latter of course producing far more stable species. The further reactions of diazonium ions are of immense synthetic interest and are the subject of numerous works[47, 48]. Tertiary amines react only slowly with nitrosating agents, via the formation of an iminium ion, to give a carbonyl compound and a secondary amine[49], which can of course react further, as shown below in Scheme 2.2.
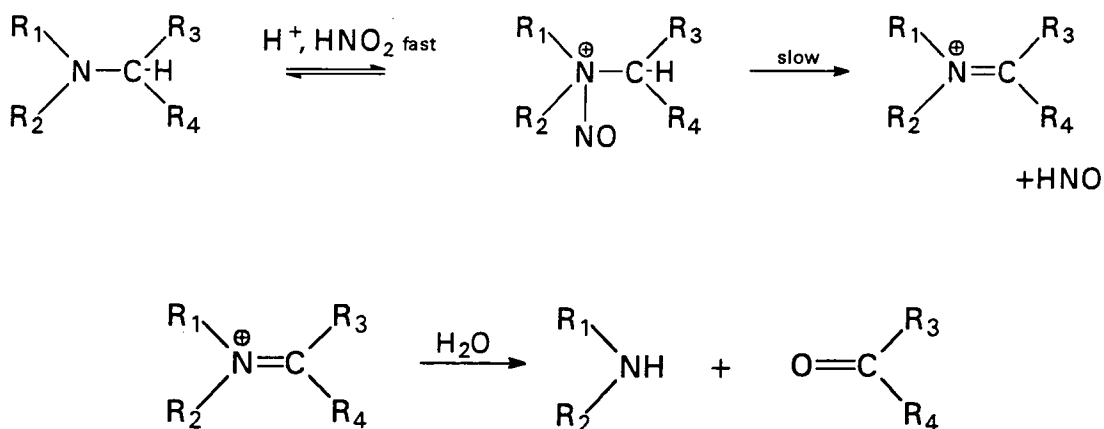
Scheme 2.2

Some amines are used as scavengers of nitrous acid in reactions - these include urea, hydrazine and sulphamic acid.

The reactions of aliphatic and aromatic secondary amines to form nitrosamines have acquired potentially great significance since the discovery that they are potent carcinogens[50] in all animal species tested. It has been theorised that nitrosamines could be formed *in vivo* from the reaction of dietary secondary amines with nitrite or nitrate in the acidic medium of the stomach[51]. Nitrite is present in canned meats (as described in Chapter 1) whilst nitrate is present in many water supplies as a result of over-application of fertilisers. While the toxic and carcinogenic effects of nitrosamines are not in doubt[52, 53], there is still uncertainty about the exact role they play in the incidence of cancer in various populations[54].

2.5 O-nitrosation

The reaction between an alcohol and nitrous acid in acid solution is the commonest example of O-nitrosation. The product, an alkyl nitrite, has already received mention in Chapter 1 as an early example of a vasodilator (Equation 2.20).

$$ROH \xrightarrow[H^+]{HNO_2} RONO$$
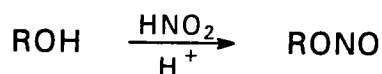
Equation 2.20

The reaction retains the chirality of the alcohol and is reversible[55]. Although steric properties of the alcohol affect the equilibrium position, in practice the alkyl nitrites are readily obtained by fractional distillation as their boiling points are lower than the corresponding alcohol. One interesting example is the nitrosation of ascorbic acid (vitamin C)[56]. It reacts very rapidly with two equivalents of nitrous acid to give dehydroascorbic acid and nitric oxide (see Equation 2.4). As is generally the case, the reaction is catalysed by halide ions and thiocyanate ions. This reaction is of great biological significance, since it is known[57] that, along with vitamin E, vitamin C protects against cancers. This is due to its competitive inhibition of the nitrosation of secondary amines in the stomach, as previously mentioned.

Alkyl nitrites are often used as nitrosating agents themselves, especially where non-aqueous solvent systems are required[58]. The full range of reactants already mentioned can be nitrosated, as well as alcohols and thiols. Studies have shown that in acidic aqueous solution the reaction proceeds, for a typical variety of reagents, via reversible hydrolysis of the alkyl nitrite to yield free nitrous acid, which is the actual nitrosating agent[59]. Where nitrosation by alkyl nitrites is slow, the addition of halide ions or thiourea can greatly increase the rate of reaction. This is effected by the formation of a nitrosyl intermediate e.g. with bromide ion[60] (Scheme 2.3).

$$\text{RONO} \; \underset{H^+}{\overset{}{\rightleftharpoons}} \; \overset{\oplus}{\underset{H}{\text{R} \overset{|}{\text{O}} \text{NO}}} \; \underset{Br^-}{\overset{}{\rightleftharpoons}} \; \text{ROH} \; + \; \text{BrNO}$$

$$\text{BrNO} \; + \; \text{Substrate} \; \xrightarrow{\text{rate determining step}} \; \text{Nitrosated Product}$$
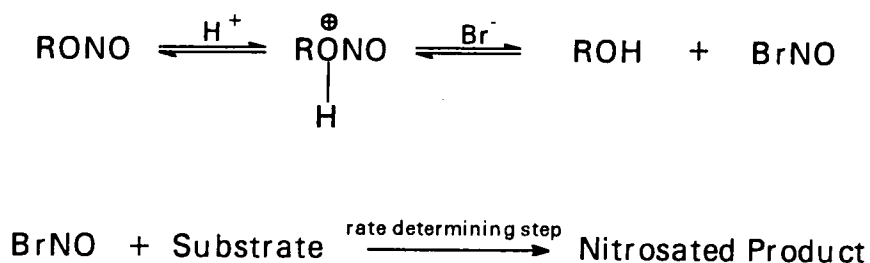
Scheme 2.3

The transnitrosation reaction between alkyl nitrites and alcohols in acid solution also occurs via formation of a protonated alkyl nitrite, which then reacts with the solvent/substrate alcohol[61].

The nitrosation of a sulphur moiety is analogous to the O-nitrosations discussed, but unlike the latter, the corresponding S-nitrosations generally are irreversible and much faster. Thus studies have shown that N-acetylpenicillamine (SNAP, an analogue for t-butyl thiol) is several orders of magnitude more reactive than t-butyl alcohol[62] and that the acid-catalysed hydrolysis of nitrosothiols is similarly slower than that of alkyl nitrites[63].

The explanation lies in the fact that, being a larger atom, sulphur is more polarisible than oxygen and hence more nucleophilic. This favours the nitrosation of sulphur by whatever reagent. Also, as oxygen is more basic than sulphur it will be more liable to denitrosation by proton attack, as shown in Scheme 2.4 below.

$$\text{RSH} \; + \; \text{XNO} \; \rightleftharpoons \; \overset{\oplus}{\underset{H}{\text{R} \overset{|}{-} \text{S} \overset{|}{-} \text{NO}}} \; \xrightarrow[\substack{\text{essentially} \\ \text{irreversible}}]{H_2O} \; \text{RSNO} \; + \; H^+ \; + \; X^-$$

$$\text{ROH} \; + \; \text{XNO} \; \rightleftharpoons \; \overset{\oplus}{\underset{H}{\text{R} \overset{|}{-} \text{O} \overset{|}{-} \text{NO}}} \; \underset{\text{reversible}}{\overset{H_2O}{\rightleftharpoons}} \; \text{RONO} \; + \; H^+ \; + \; X^-$$
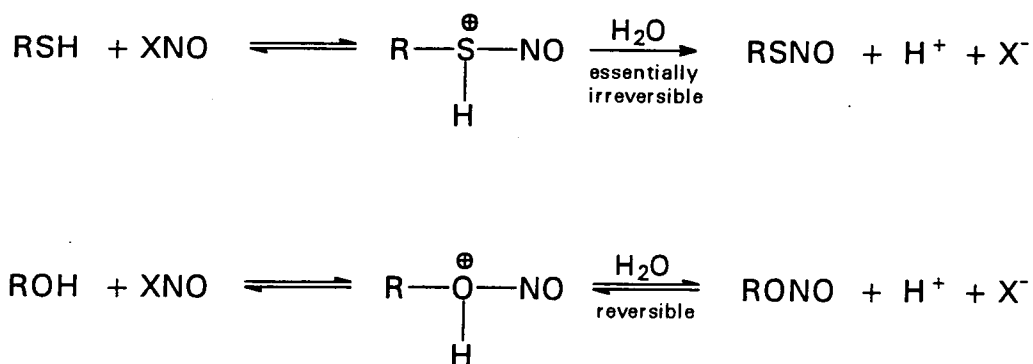
Scheme 2.4

2.6 S-nitrosation

The nitrosation of thiols to form S-nitrosothiols (or thionitrites as they are alternatively known) has a history[64] dating back to 1837. Due to their general instability however, less is known about S-nitrosation processes than those at the other centres already described. Both aliphatic and aromatic thiols react easily with a wide range of nitrosating agents (nitrous acid[65], dinitrogen tetroxide[66], nitrosyl chloride[67], alkyl nitrites[68] etc) in both aqueous and organic solvents to form S-nitrosothiols, as in Equation 2.21 below.

$$RSH \ + \ XNO \ \longrightarrow \ RSNO \ + HX \qquad \textbf{Equation 2.21}$$

An early synthesis was of phenyl S-nitrosothiol by treatment of benzenethiol with nitrosyl chloride[69] (Equation 2.22).
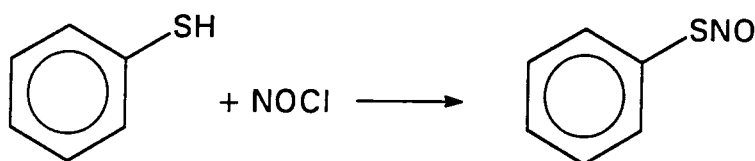
Equation 2.22

Characteristically, this unstable red substance decomposed rapidly to the diphenyl sulphide and nitric oxide (Equation 2.23).
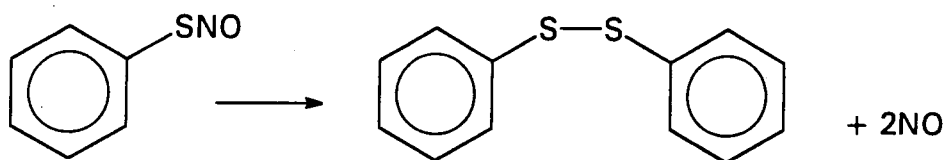
Equation 2.23

Convenient synthetic methods include the treatment of the thiol with N_2O_4 in inert solvents such as chloroform[70], while the use of t-butyl S-nitrosothiol in chloroform has been proposed as a simple procedure giving quantitative yields[71]. Alkyl nitrites have a similar use in alcohol solvent systems[60]. More uncommon is the formation of
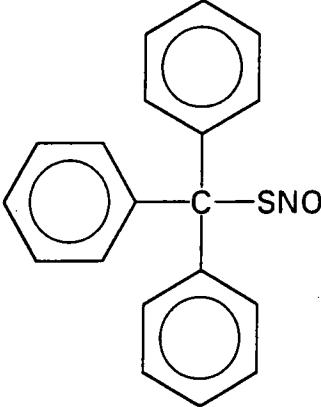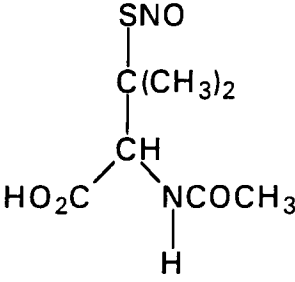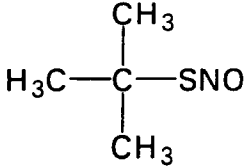
S-nitrosothiols in the vapour phase e.g. the formation of methyl S-nitrosothiol from dimethyl sulphide and nitric oxide by photolysis[72] (Equation 2.24).

$$CH_3S—SCH_3 \xrightarrow[h\nu]{heat} [CH_3S^\bullet] \xrightarrow{2NO} 2CH_3SNO$$
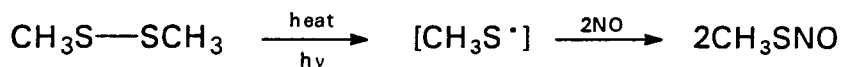
Equation 2.24

As mentioned, S-nitrosothiols are typically red or green compounds, that are light and heat sensitive to varying degrees and are best stored in a freezer if not used immediately (see Table 2.1).

Table 2.1

S-nitrosothiol Structure	Colour and form (room temp.)
	Green crystals S-nitroso-triphenylmethane
	Green crystals S-nitroso-N-acetylpenicillamine (SNAP)
	Red-green liquid S-nitroso-trimethylmethane

S-nitrosothiol Structure	Colour and form (room temp.)
SNO CH_2 CO_2H $(CH_2)_2CON-C-CONHCH_2$ CH H H H_2N CO_2H	Pink crystals S-nitroso-glutathione (SNOG)

Compound 2 (SNAP) is the most stable example known. It is indefinitely stable in the dark in a refrigerator. Its crystalline strucure has enabled the precise configuration of the SNO moiety to be adduced[73], as shown below in Figure 2.1.
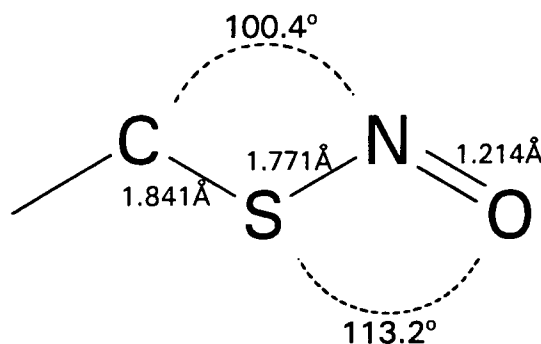
Figure 2.1 Structure of the R-SNO group

The R-SNO group is responsible for the coloured nature of the compounds, but it can be seen that the structure of the rest of the molecule may have some effect - thus a tertiary carbon seems to produce green coloured compounds. They have a characteristic absorbance maximum around 340nm (ε = 1000 mol^{-1} l cm^{-1}) with a secondary maximum (ε = 15 mol^{-1} l cm^{-1}) around 540nm for the red compounds and around 590 nm for the green compounds. The coloured property of S-nitrosothiols has led to their use in the identification of thiols in solution[74]. Almost all S-nitrosothiols are unstable at room temperature and decompose to give the corresponding disulphide and nitric oxide (Equation 2.25).

$$2RSNO \longrightarrow R-S-S-R + 2NO$$

<div align="right">**Equation 2.25**</div>
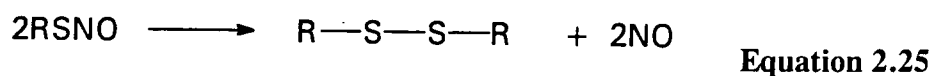
Quantitative conversion can be achieved by refluxing the S-nitrosothiol in methanol for one hour, even with a stable compound like SNAP[73]. The reaction is thought to proceed by a homolytic mechanism, as photolysis of S-nitrosothiols yields the same products e.g. with benzyl S-nitrosothiol[75] (Equations 2.26 and 2.27).
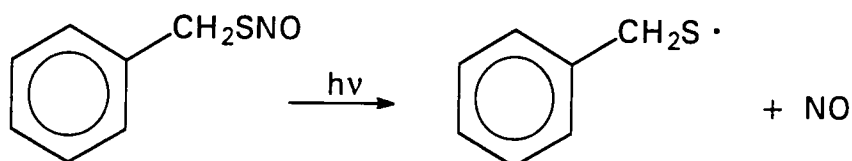
<div align="right">**Equation 2.26**</div>
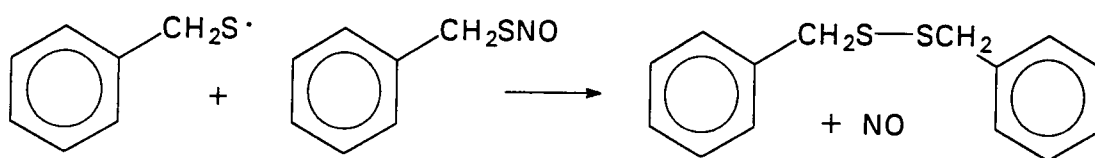
<div align="right">**Equation 2.27**</div>

Reactions of S-nitrosothiols with thiols in chloroform, using N_2O_4 as initial nitrosating agent, give unsymmetrical disulphides in excellent yields[66, 70]. S-nitrosothiols can be oxidised quite easily by a variety of reagents. Thus t-butyl S-nitrosothiol has been oxidised to the corresponding thionitrate by fuming nitric acid[76] (Equation 2.28).
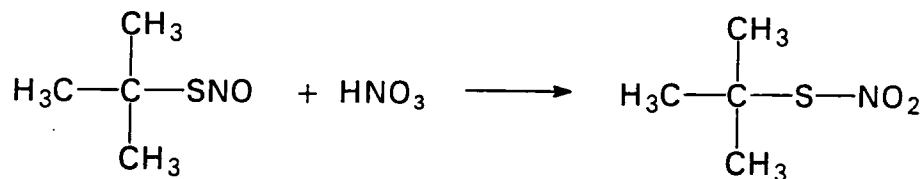
<div align="right">**Equation 2.28**</div>

An alternative method is simple oxidation with air e.g. ethyl S-nitrosothiol has been oxidised by passing air into it for three hours[77], yielding diethylsulphide and dinitrogen tetroxide (Equation 2.29).

$$2CH_3CH_2SNO \ + \ O_2 \ \longrightarrow \ CH_3CH_2\text{-}S\text{-}S\text{-}CH_2CH_3 \ + \ N_2O_4$$

<div align="right">
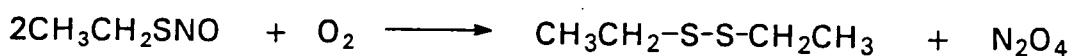
Equation 2.29

</div>

Reduction is possible with mercury(II) ion to give the corresponding mercury mercaptide e.g. with cysteine S-nitrosothiol (Equation 2.30).

$$
\underset{\substack{\\ \\ \\ \\ \\}}{
\begin{array}{c}
SNO \\
| \\
CH_2 \\
| \\
CH \\
H_2N \quad CO_2H
\end{array}}
\ \xrightarrow[H_2O]{Hg^{2+}} \
\begin{array}{c}
\overset{\oplus}{S}\text{---}Hg \\
| \\
CH_2 \\
| \\
CH \\
H_2N \quad CO_2H
\end{array}
\ + \ HNO_2 \ + \ H^+
$$

<div align="right">
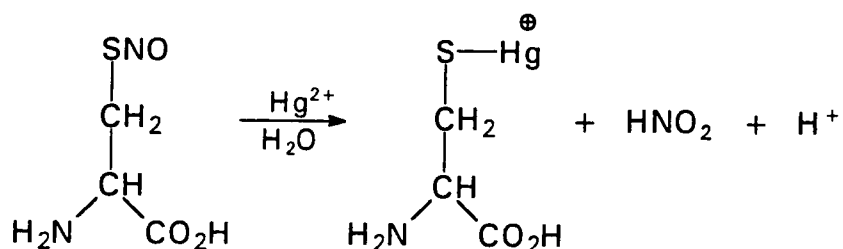
Equation 2.30

</div>

This reaction forms the basis of a procedure for the quantitative analysis of thiols in proteins etc. introduced by Saville[78], using ammonium sulphamate as a nitrous acid scavenger.

An S-nitrosothiol such as t-BuSNO reacts with various arylamines in the presence of anhydrous copper (II) halides to give the corresponding aryl halide in excellent yield[79] at room temperature e.g. as in Equation 2.31.
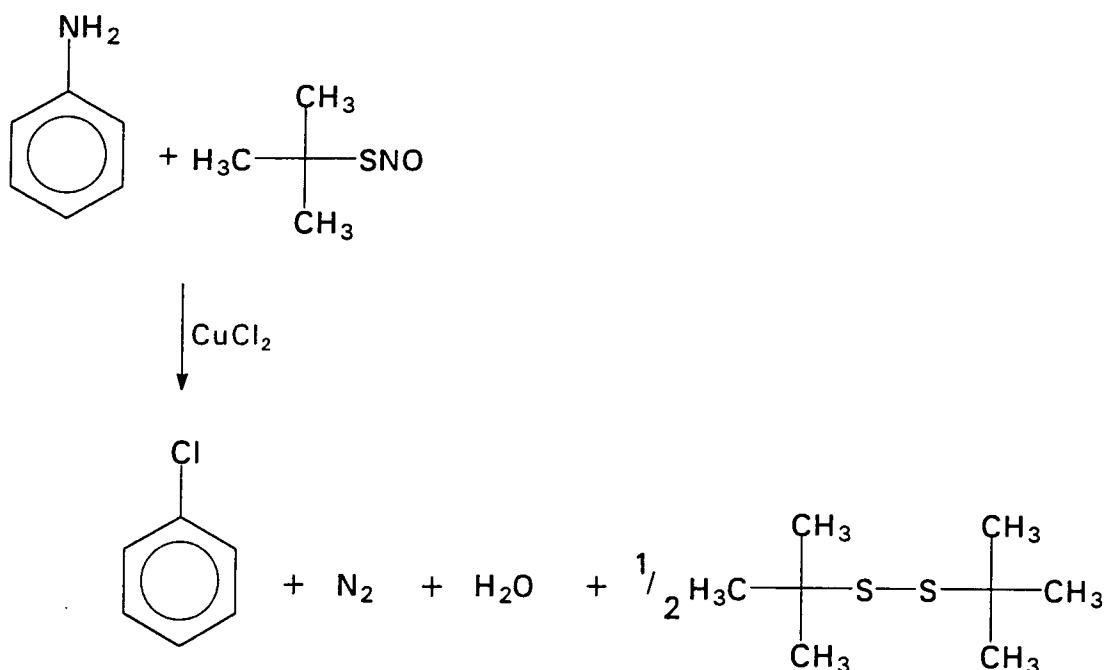
Equation 2.31

N-methylaniline reacts with the same compound alone to give N-nitroso-N-methylaniline[70] (Equation 2.32).
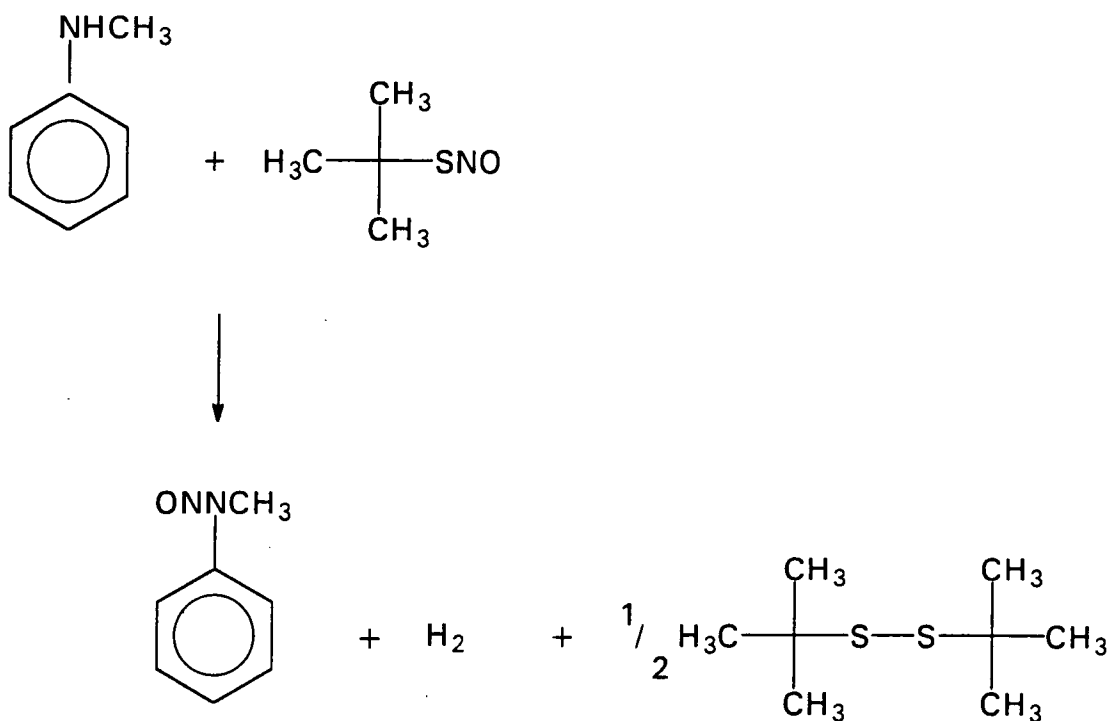
Equation 2.32

This reaction is general for the nitrosation of secondary amines by S-nitrosothiols[80, 81]. S-nitrosothiols can also yield azo dyes after reaction with aniline (as the hydrochloride) and coupling with β-naphthol[73]. In these reactions it remains to be determined whether nitrosation is directly attributable to the S-nitrosothiol or whether another nitrosating agent is formed from the S-nitrosothiol prior to this.

The mechanistic details of S-nitrosation of thiols have been studied and the following rate law established (Equation 2.33).

$$\text{Rate} \;=\; k\,[HNO_2]\,[H^+]\,[RSH] \qquad\qquad \textbf{Equation 2.33}$$

The initial work was on t-butyl thiol nitrosation by nitrous acid in 50% aqueous dioxan[68], but has received support from further work[82, 83] on cysteine and mercaptocarboxylic acids. The equation can be interpreted in terms of a rate-limiting electrophilic attack on the sulphur atom by nitrous acidium ion or nitrosonium ion ($H_2NO_2^+$ or NO^+ respectively). This is followed by rapid proton loss from the protonated S-nitrosothiol, as shown in Scheme 2.5 below.

$$HNO_2 \;+\; H^+ \;\underset{}{\overset{fast}{\rightleftharpoons}}\; H_2NO_2^+ \,/\, NO^+ \;+\; H_2O$$

$$RSH \;+\; H_2NO_2^+ \,/\, NO^+ \;\underset{}{\overset{slow}{\rightleftharpoons}}\; R\overset{\oplus}{\underset{|\;H}{-S-}}NO$$

fast

$$RSNO \;+\; H^+$$
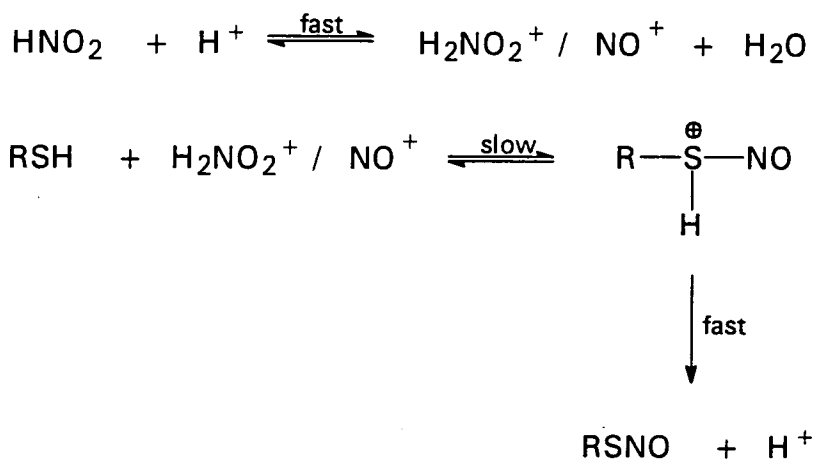
Scheme 2.5

For many reactive thiols, the reaction appears close to the encounter-controlled limit for neutral substrates (approx. 7000 l^2 mol^{-2} s^{-1})[84] as can be seen from the table[85] of third-order rate constants (k) below (Table 2.2).

Thiol	k (l^2 mol^{-2} s^{-1})
Glutathione	1080
Cysteine	443
Thioglycolic acid	2630
Mercaptopropionic acid	4760

Table 2.2

Thiols are not significantly protonated at moderate acid pH unlike basic amines where protonation reduces the effective concentration of the reactive, molecular species. Thiols thus have a use as nitrous acid scavengers. It can be seen that such fast reactions require stopped-flow spectrophotometry for their measurement. All thiols studied show catalysis by halide ion and thiocyanate ion, similar to that previously mentioned in relation to N- and O-nitrosation reactions[62]. The rate equation has been determined for nitrosation of thiols by nitrous acid with such added nucleophiles (Equation 2.34).

$$\text{Rate} = k_2 \text{ [RSH] [XNO]} \qquad \text{Equation 2.34}$$
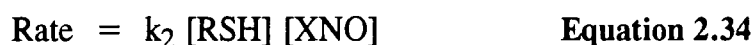
The mechanism (see Scheme 2.6 below) is thought to be one in which an equilibrium concentration of the corresponding nitrosyl compound (NOX) is formed, which then attacks the thiol.

$$HNO_2 + H^+ + X^- \rightleftharpoons XNO + H_2O$$

$$XNO + RSH \xrightarrow{\text{slow}} R-\overset{\oplus}{\underset{H}{S}}-NO + X^-$$

$$\downarrow \text{fast}$$

$$RSNO + H^+$$
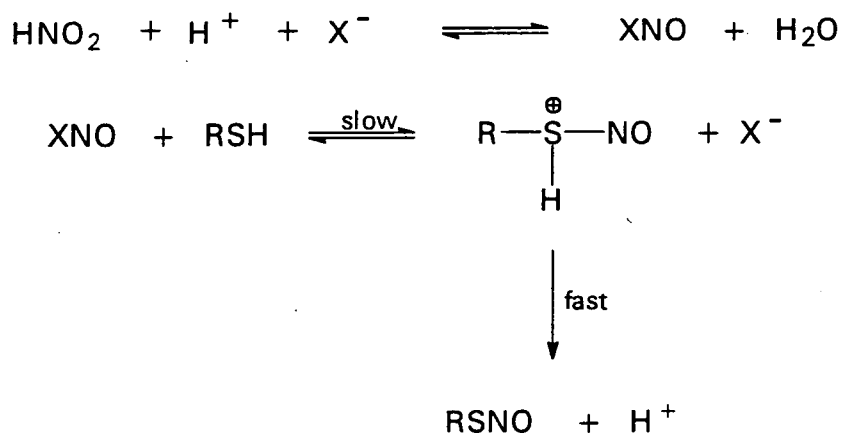
Scheme 2.6

The degree of catalysis is governed by the size of the equilibrium constant for NOX formation increasing in the series $ClNO < BrNO < NCSNO < (NH_2)_2CS^+NO$, even

though the k_2 value decreases along this series i.e. the quantity of XNO produced outweighs the lower reactivity of the species[85] (see Table 2.3 below).

	k_2 (l mol^{-1} s^{-1})		
Thiol	**ClNO**	**BrNO**	**NCSNO**
Thioglycolic acid	1.4×10^7	1.1×10^6	2.5×10^4
Glutathione	5.7×10^6	2.9×10^5	1.9×10^3
Cysteine	1.2×10^6	5.8×10^4	7.0×10^2
Cysteine methyl ester	1.0×10^6	4.9×10^4	7.0×10^2
N-acetylcysteine	1.0×10^7	4.5×10^5	1.6×10^3

Table 2.3 Second order rate constants for the reactions of ClNO, BrNO, and NCSNO with thiols in water at 25°C

It will be noticed that whereas cysteine and its ester are of similar reactivity, N-acetylcysteine is significantly more reactive. This may be due to the positively-charged sulphur of the transition state being internally stabilised by the formation of a six-membered ring structure[86], as shown below in Figure 2.2.
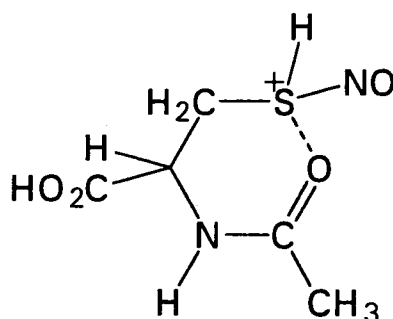
Figure 2.2

References

1. J. N. Armor, *J. Chem. Eng. Data*, 1974, **19**(1), 82

2. P. A. Leighton, in *Photochemistry of Air Pollution*, Academic Press, New York, 1961

3. M. Bodenstein, *Z. Electrochem.*, 1918, **24**, 183

4. H. H. Awad, D. M. Stanbury, *Int. J. Chem. Kinet.*, 1993, **25**, 375

5. M. Gratzel, S. Taniguchi, A. Henglein, *Ber. Bunsen-Ges. Phys. Chem.*, 1970, **74**, 488

6. M. Feelisch, E.A. Noack, *Eur. J. Pharmacol.*, 1987, **139**, 19

7. W. Brackman, P. J. Smit, *Recl. Trav. Chim. Pays-Bas*, 1965, **84**, 357

8. L. J. Ignarro, *Circ. Res.*, 1989, **65**, 1

9. J. S. Stamler *et al*, *Proc. Natl. Acad. Sci.*, U.S.A., 1992, **89**, 7674

10. D. A. Wink, J. F. Darbyshire, R. W. Nims, J. E. Saavedra, P. C. Ford, *Chem. Res. Toxicol.*, 1993, **6**, 23

11. J. Haldane, *J. Hyg.*, 1901, **1**, 115

12. D. M. P. Mingos, D. J. Sherman, *Adv. Inorg. Chem.*, 1989, **34**, 293

13. G. B. Richter-Addo, P. Legzdins, in *Metal Nitrosyls*, Oxford University Press, New York, 1992

14. M. F. Perutz, *Ann. Rev. Biochem.*, 1979, **48**, 327

15. A. R. Butler, C. Glidewell, J. Reglinski, A. Waddon, *J. Chem. Res. (S)*, 1984, 279

16. F. Bottomley, *Coord-Chem. Rev.*, 1978, **26**, 7

17. H. Maltz, M. A. Grant, M. C. Navaroli, *J. Org. Chem.*, 1971, **36**, 363

18. J. H. Swinehart, P. A. Rock, *Inorg. Chem.*, 1966, **5**, 573

19. J. H. Swinehart, W. G. Schmidt, *Inorg. Chem.*, 1967, **6**, 232

20. D. Mulvey, W. A. Waters, *J. Chem. Soc., Dalton Trans.*, 1975, 951

21. F. Z. Roussin, *Ann. Chim. Phys.*, 1858, **52**, 285

22. J. T. Thomas, J. H. Robertson, E. G. Cox, *Acta Crystallogr.*, 1958, **11**, 599

23. G. Johansson, W. N. Lipscomb, *Acta Crystallogr.*, 1958, **11**, 594

24. H. A. Croisy, H. Ohshima, H. Bartsch, *IARC Sci. Publ.*, 1984, **57**, 327

25. A. R. Butler, C. Glidewell, M. H. Li, *Adv. Inorg. Chem.*, 1988, 335

26. K. Jones, in *Comprehensive Inorganic Chemistry*, Eds. J. C. Bailar, H. J. Emeleus, R. Nyholm, A. F. Trotman-Dickenson, Pergamon Press, New York, 1973, Vol. 2, 368

27. J. Tummavouri, P. Lumme, *Acta Chem. Scand.*, 1968, **22**, 2003

28. K. Singer, P. A. Vamplew, *J. Chem. Soc.*, 1956, 3971

29. L. J. Beckman, W. A. Fessler, M. A. Kise, *Chem. Rev.*, 1951, **48**, 319

30. B. C. Challis, D. E. G. Shuker, *J. Chem. Soc., Perkin Trans. 2*, 1979, 1020

31. G. Stedman, P. A. E. Whincup, *J. Chem. Soc.*, 1963, 5796

32. T. A. Meyer, D. L. H. Williams, *J. Chem. Soc., Perkin Trans. 2*, 1981, 361

33. J. H. Boyer, in *The Chemistry of the Nitro and Nitroso Groups*, Ed. H. Feuer, Interscience, New York, 1969, Part 1, 215

34. R. G. Coombes, in *Comprehensive Organic Chemistry*, Ed. I. O. Sutherland, Pergamon Press, Oxford, 1979, Vol. 2, 305

35. E. Muller, H. Metzger, *Chem. Ber.*, 1957, **90**, 1179

36. M. Pape, Fortschr. *Chem. Forsch.*, 1967, **7**, 559

37. M. Fischer, *Angew. Chem. Internat. Edn.*, 1978, **17**, 16

38. O. Touster, in *Organic Reactions*, Ed. R. Adams, Wiley, New York, 1953, Vol. 7, 327

39. S. Veibel, *Ber.*, 1930, **63**, 1577

40. J. Suzuki, N. Yagi, S. Syzuki, *Chem. Pharm. Bull.*, 1984, **32**, 2803

41. G. M. Loudon, in *Organic Chemistry*, Benjamin/Cummings, 1988, 2nd Ed., 1019

42. H. H. Hodgson, D. E. Nicholson, *J. Chem. Soc.*, 1941, 470

43. R. A Henry, *J. Org. Chem.*, 1958, **23**, 648

44. M. Colonna, L. Greci, M. Poloni, *J. Chem. Soc., Perkin Trans. 2*, 1984, 165

45. S. Ege, in *Organic Chemistry*, D. C. Heath & Co., Toronto, 1984, 919

46. E. Kalatzis, J. H. Ridd, *J. Chem. Soc. (B)*, 1966, 529

47. H. Zollinger, in *Diazo and Azo Chemistry*, Interscience, New York, 1961

48. in *The Chemistry of Diazonium and Diazo Groups*, Ed. S. Patai, Interscience, New York, Parts 1 and 2, 1978

49. P. A. S. Smith, R. N. Loeppky, *J. Am. Chem. Soc.*, 1967, **89**, 1147

50. P. N. Magee, J. M. Barnes, *Brit. J. Cancer*, 1956, **10**, 114

51. J. S. Wishnok, *J. Chem. Educ.*, 1977, **54**, 440

52. H. A. Freund, *Ann. Intern. Med.*, 1937, **10**, 1144

53. R. Montesano, H. Bartsch, *Mutation Res.*, 1976, **32**, 179

54. D. Forman, S. Al-Dabbagh, R. Doll, *Nature* (London), 1985, **313**, 620

55. W. A. Noyes, *Org. Synth.*, 1943, Coll. II, 108

56. J. H. Ridd, *Adv. Phys. Org. Chem.*, 1978, **16**, 1

57. C. L. Walters, *Ind.- Univ. Co-op. Symp.*, 1974, 78

58. B. Bromberger, L. Phillips, *J. Chem. Soc.*, 1961, 5302

59. M. J. Crookes, D. L. H. Williams, *J. Chem Soc., Perkin Trans. 2*, 1988, 1339

60. S. E. Aldred, D. L. H. Williams, *J. Chem. Soc., Perkin Trans. 2*, 1981, 1021

61. A. D. Allen, G. R. Schonbaum, *Can. J. Chem. Comm.*, 1961, **39**, 947

62. S. E. Aldred, D. L. H. Williams, M. Garley, *J. Chem. Soc., Perkin Trans. 2*, 1982, 777

63. S. S. Al-Kaabi, D. L. H. Williams, R. Bonnett, S. L. Ooi, *J. Chem. Soc., Perkin Trans. 2*, 1982, 227

64. H. Lecher, W. Siefker, *Ber.*, 1926, **59**, 1314

65. R. Bonnett, P. Nicolaidou, *J. Chem. Soc., Perkin Trans. 1*, 1979, 1969

66. S. Oae, D. Fukushima, Y. H. Kim, J. *Chem. Soc., Chem. Comm.*, 1977, 407

67. J. Mason, *J. Chem. Soc. (A)*, 1969, 1587

68. G. Kresze, J. Winkler, *Chem. Ber.*, 1963, **96**, 1203

69. H. S. Tasker, H. O. Jones, *J. Chem. Soc.*, 1909, **95**, 1910

70. S. Oae, Y. H. Kim, D. Fukushima, T. Takata, *Chem. Lett.*, 1977, 893

71. M. P. Doyle, J. W. Terpstra, R. A. Pickering, D. M. LePoire, *J. Org. Chem.*, 1983, **48**, 3379

72. P. M. Rao, J. A. Copeck, A. R. Knight, *Can. J. Chem.*, 1967, **45**, 1369

73. L. Field, R. V. Dilts, R. Ramanthan, P. G. Lenhert, G. E. Carnahan, *J. Chem Soc., Chem. Comm.*, 1978, 249

74. G. W. Ashworth, R. E. Keller, *Anal. Chem.*, 1967, **39**, 373

75. J. Barrett, D. F. Debenhan, J. Glauser, *J. Chem. Soc., Chem. Comm.*, 1965, 248

76. H. Rheinbolt, F. Mott, *Ber.*, 1932, **65**, 1223

77. H. Lecher, W. Siefker, *Ber.*, 1926, **59**, 2594

78. B. Saville, *Analyst*, 1958, **83**, 670

79. Y. H. Kim, K. Shinhama, S. Oae, *Tet. Lett.*, 1978, 4519

80. J. Fitzpatrick, T. A. Meyer, M. E. O'Neill, D. L. H. Williams, *J. Chem. Soc., Perkin Trans. 2*, 1984, 927

81. M. J. Dennis, R. Davies, D. J. McWeeney, *J. Sci. Food Agric.*, 1979, **30**, 639

82. P. Collings, K. Al-Mallah, G. Stedman, *J. Chem. Soc., Perkin Trans. 2*, 1975, 1734

83. L. R. Dix, D. L. H. Williams, *J. Chem. Soc., Perkin Trans. 2*, 1984, 109

84. J. H. Ridd, *Adv. Phys. Org. Chem.*, 1978, **16**, 1

85. D. L. H. Williams, *Chem Soc. Rev.*, 1985, **14**, 171

86. D. L. H. Williams, in *Nitrosation*, Cambridge University Press, Cambridge, 1988, 178

Chapter Three

Aspects Of S-nitrosothiol Decomposition In Aqueous Solutions

3.1. Use of a Griess Reagent To Measure Nitrite Production

3.1.1. Introduction

One aspect of the decomposition of S-nitrosothiols is the production of nitrous acid in solution. This has been shown to be quantitative for many S-nitrosothiols and could offer a means of monitoring the decomposition of S-nitroso-N-acetylpenicillamine (SNAP). The nitrous acid produced could be detected by means of a Griess reaction[1]. This involves using the nitrous acid to diazotise an aryl amine (in acid solution), which is subsequently coupled to an appropriate aryl compound to yield an azo dye. This can be detected by the colour produced and its concentration measured at a suitable absorbance maximum.

The particular method of Saville was used[2], whereby sulphanilamide (SUL) is the diazotised substrate and N-(1-Naphthyl)-ethylenediamine (NNED) is the coupling agent (see Scheme 3.1 below).
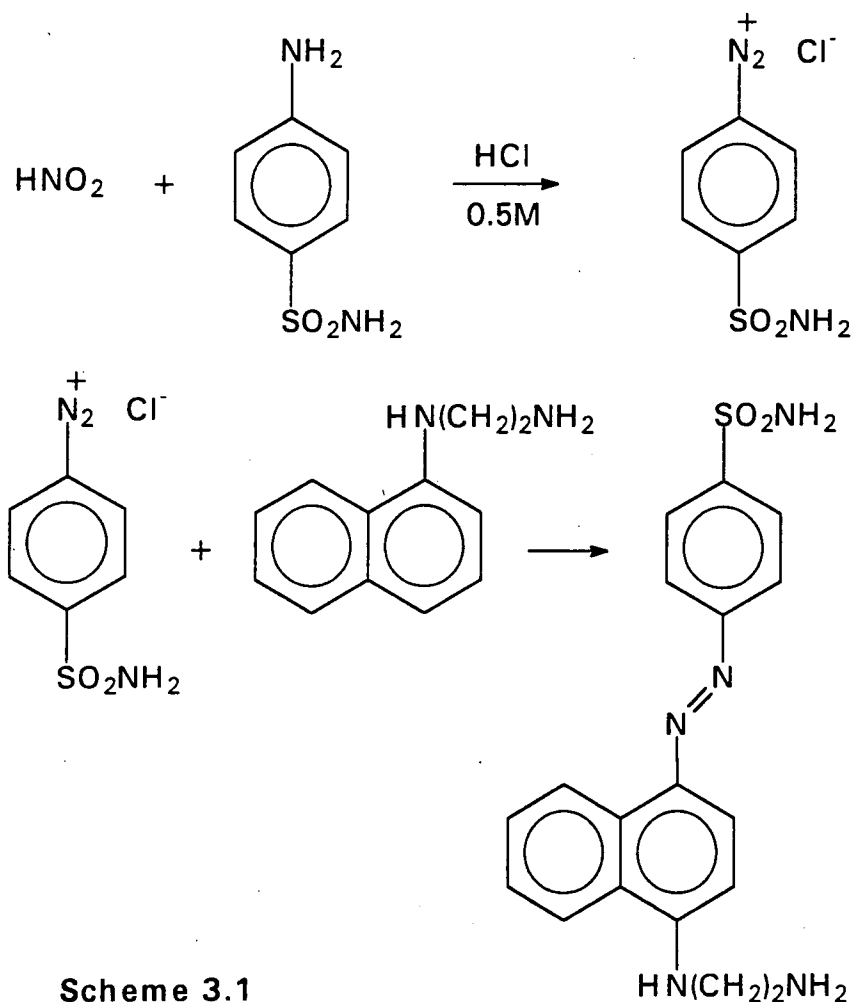
Scheme 3.1

The presence of an electron withdrawing group at one end of the molecule and an electron donating group at the other endows the molecule with a colour that is more inclined to the blue end of the spectrum. Thus this dye is red/purple in colour.

3.1.2. Calibration and Initial Set-up

Initial experiments indicated that the dye had an abs_{max} at 540nm. ($\varepsilon = 9.64 \times 10^4$ mol^{-1} l cm^{-1})

A calibration curve was produced, using stock sodium nitrite in the range 1×10^{-4} M to 8×10^{-4} M, using the data shown in Table 3.1.

10^4 x [NaNO$_2$] (M)	Abs at 540nm (Mean of 5)	25°C
8	1.588 $\pm$ 0.015	
6	1.207 $\pm$ 0.006	
4	0.823 $\pm$ 0.003	0.850 $\pm$ 0.013
2	0.422 $\pm$ 0.003	0.446 $\pm$ 0.013
1	0.211 $\pm$ 0.005	0.217 $\pm$ 0.006
0.5		0.094 $\pm$ 0.004

An excellent correlation was found (0.9998), the method being most sensitive below 4×10^{-4} M, while at 1×10^{-4} M the absorbance maximum was too low in comparison with the background reference absorbance (≈ 0.04) i.e. 4×10^{-4} M was chosen as the best compromise between high absorbance and accurate conforming to the Beer-Lambert Law. Repetition of the calibration curve work, over a lower range produced again a line with a very high correlation coefficient (0.9992). The value for the absorbance at 4×10^{-4} M was taken as the average of the two means (0.823 and 0.850) i.e. 0.837.

Some initial runs were performed on SNAP in water at 25°C, 4×10^{-4} M. These indicated that problems could arise with the reference cell (SUL/NNED plus water). A pink tinge was observed which occurred even when the reference was covered in aluminium foil. Investigation appeared to indicate that the problem arose from

inadequate washing of apparatus. (All the chemicals used were checked, including the stock 0.47M hydrochloric acid and found to be satisfactory). Pink particles in some glassware indicated that the azo dye precipitates out, especially at higher dye concentrations when left overnight.

After scrupulous washing, and use of new solutions, low reference cell absorbances ($<$ 0.04) were re-obtained.

SNAP in phosphate buffer at 25°C, pH 6.94 was allowed to decompose and the reaction progress obtained by detection of nitrous acid production. The results of three parallel runs are shown in Table 3.2.

Time (mins)	Absorbance (mean)	Time (mins)	Absorbance (mean)	Time (mins)	Absorbance (mean)
5	0.183	3.5	0.198	4	0.158
10	0.430	9.0	0.456	10	0.392
15	0.608	14	0.673	20	0.496
30	0.803	20	0.774	40	0.588
45	0.807	26	0.769	60	0.617
60	0.804	30	0.762	90	0.626
90	0.810	46	0.786	120	0.674
120	0.807	60	0.777	225	0.607

Abs_∞ value of $\approx$ 0.81 indicates SNAP concentration of 3.87 x10^{-4} M.
Actual concentration = 4 x 10^{-4} M i.e. 97% conversion to nitrite.
Abs_∞ value of $\approx$ 0.78 indicates SNAP concentration of 3.73 x10^{-4} M.
Actual concentration = 4 x 10^{-4} M i.e. 93% conversion to nitrite.

Table 3.2

i.e. the results seem to indicate a (virtually) total conversion of NO to HNO_2 in aqueous solution. This confirms recent work[3] showing that a 50:50 production of HNO_2 and HNO_3 does not occur, due to the competitive kinetics.

Checks indicated that the azo-dye was stable in solution (Av. 7.5% loss in absorbance after 3 days), while the level of HNO_2 in the reaction mixture was found to decline with time in solution, but only over many hours.

3.1.3. Decomposition of SNAP in distilled water

A trial run of SNAP in distilled water at 8×10^{-4} M at 25°C was performed (in triplicate) and the results gave a good first order plot for 95% of the reaction time as indicated in Table 3.3.

Time	Abs (mean)
5	0.292
10	0.471
15	0.600
20	0.691
25	0.741
35	0.830
45	0.858
60	0.878
80	0.896
100	0.875

$Abs_\infty = 0.900, \quad k_{obs} = 1.15 \times 10^{-3} \text{ s}^{-1}$

Table 3.3

However, this infinity value represents only 55% molar equivalence of SNAP conversion to HNO_2 i.e. the kinetics indicate a maximum when only half the stoichiometric equivalent of SNAP is converted to HNO_2. Further absorbance measurement of the aliquots (after three hours into the reaction) indicated a large increase i.e. further HNO_2 production was occurring within the coupled solution. Thus the gross mean of all the aliquots tested (25mins - 100mins inclusive) indicated a 71% HNO_2 production. After 3 hours 45 minutes this had increased to 74%. (Grand mean of the absorbance for all samples taken after 25 minutes of reaction = 1.178) After 22 hours the absorbance for the SNAP solution <u>in the flask</u> was a mean of 0.691 i.e. the HNO_2 levels had greatly declined.

The decomposition of SNAP in distilled water at 25°C (4×10^{-4} M) was measured using the Griess method, triplicate aliquots being taken at set intervals, diazotised and coupled according to a previously defined protocol (45 second diazotisation, 30 second coupling then absorbance measured). The mean values for each time interval

were plotted, but both 1st and 2nd order plots were very poor (Table 3.4 and Figure 3.1).

Time (mins)	Abs (mean of 3)
4	0.158
10	0.392
20	0.496
40	0.588
60	0.617
90	0.626
120	0.674
225	0.607

Table 3.4
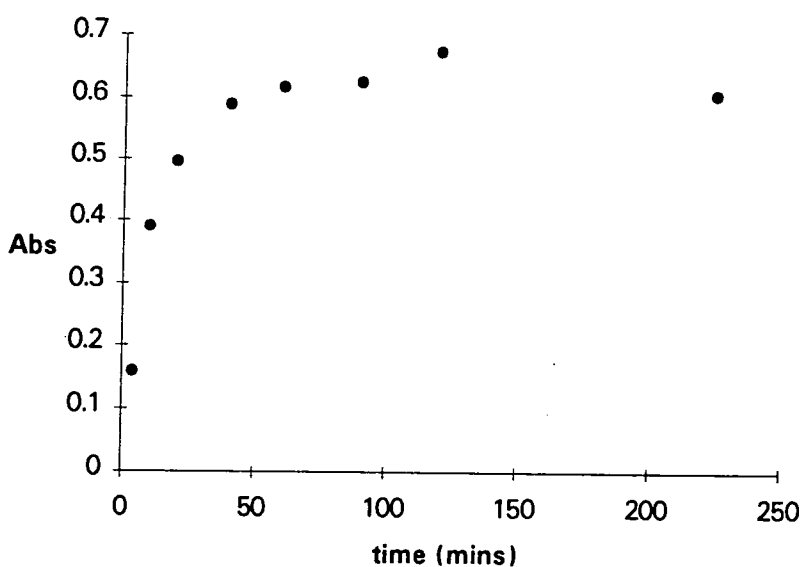
Figure 3.1

The samples were all re-checked after 21 hours of reaction time i.e. 8 x 3 = 24 samples in all. These gave a grand mean for the absorbance of 0.700 ± 0.021. This represents 84% conversion to nitrite.

3.1.4. Nitrite Production from SNAP in Different Buffers

A series of buffers were used to attempt to correlate the decomposition of SNAP (as measured by its decrease in absorbance at 340 nm), with the production of nitrite, as measured by the Griess method. The results of this work in terms of overall percentage conversion of SNAP to nitrite (at 25°C) as measured by the Griess method, for varying pHs / buffers are shown in Table 3.5

Potassium hydrogen phosphate/sodium hydroxide

pH	%conversion
6.0	91
6.9	95;92
7.0	95;95
7.9	91;92

Potassium hydrogen phthalate/sodium hydroxide

pH	%conversion
4.2	88;80
5.0	88;92
5.5	88;94
5.9	98;93

TRIS /Maleic acid/sodium hydroxide

pH	%conversion
5.0	88;89
5.6	91;91
6.0	87;92
6.8	89;87
6.9	86

Potassium hydrogen phthalate/sodium hydroxide - pH7.4
(varying concentration of solution - Standard (STD) ≈ 0.1M)

x STD	%conversion
1.0	92;94
0.5	93;92
0.25	94;95
0.125	92;89

Table 3.5

Similar to the work in distilled water, the results of SNAP decomposition in phosphate buffer were found to give poor plots.

From these results it can be seen that conversion to nitrite is usually 90% and can be much higher. It is presumed that this applies to all S-nitrosothiol decompositions, as the nature of the parent S-nitrosothiol should not affect nitrite production subsequent to decomposition. This proposition was not tested however as the only other S-nitrosothiol available in pure solid form (SNOG), was decomposed only extremely slowly under the conditions of the experiment. As generation of more labile S-nitrosothiols in acid solution in sufficient quantity would have affected buffer pH, these were not tested either. However, there seems little reason to doubt that the overwhelming product of S-nitrosothiol decomposition, apart from dimer, is nitrite anion, and not a mixture of nitrite and nitrate anions.

3.2 Effects of Buffer/pH on SNAP Decomposition (Measured by Griess Method)

A short series of runs were performed on the decomposition of SNAP in some buffers at various pH ranges, under the same conditions, measured by the Griess method (Table 3.6).

Potassium hydrogen phthalate/sodium hydroxide

pH	$10^4 \times k_{obs}$ (s^{-1})
4.15	6.5, 5.6
4.97	7.5, 8.2
5.47	19.1, 17.7
5.92	37.6, 39.5

TRIS/Maleate/sodium hydroxide

pH	$10^4 \times k_{obs}$ (s^{-1})
4.97	24.4, 22.8
5.5	14.8, 17.2
6.01	16.3, 19.0
6.80	7.5, 7.0
6.93	7.2, 8.0
7.43	4.0, 3.9

KH$_2$PO$_4$/sodium hydroxide

pH	10^4 x k_{obs} (s^{-1})
6.0	120
6.5	60.4, 58.1
7.0	28.7, 23.4
7.9	10.0, 9.5

Some of these runs were repeated, the SNAP decomposition being measured at 340nm in the UV spectrophotometer, for comparison (Table 3.7).

TRIS/Maleate/sodium hydroxide

pH	10^4 x k_{obs} (s^{-1})
4.97	25.7, 23.0
7.43	4.67, 5.05

The results indicated that the method was quite consistent for any given pH and buffer, producing good first order kinetics (but this measuring a final result of a complex series of reactions). However, the trends indicated were difficult to establish - phthalate buffer seemed to indicate increasing rate of nitrite production with increasing pH from 4 → 6, and a phosphate buffer the same trend towards a maximum rate at pH 6, but the actual rates at pH 6 seemed to be buffer dependent. This was borne out by TRIS/maleate buffer, which seemed to indicate a general rate of increase in nitrite production with decreasing pH from 7.4 → 5.0 ! The results for SNAP decomposition measured at 340 nm fitted well with the results for nitrite production with the same buffer/pH. The results overall did seem to indicate that buffer type was an important factor affecting decomposition rate i.e. pH might be subordinate to buffer salt effects in dictating SNAP decomposition rate in solution. One criticism of this was raised by the observation that in distilled water, SNAP had an observed rate constant that was comparable with the low pH data for these buffers, whereas it would have been expected to be much smaller.

3.3 Buffers as Catalysts of SNAP decomposition ?

3.3.1. SNAP Decomposition in Phosphate/NaOH Buffer at pH 7.4

It had been thought that phosphate buffer could have a catalytic effect upon the decomposition of SNAP[4] so a series of runs were devised where the SNAP concentration was kept constant but the concentration of phosphate buffer varied. The ratio of $HPO_4^{2-}:H_2PO_4^-$ was maintained by using the same ratio of KH_2PO_4 to NaOH. The buffer pH chosen was 7.4, standard for this being 50ml of 0.1M KH_2PO_4 with 40ml of 0.1M NaOH, all made up to 100ml, as shown in Table 3.8 below.

KH_2PO_4 (0.1M)	NaOH (0.1M)	Tot. Volume	Standard (STD)
50ml	40ml	100ml	STD
25ml	20ml	100ml	0.5 x STD
12.5ml	10ml	100ml	0.25 x STD
6.25ml	5ml	100ml	0.125 x STD
50ml (0.2M)	40ml (0.2M)	100ml	2 x STD
50ml (0.4M)	40ml (0.4M)	100ml	4 x STD

Table 3.8

The decomposition rates for SNAP (4×10^{-4} M in solution) in these various phosphate buffer solutions were examined using the Griess method (monitoring HNO_2 production) and by UV (monitoring SNAP decline at 340nm). The results are shown below in Table 3.9 (all k_{obs} values taken over > 95% reaction time).

[Buffer]	10^4 x k_{obs} (s^{-1})	
	540nm (Greiss)	340nm (UV)
4 x Standard	-	31.3 (0.980)
		25.6 (0.979)
2 x Standard	-	16.8 (0.962)
		15.0 (0.986)
Standard	19.2 (0.985)	22.1 (0.964)
	21.8 (0.962)	21.2 (0.976)
0.5 x Standard	37.8 (0.931)	34.1 (0.931)
	32.5 (0.962)	33.5 (0.96)
0.25 x Standard	40.8 (0.953)	41.3 (0.916)
		53.6 (0.946)
0.125 x Standard	10.2 (0.977)	6.2 (0.997)
	15.0 (0.986)	7.4 (0.972)

Table 3.9

Examination indicated that in both cases the rate of SNAP decomposition increased with <u>decreasing</u> concentration of phosphate buffer, but that at the highest concentration, the reaction increased again, i.e. the slowest rate was found at the lowest concentration and the fastest at 0.25 x Standard concentration ! The observed decomposition did fit first order kinetics reasonably well, graphical plots indicating a faster (than theoretically expected) reaction in the later phase. This seemed to indicate that decomposition was enhanced by some factor(s).

The results appeared to indicate that phosphate buffer was <u>not</u> catalytic with respect to SNAP decomposition at pH 7.4. Given this case, it would have been expected that the decomposition rate was reasonably constant throughout the concentration range. The fact that the observed rate constant increased with increasing concentration, then decreased, then increased again (as shown by both methods) indicates complicating factors. It could be simply that the values obtained are inaccurate due to poor fit to first order kinetics, despite the reasonable correlation coefficients, or that indeed unknown factors are involved. A possible explanation for the decrease in k_{obs} at lowest dilution could be that the buffer capacity has been overwhelmed by the acid production from the reaction, lowering the pH to a level where SNAP decomposition is slower. Unfortunately, no check was made of this.

3.3.2. SNAP decomposition in TRIS/HCl buffer at pH 7.4

The decomposition behaviour of SNAP in a commonly-used biological buffer, tris(hydroxymethyl) aminomethane/HCl (TRIS/HCl), was examined at pH 7.4, to compare the results with those obtained by workers at St Andrews University - it had been noticed in contacts between our two research groups that their values for the half-lives of SNAP in buffers were considerably lower than those obtained by ourselves. (The St Andrews group were primarily interested in the use of SNAP as an NO source in biological systems, using it at physiological pH (7.4).)

The decomposition of SNAP was examined, using varying concentrations of TRIS/HCl i.e. Standard (50ml 0.1M TRIS + 42ml 0.1M HCl → 100ml) and variations thereof (x 0.125, x 0.25, x 0.5, x 2). SNAP was added as a concentrated solution in methanol and its decay at 340nm measured. The results showed that a half order plot gave a much better fit than a first order one, in terms of the correlation coefficient obtained i.e. the plots were found to conform much better to <u>half</u> <u>order</u> kinetics - a plot of $2(A_\infty - A_t)^{0.5}$ against time gave a good straight-line fit over the reaction time. The two analyses are shown below in Tables 3.10 and 3.11.

First order analysis

Absorbance at 340nm   TRIS/HCl pH 7.4 buffer

Conc^n (x STD)	10^4 x k_{obs} (s^{-1})
2	2.0 (0.816); 2.55 (0.835)
1	4.96 (0.991); 6.15 (0.967); 8.47 (0.961); 7.12 (0.967)
0.5	19.5 (0.959); 18.8 (0.974); 16.6 (0.978)
0.25	23.5 (0.975); 24.2 (0.973); 25.0 (0.985)
0.125	12.8 (0.908); 12.8 (0.913); 9.4 (0.919)

Table 3.10

Half order analysis

Absorbance at 340nm   TRIS/HCl pH 7.4 buffer

Conc^n (x STD)	10^4 x k_{obs} ($Abs^{\frac{1}{2}}$ s^{-1})
2	0.65 (1.0); 0.79 (0.999)
1	2.15 (0.999); 2.41 (0.997); 3.16 (0.998); 2.79 (0.997)
0.5	6.56 (0.997); 7.09 (0.998); 6.59 (0.997)
0.25	8.29 (0.998); 9.16 (0.996); 8.50 (0.998)
0.125	3.95 (0.806); 3.46 (0.829); 2.72 (0.917)

Table 3.11

[It can be derived that $2([A]_t - [A]_\infty)^{1/2} - 2([A]_0 - [A]_\infty)^{1/2} = -k_0 t$

A plot of $2([A]_t - [A]_\infty)^{1/2}$ against time (t) gives a slope of $-k_0$ and an intercept of $-2([A]_0 - [A]_\infty)^{1/2}$ Half order kinetics are unusual and are taken to be indicative of reactions whose mechanisms involve free-radicals.]

As a crude measure, the half-life in standard buffer was found to be approximately 25 minutes. The St Andrews group found a half-life under these conditions of approximately 3 hours ! A sample of SNOG under the same conditions was found to decompose at a very slow rate - after 2 hours the absorbance at 335nm (λ_{max}) had decreased only by 5%.

The first order kinetic analysis was not of a high correlation, even at standard buffer strength and declined sharply with increase or decrease in concentration. The (very) general trend was that decreasing buffer concentration increased k_{obs} until the lowest concentration was reached. The half order kinetic analysis was very well correlated to the data except at the lowest concentration of buffer. Again, the general trend was the same as that indicated by first order analysis. The change at lowest buffer concentration could be due to the pH altering upon the addition of SNAP, due to lack of buffering capacity. The elementary check of the effect upon pH of SNAP addition was not done. However, from the results it did not seem that there was any basis for the view that either phosphate or TRIS/HCl buffer had any catalytic effect, yet the results still differed greatly from work done (ostensibly under identical conditions) by the St Andrews group, where SNAP decomposition was found to be much slower.

3.3.3. SNAP decomposition in TRIS/Maleic Acid/ NaOH buffer at low pH

The decomposition of SNAP, measured at 340nm at 4×10^{-4} M in standard TRIS/Maleate/NaOH buffer was examined.

Added (to 250ml) NaOH (ml)	pH of buffer (TRIS/Maleate)	$10^4 \times k_{obs}$ (s^{-1})
NONE	3.9	16.3 (0.998); 17.5 (0.999)
1.0	4.2	30.8 (0.997)
2.0	4.4	34.2 (1.0); 35.0 (1.0)
3.0	4.6	57.5 (1.0); 51.5 (1.0)

Table 3.12

The effect on the pH of the solution of SNAP addition was examined in this instance. Addition of SNAP in all cases caused no more than a drop of 0.2 pH units by the end of the reaction time.

Typically, 62.5ml of 0.2M TRIS/Maleate solution was made up to 250ml, with the inclusion of (say) 1.0ml NaOH 0.19M solution to give a pH 4.17 solution. At the end of 60 minutes, the pH had fallen to 3.94. The kinetics were an extremely good fit to first order analysis. The general trend seemed to be that addition of only a very small quantity of NaOH caused a rapid rise in k_{obs} (SNAP decomposition). At the time it seemed unusual that such a rapid change in the observed rate of decomposition should occur over such a small pH change. It can now be explained in terms of the significant increase in Cu^{2+} ions which occurs upon the addition of even a small quantity of sodium hydroxide solution.

3.4 Decomposition of SNAP in DGA/NaOH Buffer

Some variables regarding SNAP decomposition in 2,2-dimethylglutaric acid (DGA)/NaOH buffer were examined.

3.4.1. Varying pH

SNAP decomposition in DGA/NaOH buffer at varying pH was measured at 340 nm using 1,4-dioxan as SNAP solvent, 0.1 ml being added to 2.4 ml of buffer, all at 25°C, SNAP in-cell concentration being 4×10^{-4} M. The results are shown below in Table 3.13.

	SNAP in dioxan ([SNAP] = 4×10^{-4} M) $10^3 \times k_{obs}$ (Abs$^{1/2}$ s^{-1})	Correlation coeff.
DGA pH 7.5	3.21	(0.950)
	4.35	(0.974)
	4.88	(0.987)
DGA pH 7.0	5.42	(0.984)
	5.64	(0.989)
	5.68	(0.967)
	5.42	(0.976)
	5.30	(0.991)
DGA pH 6.1	10.20	(0.971)
	11.10	(0.984)
	10.72	(0.984)
	10.14	(0.966)
DGA pH 5.0	4.20	(0.930)
	4.22	(0.925)
	4.38	(0.926)
	$10^3 \times$ (s^{-1})	
DGA pH 4.0	3.5	(0.994)
	3.6	(0.988)
	3.7	(0.993)
Dry SNAP in pH 4.0	3.8	(0.999)

Table 3.13

It can be seen that there is an increase in decomposition with decreasing pH, down to pH 6, the kinetics appearing to fit half order reasonably well according to the correlation coefficients, but below this pH level, the kinetics change. At pH 5.0, there is poor correlation to both half and first order kinetics, and they become more

similar to first order kinetics at pH 4.0. Clearly, the reality is that complex decomposition is occurring which has some unknown relation to pH.

3.4.2. SNAP as a dry solid

SNAP was dissolved directly in the buffer as the dry solid and its decomposition at 340nm examined, at 4×10^{-4} M in cell, in pH 7.0 buffer. The results are as shown in Table 3.14.

SNAP (dry) 4×10^{-4} M DGA pH 7.0	
$10^3 \times k_{obs}$ (Abs$^{1/2}$ s^{-1})	Correl.
1.58	(0.999)
1.67	(0.999)
1.70	(0.999)
1.67	(0.999)
1.56	(0.999)
1.79	(0.999)
1.66	(0.999)

Mean $= 1.66 \times 10^{-3} \pm 0.36$

Table 3.14

It can be seen that an excellent fit to half order kinetics was obtained, but the k_{obs} values, while being consistent within the group, (as are the comparable dioxan results) show a significant difference from the latter, being definitely lower.

The effect is presumably to do with the dioxan solvent.

3.4.3. Presence of Oxygen

The possibility of dissolved oxygen having an effect was examined by using sonication and water pump vacuuming to remove air, followed by bubbling with nitrogen, for ten minutes and repeating the procedure twice. For dioxan, the results were as shown in Table 3.15, using SNAP at 5×10^{-4} M in-cell, in DGA/NaOH pH 7.4 buffer.

	$10^3 \times k_{obs}$ (Abs$^{1/2}$ s^{-1})	Correlation
Dioxan, aerated	5.07	(0.923)
	4.63	(0.910)
	4.79	(0.904)
	4.54	(0.908)
Dioxan, deoxygenated	4.59	(0.932)
	4.42	(0.921)
	4.48	(0.929)

Table 3.15

Essentially, there appeared to be no difference between the two sets of runs. When this experiment was repeated using SNAP as a dry solid in buffer, but under otherwise identical conditions, the results were the same, i.e. oxygen had no apparent effect and although in this case the traces gave poor correlation to both half and first order kinetics, the traces were effectively identical for all runs.

3.4.4. Parallel Study

Colleagues at St Andrews University were known to have similar problems to ourselves regarding the various anomalies of SNAP decomposition in buffer systems, which they were using for work of a biological nature (see Appendix A), at 30°C. To allow a valid comparison between results a sample of SNAP prepared in the laboratory in Durham was divided and one half taken to St Andrews. Using this SNAP in DGA pH 7.4 buffer as a dry solid at 5 x 10^{-4} M in-cell, under normal aerated conditions, the results obtained were as shown in Table 3.16

SNAP, DRY SOLID, 5 x 10^{-4} M, DGA/NaOH pH 7.4 AERATED BUFFER @ 25°C

<u>Durham</u> $10^3 \times k_{obs}$ (Abs$^{1/2}$ s^{-1})

7.50 (0.992); 7.78 (0.992); 8.37 (0.994); 6.09 (0.995); 7.45 (0.997)
7.18 (0.997); 7.29 (0.995)

<u>St Andrews</u> 0.137 (0.963); 0.177 (0.985); 0.116 (0.965); 0.159 (0.972);
0.128 (0.971)

Results from St Andrews courtesy of Stuart Askew[5].   **Table 3.16**

It is very evident that a great difference (approximately 20x) exists between the two sets of results. The only differences possible were in the DGA and NaOH used to make the buffer and the water used. Although puzzling at the time, this work did confirm that the differences in repeated decomposition rates/half-lives for SNAP between the two groups were not just a matter of interpretation and/or differences in SNAP sample or technique. With hindsight, the difference could be seen to be due to the better quality of distilled water used at St Andrews, i.e. water containing a lot less Cu^{2+} ion.

3.4.5. Presence of free thiol

The presence of unconverted NAP in SNAP (i.e. free thiol) might have been expected to have an effect upon SNAP decomposition. This was tested by adding approximately 10% NAP to dry SNAP dissolved in DGA/NaOH pH 7.4 buffer, at 4×10^{-4} M in-cell. However, the decomposition appeared to be unaffected and this was not investigated further.

3.4.6 Summary

The effect of the presence of SNAP dimer was <u>not</u> investigated. This was an unfortunate oversight, but no excuses can be made as earlier work on SNAP purity (using TLC) had indicated that a significant minor contaminant of the solid SNAP was the dimer (see Appendix B). Ironically, the same work had also shown that (unconverted) NAP was <u>not</u> a minor contaminant.

3.5 Dissolution of SNAP in Buffer

A brief examination of the dissolution of SNAP was performed. It was felt that the SNAP might precipitate out when added to buffer, particularly at higher concentrations. SNAP was dissolved in 5 ml Analar methanol at varying concentrations and 0.1 ml added to 2.4 ml of DGA/NaOH buffer pH 7.0 at 25°C, to produce a series of in-cell concentrations of 2, 4, 8, 16 and 32 x 10^{-4} M SNAP. The decomposition of SNAP was followed at 340nm (See Figure 3.2).
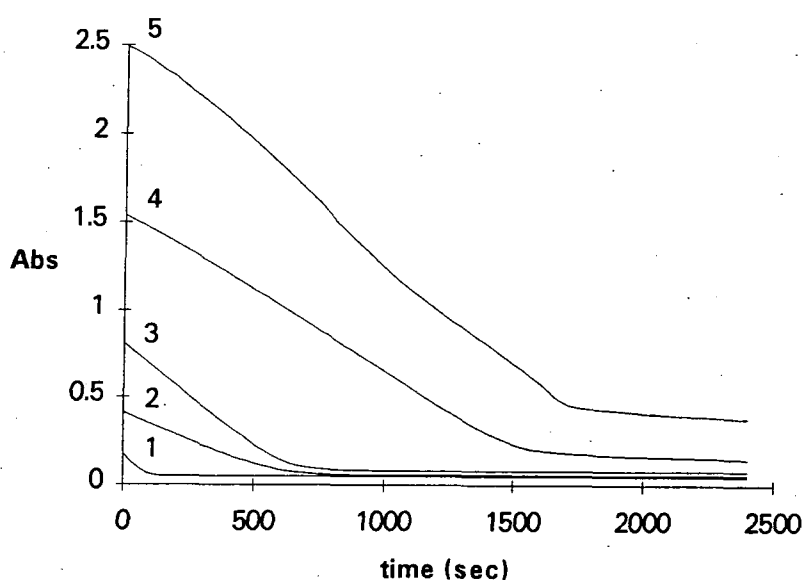
1. SNAP at 2 x 10^{-4} M   2. SNAP at 4 x 10^{-4} M
3. SNAP at 8 x 10^{-4} M   4. SNAP at 16 x 10^{-4} M
5. SNAP at 32 x 10^{-4} M

Figure 3.2

The traces gave very good correlations for half order kinetics (See Table 3.17).

	2	4	8	16	32
$10^3 \times k_{obs}$ (Abs$^{1/2}$s^{-1})	4.95 (0.998)	1.55 (0.997)	2.05 (0.994)	1.23 (0.991)	1.25 (0.994)
	5.80 (0.999)	1.50 (0.997)	2.17 (0.995)	1.24 (0.992)	1.10 (0.993)
	4.60 (0.995)	1.47 (0.997)	1.88 (0.995)	1.15 (0.992)	1.02 (0.987)
Mean	5.12 ± 0.05	1.51 ± 0.03	2.03 0.12	1.21 ± 0.04	1.12 ± 0.04

Table 3.17

The trend in the results is that above the smallest concentration, the k_{obs} value seems to be more or less constant i.e. SNAP decomposition becomes independent of concentration. In fact, the traces do appear similar to those obeying zero order kinetics. If the slopes of the traces are read directly from the graphs i.e. in terms of absorbance unit change per second, the following results are obtained (Table 3.18).

10^4 x [SNAP] (M)	Slope (Abs change/sec) (x 10^3)	Mean
2	1.23, 1.35, 1.17	1.25 $\pm$ 0.08
4	0.61, 0.61, 0.58	0.60 $\pm$ 0.01
8	1.20, 1.09, 1.16	1.15 $\pm$ 0.05
16	0.96, 0.97 0.90	0.94 $\pm$ 0.03
32	1.38, 1.31, 1.23	1.31 $\pm$ 0.06

Table 3.18

No pattern is evident and the rate of decomposition of the SNAP appears to be more or less constant no matter what the SNAP concentration. It would be expected that k_{obs} would be smaller for these concentrations where the SNAP had precipitated out of solution, before re-dissolving in the buffer, but this is clearly not the case.

In the light of the knowledge of the Cu^{2+} catalysis, it might be expected that the observed rates of decomposition would be very similar, particularly at higher SNAP concentrations. The intrinsic Cu^{2+} concentration in DGA/NaOH pH 7.0 buffer is low and it may be the case that the catalytic decomposition mechanism has become saturated i.e. Cu^{2+} concentration/activity has become a limiting factor.

3.6 Decomposition of SNAP in NaOH/Distilled Water

3.6.1. Effect of Initial pH upon SNAP Decomposition

i) Introduction

An attempt was made to examine the decomposition of SNAP (as a solution in methanol) in distilled water at 25°C. It was hoped to obtain a solution of sodium hydroxide that would be just sufficient to neutralise the SNAP in solution, so that the initial conditions would be pH 7. A stock solution of sodium hydroxide in distilled water was produced which would approximate to this equivalence with SNAP. This consisted of 1.4ml of exactly 0.1M sodium hydroxide made up to 100ml with distilled water. This 100ml flask of dilute sodium hydroxide solution was used as stock. A check was made on the response time of the pH meter used. Addition of 5ml of 0.1M HCl to 5ml of 0.1M NaOH, pH 12.9 produced a change to pH 1.8 in 2 seconds. This was repeated, the pH changing to 1.9 in one second, pH 1.8 in 2 seconds and steady at pH 1.8 after 60 seconds, i.e. the response time of the electrode to a very wide and rapid pH change was very good. The SNAP/methanol solution was kept completely covered in aluminium foil and was found to be very stable (13% decomposition in 41 hours at room temperature as measured by absorbance decline at 340nm).

A series of measurements of pH fall with time, for various proportions of stock solution and distilled water with a fixed quantity of SNAP in pure methanol, were performed. Typically, a constant 0.6ml of SNAP/methanol solution (0.0220g in 5ml of methanol, equivalent to 1×10^{-3} M SNAP in the final solution) was added to a series of dilutions of the stock solution, the final volume always being 12.0ml. The increments were as shown in Table 3.19.

SNAP/methanol (ml)	NaOH stock (ml)	Distilled water (ml)	Final vol. (ml)
0.6	0	11.4	12.0
0.6	6.6	4.8	12.0
0.6	7.8	3.6	12.0
0.6	9.0	2.4	12.0
0.6	10.2	1.2	12.0
0.6	11.4	0	12.0

Table 3.19

The 12.0ml volume was sufficiently large to allow a pH probe tip to be fully immersed in the reaction solution, which was in turn immersed in a 25°C water bath, as were all the reaction solutions prior to mixing. Solutions were mixed and allowed to equilibrate before addition of the SNAP solution, to minimise temperature changes. The runs were done at least three times for each strength of NaOH mixture.

ii) Results

Typical results are given below (Tables 3.20 - 3.25 and Figures 3.3 - 3.5).

0.6ml SNAP/methanol + 7.8ml NaOH/water + 3.6ml distilled water.

Initial pH of solution = 11.05

Time (sec)	pH	Time (sec)	pH	Time (sec)	pH	Time (sec)	pH
0		15	4.15	30	4.02	45	3.95
60	3.91	75	3.88	90	3.87	105	3.85
120	3.83	135	3.82	150	3.81	165	3.80
180	3.80	195	3.79	210	3.79	225	3.78
240	3.78	300	3.76	360	3.75	420	3.75

Table 3.20
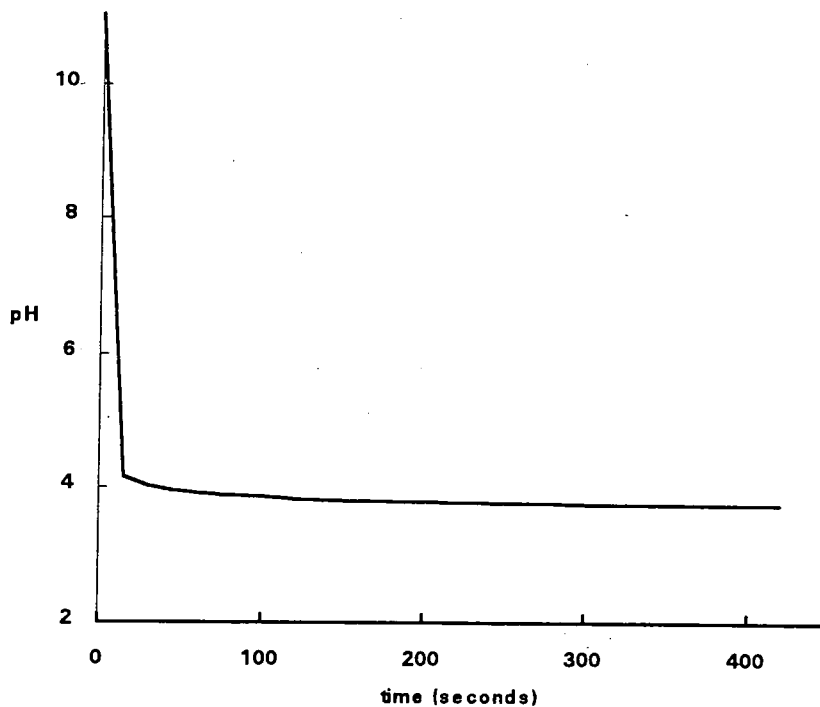
Figure 3.3

0.6ml SNAP/methanol + 10.2ml NaOH/water + 1.2ml distilled water.
Initial pH of solution = 11.18

Time (sec)	pH	Time (sec)	pH	Time (sec)	pH	Time (sec)	pH
0		15	9.48	30		45	
60	9.33	120	9.11	180	8.71	195	8.53
210	8.27	225	7.87	240	7.33	255	6.71
270	6.12	285	5.57	300	5.16	315	4.83
330	4.60	345	4.45	360	4.35	375	4.28
390	4.24	405	4.20	420	4.18	480	4.13
540	4.09	600	4.07	900	4.00	1200	3.96

Table 3.21

Initial pH of solution = 11.13

Time (sec)	pH	Time (sec)	pH	Time (sec)	pH	Time (sec)	pH
0		15	8.26	30	7.81	45	6.52
60	5.26	75	4.7	90	4.54	105	
120	4.30	180	4.09	240	4.02	300	3.98

Table 3.22

68

Time (sec)	pH	Time (sec)	pH	Time (sec)	pH	Time (sec)	pH
0		15	8.71	30	8.41	45	8.10
60	7.51	75	6.29	90	5.42	105	4.94
120	4.67	135	4.50	150	4.40	165	4.33
180	4.26	195	4.24	210	4.22	225	4.20
240	4.17	300	4.13	360	4.10	420	4.07
480	4.05	540	4.04	600	4.03		

Table 3.23
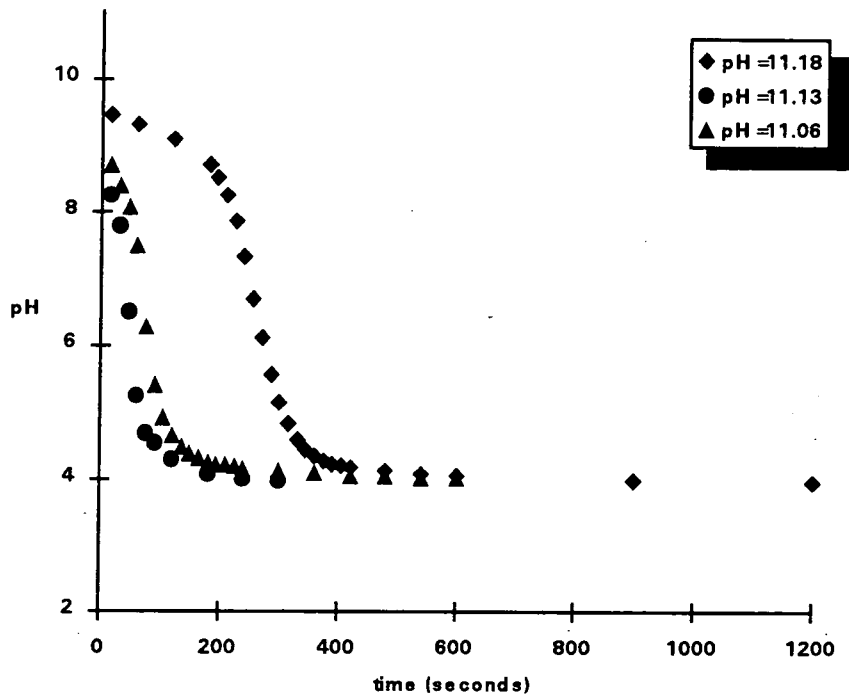
Figure 3.4

0.6ml SNAP/methanol + 11.4ml NaOH/water

Initial pH of solution = 11.32

Time (sec)	pH	Time (sec)	pH	Time (sec)	pH	Time (sec)	pH
0		15	9.81	60	9.62	120	9.49
180	9.38	240	9.23	300	8.96	360	7.93
375	7.65	390	7.38	405	7.14	420	6.90
435	6.67	450	6.45	465	6.24	480	5.99
495	5.69	510	5.39	525	5.07	540	4.75
555	4.45	570	4.30	585	4.22	600	4.18
660	4.12	720	4.09	780	4.07	840	4.06
900	4.05						

Table 3.24

Initial pH of solution = 11.28

Time (sec)	pH	Time (sec)	pH	Time (sec)	pH	Time (sec)	pH
0		15	10.27	60	10.26	120	10.25
180	10.18	240	10.13	300	10.09	360	10.04
420	9.98	480	9.89	540	9.79	600	9.66
660	9.48	720	9.27	780	9.00	840	8.71
900	8.26	915	6.34	930	7.80	945	7.45
960	7.01	975	4.45	990	5.51	1005	4.92
1020	4.60	1035	4.25	1050	4.38	1065	4.34
1080	4.32	1140		1200	4.22	1500	4.15

Table 3.25
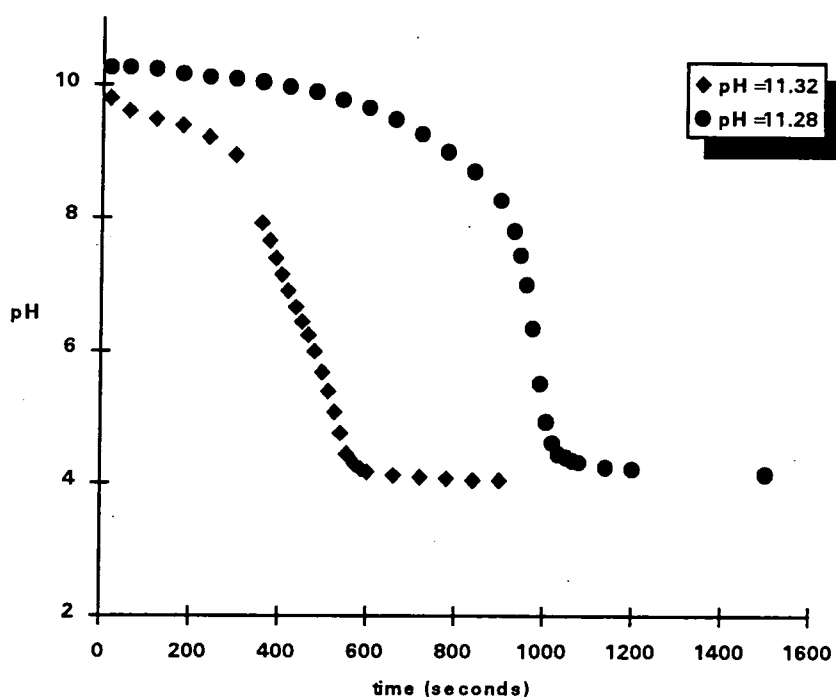
Figure 3.5

To check whether the pH changes were associated with sunlight (bright sunlight was present in the laboratory), the whole probe and sample tube were covered in aluminium foil for this experimental run, shown in Table 3.26 and Figure 3.6 below.

0.6ml SNAP/methanol + 11.4ml NaOH/water

Initial pH of solution = 11.30

Time (sec)	pH	Time (sec)	pH	Time (sec)	pH	Time (sec)	pH
0		15	9.49	60	9.45	120	9.43
180	9.32	240	9.30	300	9.29	600	9.19
900	8.96	1020	8.6	1080	8.27	1140	7.79
1170	7.51	1200	7.2	1215	7.02	1230	6.81
1245	6.67	1260	6.5	1275	6.33	1290	6.19
1305	6.04	1320	5.9	1335	5.76	1350	5.61
1365	5.47	1380	5.32	1440	4.81	1500	4.46
1560	4.26	1620	4.17	1680	4.13	1740	4.11
1800	4.09						

Table 3.26
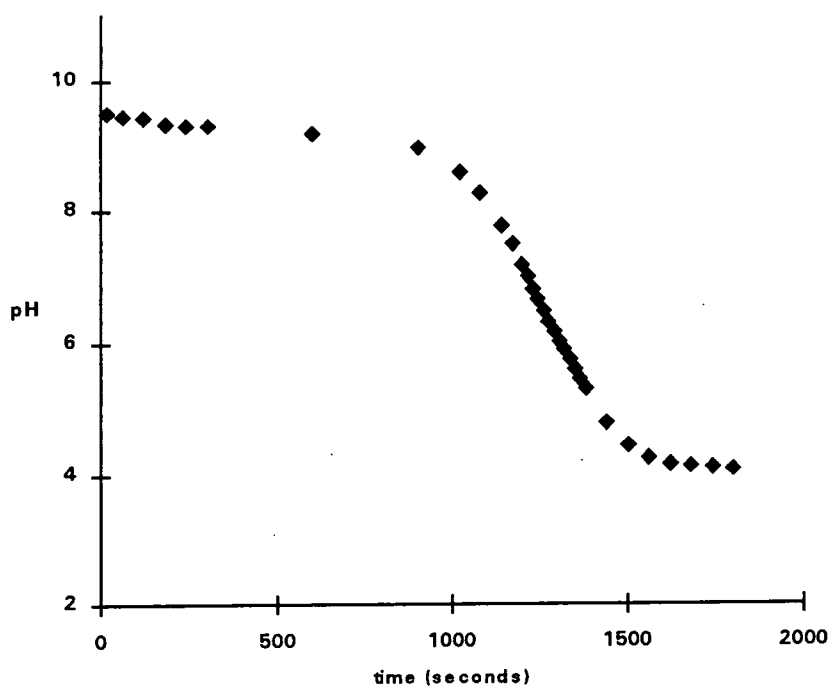
Figure 3.6

iii) Discussion

It was found that with no sodium hydroxide solution, the pH plunged immediately to 3.1, representing the acidic nature of SNAP when added to distilled water (initial pH of water = 6.3). With increasing proportions of sodium hydroxide solution, no change occurred, (beyond the final pH becoming 3.7 e.g. as in the graph for 7.8ml

sodium hydroxide) until 10.2ml were added. At this proportion, the SNAP solution was <u>just</u> neutralised, so that the pH of the solution changed from >11.0 to 8 or 9, before falling after a varying time to pH 4. With increased sodium hydroxide (i.e. 11.4ml), the delay before decline to pH 4 was even more prolonged (see graphs).

It was found that the delay before rapid decline to pH 4 depended upon the precise quantity of sodium hydroxide added. Thus the greater the initial drop from the original alkaline pH (11+) of the sodium hydroxide solution, the faster the onset of rapid decline to pH 4. As all of the SNAP had been neutralised by the sodium hydroxide, any pH fall must be due to the products of SNAP decomposition (nitrous acid). The sensitivity to sodium hydroxide concentration was demonstrated by the fact that leaving the sodium hydroxide solution exposed to air during the experiment caused a progressive decrease in the time taken before pH decline, over a series of experiments, presumably due to absorption of carbon dioxide from the atmosphere. Keeping the sodium hydroxide solution in sealed flasks prevented this.

As the work was performed in bright sunlight, a check was performed to determine if this had any effect. Keeping the sample bottle and pH probe covered in aluminium foil did slow down the reaction - the onset of rapid decline was considerably delayed in comparison to a sample which started at the same initial pH of 9.5 (16 minutes compared to 3 minutes). See graphs above.

3.6.2. Absorbance and pH decline with SNAP

A check was made upon the decomposition of SNAP, as indicated directly by reduction in absorbance at 340nm and indirectly by reduction in pH, with time. An initial run was performed, with SNAP solution added to sodium hydroxide solution known to be just sufficient to neutralise the added SNAP. After mixing (using the pH probe !) a quantity was transferred to a pre-warmed cuvette and the absorbance measured at 340nm. The results appeared to indicate, as might be expected, a time-lag between the absorbance decline and pH decline, the former preceding the latter.

A further experiment was performed, with precise time-keeping made via a clock started at the moment of addition and mixing of the SNAP/methanol solution to the sodium hydroxide solution in the large sample bottle in the water bath. A cuvette warmed in the water bath was filled and note taken of the exact time of first data capture of absorbance. The pH was measured at +120 seconds reaction time and the absorbance at +70 seconds reaction time. The results are shown below in Table 3.27, 3.28 and Figure 3.7. (—— = pH   ----- = Absorbance)

Time (sec)	Abs_{340}	Time (sec)	Abs_{340}	Time (sec)	Abs_{340}
0	0.403	630	0.238	1260	0.173
30	0.407	660	0.231	1320	0.168
60	0.407	690	0.227	1380	0.167
90	0.407	720	0.221	1440	0.163
150	0.401	750	0.216	1500	0.159
180	0.393	780	0.211	1560	0.156
210	0.386	810	0.209	1620	0.154
240	0.377	840	0.204	1680	0.152
270	0.370	870	0.202	1740	0.150
300	0.358	900	0.199	1800	0.146
330	0.346	930	0.195	1860	0.144
360	0.335	960	0.193	1920	0.141
390	0.323	990	0.190	1980	0.137
420	0.308	1020	0.187		
450	0.299	1050	0.185		
480	0.286	1080	0.183		
510	0.273	1110	0.180		
540	0.262	1140	0.180		
570	0.254	1170	0.177		
600	0.246	1200	0.176		

Table 3.27

| Time (sec)	pH	Time (sec)	pH	Time (sec)	pH
0	9.5	630	8.69	1260	5.11
30	10.06	660	8.55	1320	5.01
60	10.07	690	8.40	1380	4.93
90	10.06	720	8.22	1440	4.85
150	10.04	750	8.00	1500	4.79
180	10.01	780	7.80	1560	4.73
210	9.97	810	7.57	1620	4.68
240	9.93	840	7.33	1680	4.64
270	9.88	870	7.08	1740	4.60
300	9.84	900	6.84	1800	4.56
330	9.80	930	6.61	2100	4.42
360	9.74	960	6.40	2400	4.33
390	9.62	990	6.20		
420	9.48	1020	6.01		
450	9.36	1050	5.84		
480	9.26	1080	5.69		
510	9.15	1110	5.55		
540	9.04	1140	5.43		
570	8.92	1170	5.34		
600	8.81	1200	5.25		

Table 3.28
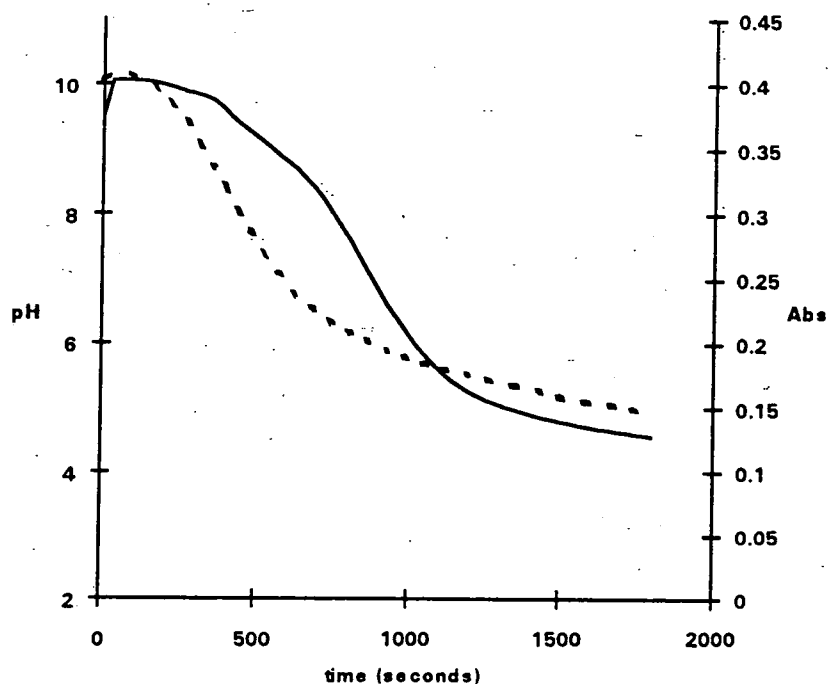
Figure 3.7

It can be seen from the graph that a distinct lag-time of approximately four minutes is present, between the start of decline in absorbance at 340nm and the corresponding

74

fall in pH. This lag can be explained as being the time required for production of nitrous acid (to neutralise the excess sodium hydroxide) after initial decomposition of RSNO (SNAP). The complex series of reactions, previously outlined, would require a reasonable time scale, neutralisation itself being taken as instantaneous. The final decline is very slow as both pH and absorbance take several hours (+5 hours) to reach a steady value.

An explanation can now be given for the above results. It can be assumed that the SNAP is decomposing catalytically due to the presence of trace amounts of copper in the water supply <u>and</u> the sodium hydroxide (see chapter 4). This catalysis will be very slow at pH 9 - 10, as the copper will be largely unavailable for reaction due to complex formation with OH^-. As SNAP does decompose however, it generates protons (nitrous acid) which, by neutralising excess OH^- ions, lower the pH and produce a cascade effect as more and more copper(II) ions become available for reaction as the pH is lowered. This results in the rapid decline phase for SNAP decomposition (and pH lowering) until acid pH is reached. The reaction will then slow down as the SNAP concentration is greatly decreased and the acid pH inhibits further decomposition, producing an overall sigmoidal curve. The effect of strong sunlight may be most pronounced at the margins of reactivity i.e. in the initial lag phase, where any slight photolytic decomposition of SNAP (again producing protons) will help to speed up the induction of the rapid decline phase. Hence exclusion of light should delay decline for any given initial pH, in the 9-10 range.

3.6.3. Effect of Nitrogen, Oxygen and Carbon Dioxide

An attempt was made to determine whether the presence of nitrogen, oxygen or carbon dioxide had any effect upon the decomposition of SNAP in the sodium hydroxide solution. The stock sodium hydroxide solution was thoroughly degassed by sonication and vacuuming, then pure nitrogen or oxygen were bubbled through, or carbon dioxide added as dry ice. As expected, the solution with carbon dioxide

produced rapid decomposition, for reasons given above, but there was little discernible difference between solutions containing nitrogen or oxygen. The results would appear to suggest that oxygen does not play a part in initiating SNAP decomposition, although the results can be criticised as being too small a sample to allow valid interpretation. (See Table 3.29.)

	Nitrogen	Oxygen	Carbon dioxide
$10^3 \times k_{obs}$ (s^{-1})	5.7 (0.996) 6.6 (0.993) 5.7 (0.995) 6.0 (0.996)	5.0 (0.996) 5.4 (0.995) 6.3 (0.992) 5.1 (0.996) 5.9 (0.994)	12.3 (0.976) 12.6 (0.974) 12.1 (0.976) 11.6 (0.977) 11.7 (0.974) 11.9 (0.974)
$10^3 \times$ Mean (s^{-1})	6.0 $\pm$ 0.4	5.5 $\pm$ 0.5	12.0 $\pm$ 0.3

Table 3.29

3.7 Anomalous Decomposition of SNAC

During experiments to examine the decomposition of various S-nirosothiols in DGA/NaOH buffer, pH 7.4, the relatively slow decomposition of SNOG, SNAC and SNOCAP at 335nm was examined over a longer period. An attempt was made to see if bromide or thiocyanate could catalyse the decomposition of these stable S-nitrosothiols. No noticeable difference was seen when concentrations of 1:1 and even 100: 1 stoichiometry of 'catalyst' to SNOCAP were used. A check was then made of the decomposition of all three S-nitrosothiols overnight. With SNOG and SNOCAP it was found that the very slow, steady decline continued, even after five days, as shown in Table 3.30 below

RSNO	Absorbance at 335nm		
	72 hours	94 hours	137hours
SNOCAP	0.733	0.730	0.716
SNOG	0.755	0.744	0.720

Table 3.30

In all cases, the S-nitrosothiols were added as the freshly-prepared, dry solid to the buffer, each being prepared by the same general method, with slight variation, as indicated in Chapter 6. With SNAC, the initial steady decline occurred, but then a phase of rapid decline occurred.

This was found to obey first order kinetics with good correlation. With DGA/NaOH buffer, pH 4.0, a steady, regular decline occurred, while with Borax/NaOH buffer, pH 10.0, a rapid decline occurred immediately. The latter bore a strong resemblance to the curves of SNAP decomposition at pH 7.4 ! A check was made to see if the amount of solid SNAC initially added affected the delay time to the start of the decline phase. This was not the case. There appeared

to be no link between initial absorbance value and the start of rapid decline, or of the value for k_{obs} for the decline phase. (See Table 3.31 below).

Initial Abs. value	Start of decline (mins)	10^4 x k_{obs} (s^{-1})	Correl.
0.43	130	2.23 ± 0.01	0.986
0.57	210	1.46 ± 0.00	0.979
0.63	250	1.22 ± 0.00	0.986
0.93	180	2.15 ± 0.01	0.972
1.22	220	0.54 ± 0.00	0.984
0.89	310	0.48 ± 0.00	0.988

Table 3.31

It will be noticed that no link can be made between the time for start of decline and the subsequent k_{obs} value. It should be noted that while SNOCAP and SNOG can be prepared as dry solids of quite high purity (>95%), the SNAC used was always approximately 35% pure i.e. a large amount of dimer and possibly some unchanged free thiol existed in the sample, as well as traces of the nitrite. These compounds could have some effect upon the stability of the SNAC. Subsequent work using SNAC generated in acid has shown that when used in this (relatively pure) state it does not undergo the sudden rapid decline observed here.

With SNAP, addition of free thiol (NAP) to a solution in DGA/NaOH buffer, pH 7.4, did not appear to alter the decomposition rate, nor did addition (10%) of SNAP dimer. This was not performed on SNAC, so the reasons for its anomalous decomposition must remain conjecture.

3.8 Analysis of SNAP Decomposition Products

Although it is generally assumed that the products of S-nitrosothiol decomposition are always the dimer[6], it was thought necessary to check this as far as possible, as well as examining any contaminants present in the dry SNAP samples prepared.

3.8.1. UV Spectra

The products of SNAP decomposition in distilled water were examined by u.v. spectrophotometry. SNAP at a concentration of 1×10^{-4} M was used, as this allowed any decomposition products to remain at a sufficiently low absorbance level to enable accurate scanning. The SNAP solution was left in the dark at room temperature for three days and then its spectrum compared with three day old solutions (in distilled water) of

a) sodium nitrite (1×10^{-4} M)
b) sodium nitrate (1×10^{-4} M)
c) authentic NAP dimer (0.5×10^{-4} M)

The dimer is formed as 1 mole from 2 moles of SNAP, and was produced by the method described by Field[7]. From the traces below it can be seen that the u.v. spectrum of SNAP decomposition is compatible with any and all of the u.v. spectra of the putative products (Figure 3.8).
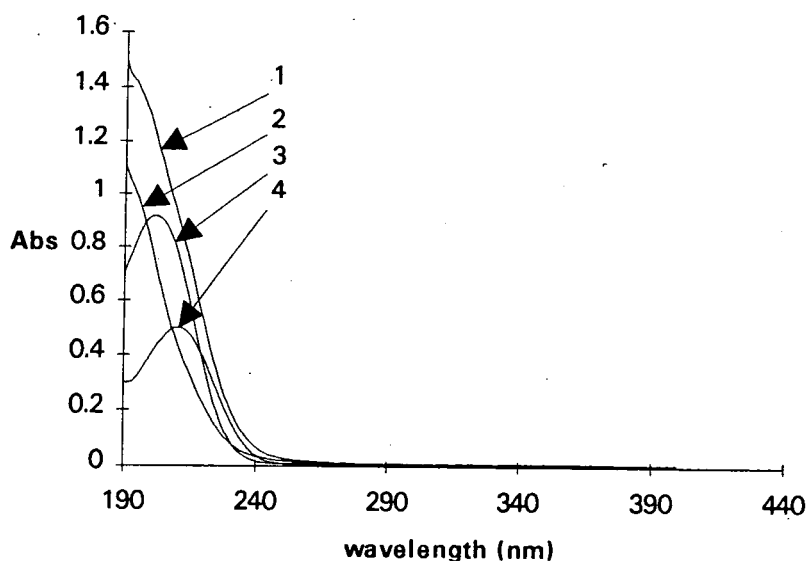

Figure 3.8   1 = SNAP   2 = Dimer   3 = Nitrite   4 = Nitrate

3.8.2. Thin Layer Chromatography (TLC)

Contaminants of the SNAP as a dry solid were thought to be possible, and this was examined by TLC. After some experimentation, during which it was found that dichloromethane alone and dichloromethane/acetonitrile (1:1) were too polar, it was found that Analar dichloromethane/ether (1:1) gave a good separation between SNAP and NAP. Running SNAP alone, NAP alone, and a mixture of the two showed that NAP was not a discernible contaminant of the SNAP. It can be assumed therefore that the nitrosation of the NAP goes to completion during the synthesis of SNAP. (N.B. The TLC must be run in the total absence of light, using aluminium foil. The SNAP spot must be highlighted in pencil before using a u.v. lamp to examine the TLC as its green spot disappears within seconds of using the u.v. lamp on the TLC sheet.)

The possibility of NAP dimer as a contaminant was examined using Analar dichloromethane/acetone (3:1) as solvent. Running SNAP alone, pure NAP dimer alone and a mixture of the two showed that the dimer is a contaminant of the SNAP, in the dry solid form. The disulphide must be present either as a contaminant of the NAP, or (much more likely) is a product of a side-reaction during SNAP synthesis e.g. from SNAP itself.

3.8.3. NMR.

NMR was used to check the products of SNAP decomposition in aqueous alkali (which would ensure slow SNAP decomposition due to the neutral to high pH and therefore allow sufficient time for manipulation etc.). NaOH was dissolved in 10 ml D_2O and this solution diluted by 10 in D_2O. 0.95 ml was added to an NMR tube, and 0.05 ml of a SNAP solution in CD_3OD was added. Final concentrations of NaOH and SNAP were both 1×10^{-2} M. The mixture was immediately subjected to NMR. The initial spectrum showed a mixture of dimer and SNAP (as compared to authentic samples of each alone). After two days the mixture was re-examined. It now seemed

to show that only dimer was present, but the presence of a large peak (OH⁻ ?) detracted from the quality of the spectrum.

The NMR work was repeated, this time using NaOD in place of NaOH. Runs were performed on NMR tubes as follows:

a) SNAP in CD_3OD added to an equal volume of D_2O. SNAP was 0.015M in the NMR tube. It remained green throughout the experimental period and was still green several days later. The NMR spectrum showed the presence of a small amount of dimer initially, increasing to become quite obvious after five hours. The solution was approximately pH 4 after many days, using universal indicator paper.

b) SNAP in CD_3OD added to NaOD in D_2O, giving a 60% excess of NaOD. The solution remained green for several days. The NMR spectrum showed traces of dimer, increasing slightly over five hours, although not as obviously as with SNAP/CD_3OD in D_2O. The solution was still pH 10 after many days using universal indicator paper.

c) Cysteine in D_2O was added to $NaNO_2$ in D_2O, plus one drop of concentrated $HClO_4$. The solution (5 x 10^{-5}M with respect to cysteine) immediately turned red, but the NMR spectrum produced was very poor. After several days the solution was pH 1 as shown by universal indicator paper.

d) SNAP in CD_3OD was added to an equal volume of cysteine in D_2O (both 5 x 10^{-5} M in the tube). The solution went pink immediately but over five hours produced a pink solid which collected at the top of the solution above a pocket of gas. This could be the mixed dimer of SNAP and cysteine, the dimer of cysteine alone, the dimer of SNAP alone, or all three. The NMR spectrum was not clear. Repeated on a larger scale, using non-deuterated solvents, a white precipitate was produced below a pink solution, the pink colour slowly

discharging to a colourless solution and a further white precipitate. After several days the solution was pH 3/4 as shown by universal indicator paper.

The experiments using cysteine and SNAP were repeated, using fresh CD_3OD, D_2O and D_2SO_4 as acid for generating DNO_2 in nitrosating cysteine, as well as NaOD. They were not successful, as D_2O is not a very good NMR solvent for TMS and the alternatives (DSS - 3-(trimethylsilyl) propanesulphonic acid Na or TSP - 3-(trimethylsilyl) tetradeutero sodium propionate) were not good either[8]. An alternative would be to use only CD_3OD as a solvent, but cysteine proved to be insoluble in this, even after hours of sonication.

3.8.4. Titration of Decomposed SNAP solution

If SNAP was allowed to decompose in just sufficient alkaline solution to neutralise it initially, then the H^+ ions produced in the reaction could be back-titrated using more of the same alkali solution. A 1:1 SNAP:H^+ stoichiometry would result in the same volume of alkali being required for back-titration as was required for neutralisation.

Four sets of test solutions were used, each with 5 ml SNAP (0.02007M) in Analar methanol to which was added an exact equivalent of NaOH (as 45.51 ml of 0.002005M solution). These were left at room temperature, in the dark, overnight. They were then back-titrated with the same stock NaOH solution, using phenol red[9] in methanol as indicator - yellow in acid, pink in alkali, pH range 6.8 - 8.4.

For all four sets, an approximate end-point was found at 20 ml of added alkali, but this faded over 2 - 3 minutes. Over the course of an afternoon, several ml were added to restore the pink colour. Next day, further aliquots were required, so that approximately 30 ml of alkali had been added in total. Each "end-point" took place over a range of approximately 0.5 ml ! It seemed that H^+ was produced slowly over a period of time (i.e. an equilibrium situation ?) to the extent of 75% of equivalence of SNAP. All four test solutions gave the same approximate results. This was

unexpected, as it had been assumed that the following stoichiometry would prevail (Scheme 3.2).

$$2SNAP \xrightarrow{\text{decomposition}} 2NO + \text{dimer}$$

$$2NO + \tfrac{1}{2}O_2 \longrightarrow N_2O_3$$

$$N_2O_3 + H_2O \longrightarrow 2NO_2^- + 2H^+$$

$$\text{i.e. } 2SNAP \longrightarrow 2NO \longrightarrow 2H^+$$
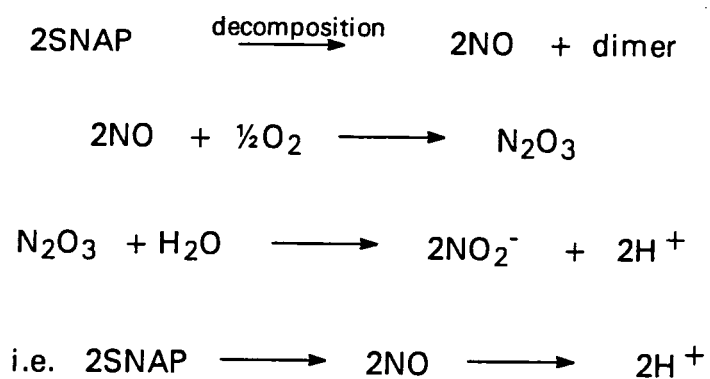
Scheme 3.2

The reasons for the observations remain unclear.

3.9 Use of Free-Radical Trapping Reagents

3.9.1. Introduction

From some of the observations regarding the decomposition of SNAP and other S-nitrosothiols in a variety of solutions, it seemed quite possible that the initial step in S-nitrosothiol decomposition pathways was the formation of two free-radicals as in Equation 3.1.

$$RSNO \rightleftharpoons RS^\bullet + NO^\bullet$$

Equation 3.1

This was thought to be particularly true when the solution was irradiated with bright sunlight. If this was the case, then the use of free-radical trapping reagents should have a pronounced effect on the decomposition rate of S-nitrosothiols. By combining with $NO^\bullet$ (or $RS^\bullet$) as soon as they were formed, a free-radical trapping agent (or spin trapping reagent) would shift the equilibrium towards the right and favour RSNO decomposition. Alternatively, the reagent could work by combining directly with the RSNO molecule and removing $NO^\bullet$.

Spin trapping reagents have a long history of use in chemistry[10, 11], particularly in the field of gas-phase kinetics. One of the problems that was immediately apparent was to obtain a free-radical trapping reagent that was sufficiently water soluble for use in aqueous buffer solutions. Upon reading the literature, several reagents had to be discounted, even though they were considered to be good traps for $NO^\bullet$ or thiyl radicals ($RS^\bullet$) because they were only soluble in organic solvents[12, 13].

3.9.2 SNAP Decomposition in DGA/NaOH Buffer

A buffer was chosen which would have very little u.v. interference and no possibility of reaction with NO, for use with the free-radical trapping agents to be tried. A buffer which fitted these criteria was 2,2-dimethylglutaric acid (DGA) with NaOH,

which was suitable for use between pH 3.2 and 7.6. Runs were performed in pH 7.0 standard strength buffer, with SNAP at 4×10^{-4} M. SNAP was added as the dry powder to the buffer and shaken quickly, producing very rapid dissolution. This produced only a 0.05 pH unit change over the entire reaction period. The decomposition followed half order kinetics extremely well and were reasonably consistent. The results are shown in Table 3.32 below.

pH	$10^4 \times k_{obs}$ (Abs$^{1/2}$s^{-1})
7.0	15.84 (0.999); 16.7 (0.999); 17.02 (0.999); 16.68 (0.999); 15.54 (0.999); 17.88 (0.999); 16.54(0.999) Mean = 16.6 $\pm$ 0.77

Table 3.32

3.9.3. Phenol

The first reagent to be tried was phenol. This is reasonably soluble in water and is known to combine with thiyl radicals by means of a radical mechanism[14], as shown below in Scheme 3.3, using SNAP.
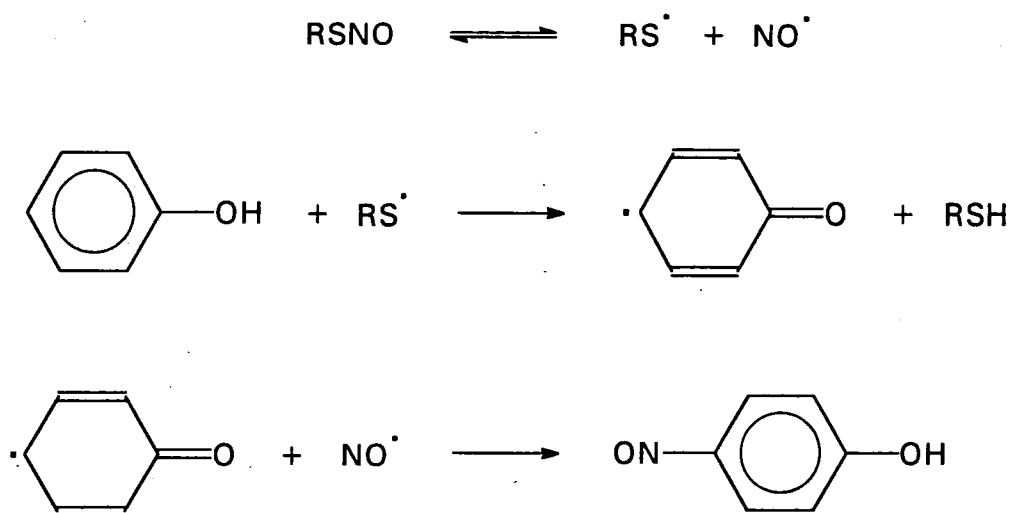
(A small quantity of the ortho-substituted nitrophenol is also formed.)

Scheme 3.3

Initial work showed that buffers such as TRIS/Maleate/NaOH, pH 7.4, absorbed in the same region (280nm) that phenol did. It was found that DGA/NaOH pH 7.0 buffer did not absorb at all in this region, or anywhere above it. Phenol was stable in

the buffer, and did not absorb above 300nm. Scans of SNAP alone in DGA/NaOH pH 7.0 buffer and with phenol (4×10^{-4} M and 2×10^{-3} M respectively) showed that a distinct peak was formed at 400nm, due to the formation of the nitrosophenol; SNAP alone did not interfere significantly here. Using the above reactant concentrations, virtually no effect was noted upon pH. Several runs were performed on SNAP alone, 4×10^{-4} M in DGA/NaOH pH 7.0 buffer at 25°C. These showed extremely good half order kinetics, taken over 95% reaction completion (Table 3.33).

$10^3 \times k_{obs}$ (Abs$^{1/2}$s^{-1})

1.58 (0.999)
1.67 (0.999)
1.70 (0.999)
1.67 (0.999)   Mean = $1.66 \times 10^{-3} \pm 0.07$ Abs$^{1/2}$s^{-1}
1.55 (0.999)
1.79 (0.999)
1.65 (0.999)

Table 3.33

The buffer, pre-equilibrated to 25°C, was added to a flask containing dry SNAP already in the water bath, made up to the mark, sealed and shaken, then a sample added to the cuvette already in position. Readings were taken approximately 60 seconds after first addition of buffer. This method was repeated for addition of phenol, which was already dissolved in the buffer, at the appropriate concentration. Phenol was added to the 4×10^{-4} M SNAP in varying equivalents i.e. 8×10^{-4} M, 2×10^{-3} M, 4×10^{-3} M and 8×10^{-3} M, all in DGA/NaOH pH 7.0 buffer. Even at these high concentrations there was virtually no effect on buffer pH.

Typical plots are shown in Figures 3.9 below for each of these increasing phenol concentrations.

400 nm
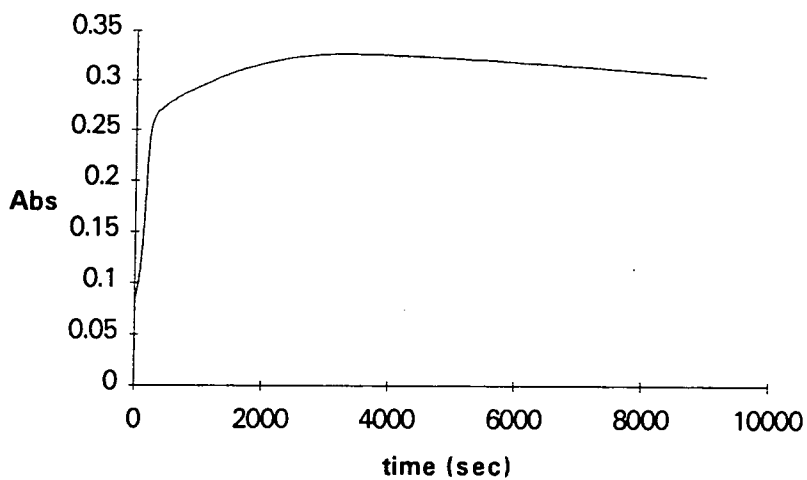
Phenol at 8×10^{-4} M

400 nm
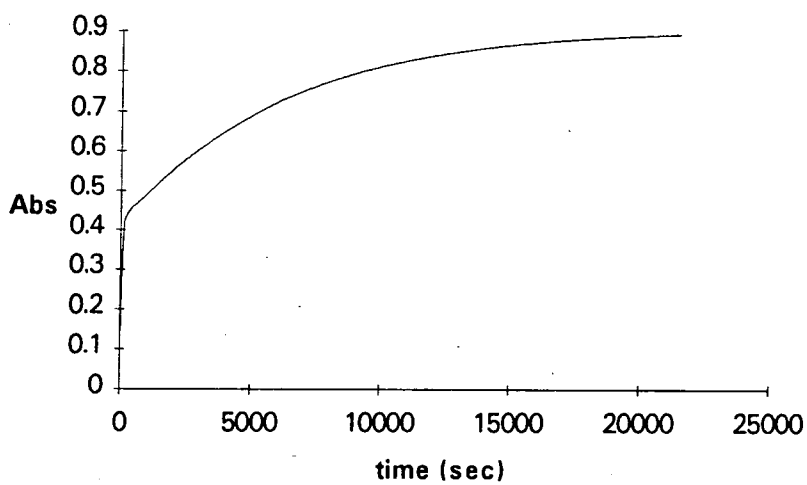
Phenol at 2×10^{-3} M

400 nm
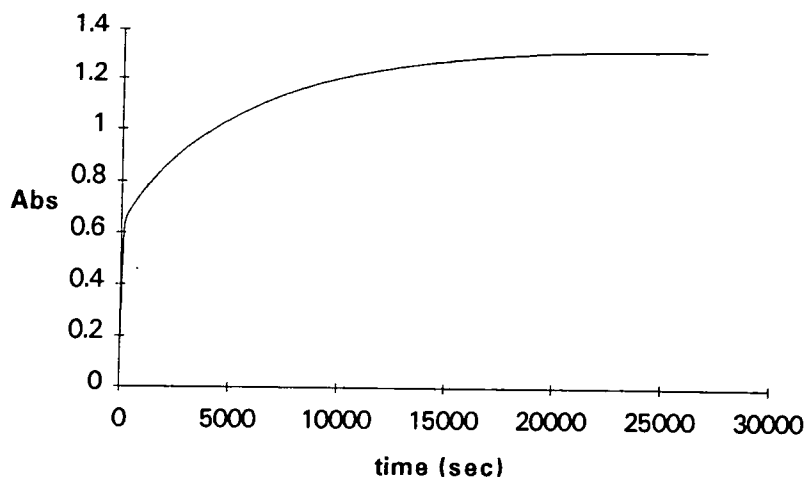
Phenol at 4×10^{-3} M

400 nm
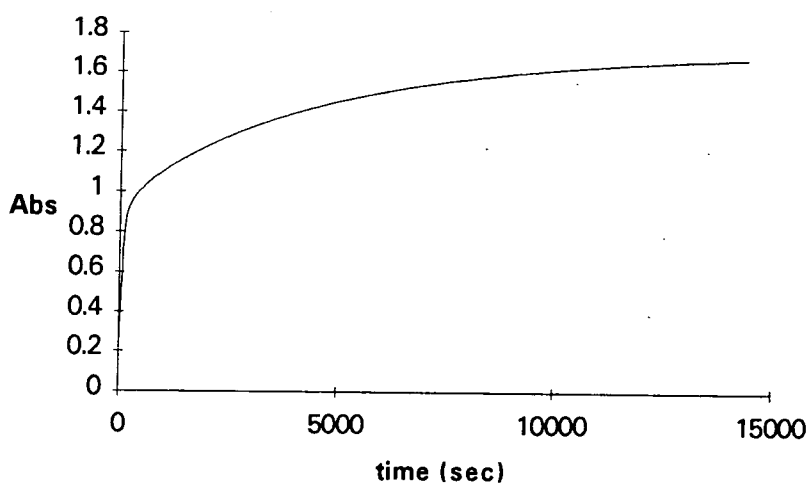
Phenol at 8×10^{-3} M

Figures 3.9

These traces were produced consistently for each concentration. It can be seen clearly that although the SNAP concentration is constant, the absorbance at 400nm increases with increasing phenol concentration. At the lowest concentration of phenol, the trace is sigmoidal. At higher concentrations, the rise is extremely rapid before changing again into a slower rate of absorbance increase. The point of changing occurs at increasingly higher absorbance levels with increasing phenol, as does the final absorbance level reached. This would appear to indicate that a phase of very rapid

nitrosation of the phenol occurs, which is dependent upon phenol concentration, as phenol must be an inefficient "scavenger" of NO. This is followed by a slower reaction where phenol is further nitrosated by another mechanism, possibly involving a nitrosation reagent derived from the reaction of NO with the solution. This seems to indicate that phenol is not a particularly good reagent for trapping free-radicals produced from SNAP decomposition, as all the SNAP would be decomposed over a period of 600 seconds. The initial nitrosation phase with phenol is over after less than 150 seconds in all cases, yet secondary nitrosation takes hours. Using KH_2PO_4 /NaOH buffer pH 7.0 produced similar results. Multiple scans over a 3 hour period of the reaction mixture indicated that there was no secondary product being formed during the slower part of the absorbance increase i.e. the same product was being formed, but in two distinct phases in terms of rate of formation.

A check was made upon the product formed between SNAP and phenol. A sample of authentic *p*-nitrosophenol (PNP) was obtained from suppliers and dissolved, by sonication, in DGA/NaOH pH 7.0 buffer and 0.1M HCl. Solutions containing PNP at 4 x 10^{-5} M in-cell were scanned. These showed the u.v. spectra for the benzenoid (colourless) and quinoid (yellow) forms of the substance.

The PNP exists in the two forms in equilibrium, which is very solvent dependent, existing mainly in the oxime form, as shown in Figure 3.10.

benzenoid   benzoquinone oxime
(colourless)   (yellow)
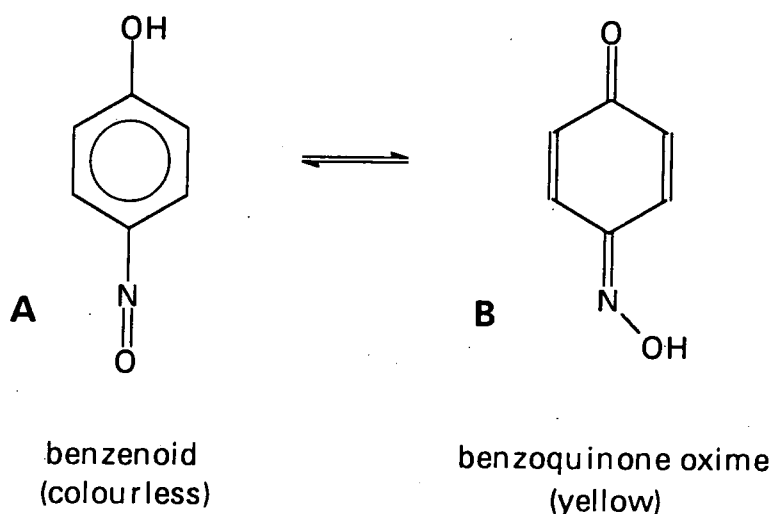
Figure 3.10

The ortho isomer only exists as the benzenoid form due to internal hydrogen bonding[15], as shown in Figure 3.11.
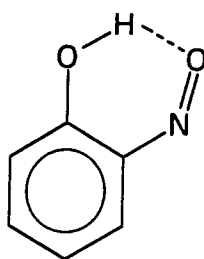
Figure 3.11
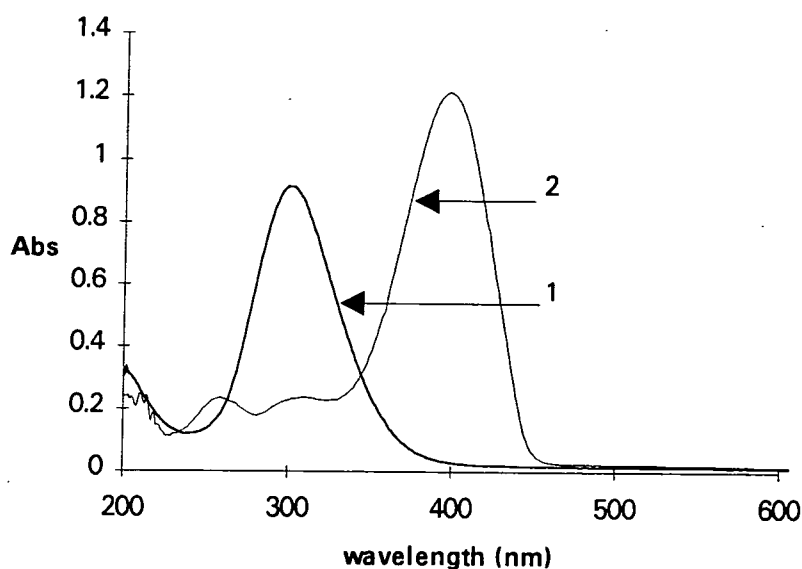
1 = benzenoid form

2 = quinoid form

Figure 3.12

The quinoid form showed the same absorbance maximum and spectrum as the product with SNAP and phenol, with an absorbance maximum at 397nm, (ε = 3.03 x 10^4 mol^{-1} l cm^{-1}) (see Figure 3.12 above).

An equimolar mixture of phenol and sodium nitrite in 0.1M HCl (both 2 x 10^{-4} M in-cell) was scanned and compared to the standard PNP solution in acid. Comparing absorbance maxima at 299nm for the PNP product in the benzenoid form, it seemed

that only a 19% conversion of phenol to PNP occurred - the reaction was very slow and was left for 70 hours before measuring.

The products of the reaction between phenol and SNAP in buffer were acidified, extracted into ether, dried over magnesium sulphate and dried by rotary evaporator to give a brown/black solid residue. Attempts were made to perform NMR measurements on this and compare it with the authentic PNP sample (also black), but these were of very poor quality for both samples, due to the presence of water.

The work was repeated, using a stock solution of SNAP in dry, Analar methanol, to which was added the phenol/buffer solution. While keeping the SNAP concentration steady at 2×10^{-4} M in-cell, runs were performed with phenol at 8×10^{-4} M, 2×10^{-3} M, 4×10^{-3} M and 8×10^{-3} M in-cell. This was then repeated with SNAP at 8×10^{-4} M in-cell, and phenol at 8×10^{-4} M, 2×10^{-3} M, 4×10^{-3} M and 8×10^{-3} M in-cell. The results of an attempt at analysis are shown in Table 3.34 below, for SNAP at 2×10^{-4} M. Typical traces are shown for each phenol concentration, in Figure 3.13.

$10^4 \times k_{obs}$ (s^{-1})	Correlation	
7.58 ± 0.02	(0.972)	
6.88 ± 0.02	(0.977)	8×10^{-4} M
11.45 ± 0.00	(0.976)	Phenol
9.87 ± 0.02	(0.981)	
6.54 ± 0.02	(0.970)	
5.84 ± 0.01	(0.977)	2×10^{-3} M
18.20 ± 0.05	(0.976)	Phenol
17.90 ± 0.05	(0.975)	
6.80 ± 0.02	(0.969)	
7.38 ± 0.02	(0.969)	4×10^{-3} M
11.10 ± 0.03	(0.969)	Phenol
8.99 ± 0.03	(0.965)	
4.89 ± 0.01	(0.976)	
5.26 ± 0.02	(0.975)	8×10^{-3} M
4.88 ± 0.01	(0.980)	Phenol
6.08 ± 0.02	(0.971)	

Table 3.34
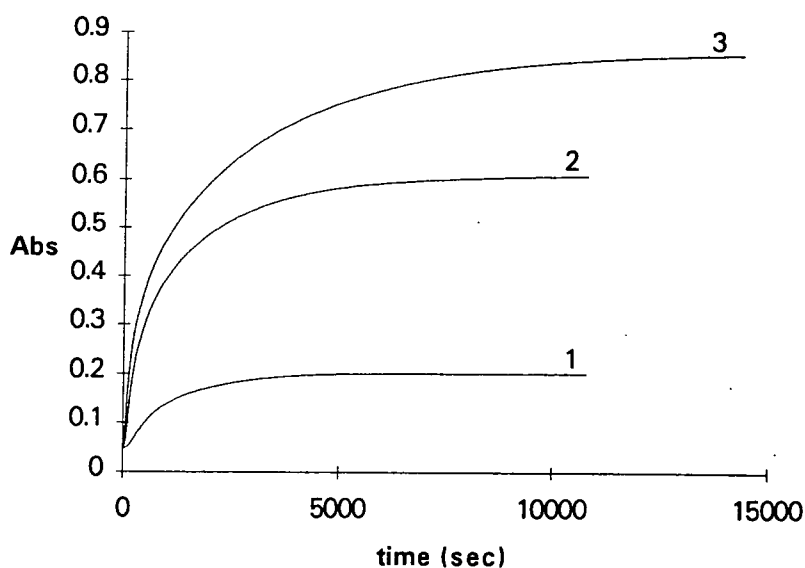
1 = Phenol at 8 x 10^{-4} M   2 = Phenol at 2 x 10^{-3} M

3 = Phenol at 4 x 10^{-3} M

Figure 3.13

These results are a poor fit to first order kinetics and merely give some idea of the rate of formation of the yellow nitrosophenol. It can be seen that this rate is approximately the same for all concentrations of phenol and may be taken as indicating a very slow rate of nitrosation of the phenol by a nitrosating agent formed <u>after</u> total SNAP decomposition. Due to the very high extinction coefficient for *p*-nitrosophenol, a small increase in concentration will have a large absorbance effect. Increasing the concentration of phenol will merely increase the final quantity of *p*-nitrosophenol produced, not the <u>rate</u> of formation.

It was felt that phenol would not offer further fruitful examination, and attempts were made with other reagents.

3.9.4. Furan

This proved to be of no use and did not appear to have any reaction with SNAP or its decomposition products, in aqueous solution.

92

3.9.5. Salicylic acid

Attempts were made to use salicylic acid (2-hydroxybenzoic acid) as a free-radical trap for SNAP decomposition, in a similar manner to phenol. Checks were made to ensure that no interference occurred between the salicylic acid (SAL), buffer (DGA/NaOH pH 7.0) and SNAP. No reaction appeared to occur between SNAP and SAL in buffer. When the SAL was added to sodium nitrite in 0.1M HCl, no reaction occurred. When the solution was left over the weekend and re-examined after 64 hours it had gained a very pale yellow colour and absorbance had increased in the region between 350nm and 400nm. However, it was clear that any nitrosation was far too slow to be of any use.

3.9.6. Tetramethyl pyrroline N-oxide (M4PO)

A final attempt was made to obtain a water soluble free-radical trap that would trap out thiyl radicals (RS$^{\bullet}$). A literature search showed that there were many thiyl radical traps available, but these were usually unsuitable as they were not water soluble. However one compound was found[16] that appeared to be both a good thiyl radical trapping agent and water soluble - this was tetramethyl pyrroline N-oxide (M4PO) as shown in Figure 3.14.
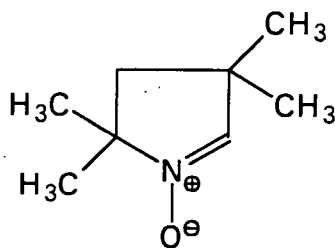
Figure 3.14

SNAP was dissolved in 1,4-dioxan and this solution added to DGA/NaOH buffer pH 4.0 or 7.0 to produce an in-cell concentration of 4×10^{-4} M (0.1 ml SNAP solution added to 2.4 ml buffer). The M4PO was dissolved directly in the buffer prior to use after thermostatting the buffer in a water bath at 25°C. A check of the stability of

SNAP in 1,4-dioxan showed that a 19% drop in absorbance at 340nm occurred for the solution, stored at room temperature in the dark, over a period of 23 hours. The SNAP/dioxan solution was always freshly prepared and kept covered in aluminium foil. A solution of M4PO was scanned and found to have no absorbance above 260nm. Work was performed with DGA/NaOH buffer, pH 7.0 and later pH 4.0.

i) pH 7.0

SNAP decomposition was examined in the buffer alone and with increasing concentrations of M4PO (SNAP was 4×10^{-4} M and 8×10^{-4} M in-cell). The kinetics were poor, the only fit at lower concentrations being half order kinetics, while at the highest concentration of M4PO, a 1:20 stoichiometric ratio, the traces could be explained in terms of first order kinetics, but again the correlation was still quite poor. (See Table 3.35.)

	$10^3 \times k_{obs}$ (Abs$^{\frac{1}{2}}$ s^{-1})	Correl.
SNAP alone (4×10^{-4} M)	5.42	(0.984)
	5.64	(0.989)
	5.68	(0.967)
	5.42	(0.976)
	5.30	(0.991)
SNAP + M4PO (1×10^{-3} M)	5.80	(0.989)
	5.30	(0.993)
	5.12	(0.992)
SNAP + M4PO (4×10^{-3} M)	2.80	(0.997)
	2.52	(0.998)
	2.52	(0.998)
SNAP + M4PO (8×10^{-3} M)	1.05	(0.997)
	1.05	(0.999)
	1.13	(0.999)

Table 3.35

It can be seen that the increasing addition of M4PO seems to have the effect of reducing the rate of SNAP decomposition. A comparison of the type of decomposition given at a lower pH (4.0) with that at pH 7.0, under otherwise identical conditions (M4PO = 4×10^{-3} M) is shown below in Figure 3.15. It can be seen that there is a marked difference between the two.
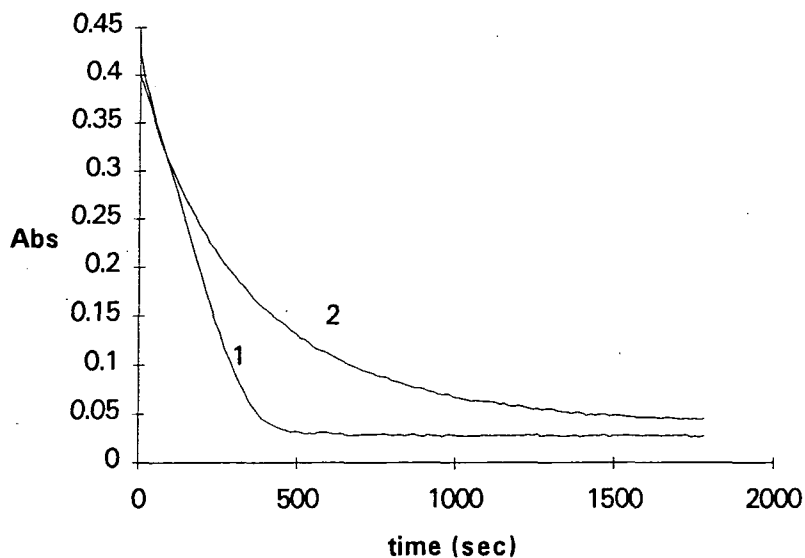
$1 = $ pH 7.0 $2 = $ pH 4.0

Figure 3.15

De-aeration

A check was made to ascertain whether the presence of oxygen in the buffer had any effect upon the decomposition. All solutions were deoxygenated by sonication/vacuuming on a water pump followed by bubbling with nitrogen gas. This was repeated twice. Cells were also flushed with nitrogen immediately prior to use. SNAP decomposition in de-aerated buffer alone was checked, then with M4PO at 8 x 10^{-3} M. (See Table 3.36.)

	10^3 x k_{obs} (Abs$^{\frac{1}{2}}$ s^{-1})	Correl.
SNAP alone (4 x 10^{-4} M)	3.92	(0.977)
	3.10	(0.995)
	3.66	(0.986)
	4.44	(0.996)
	4.42	(0.994)
SNAP + M4PO (8 x 10^{-3} M)	3.64	(0.918)
	3.34	(0.930)

Table 3.36

When the solution was reoxygenated by bubbling with air, the following value of $k_{obs} = 3.23 \times 10^{-3}$ s^{-1} (0.890) was obtained.

After thorough de-aeration again the value for k_{obs} of 3.34×10^{-3} s^{-1} (0.939) was obtained. It was observed that during this sequence the infinity level absorbance was quite high with de-aerated solution, but low with aerated solution. This was repeatable i.e. in the deoxygenated solution, something was being formed that was not present in the aerated solution. (See Figure 3.16.)
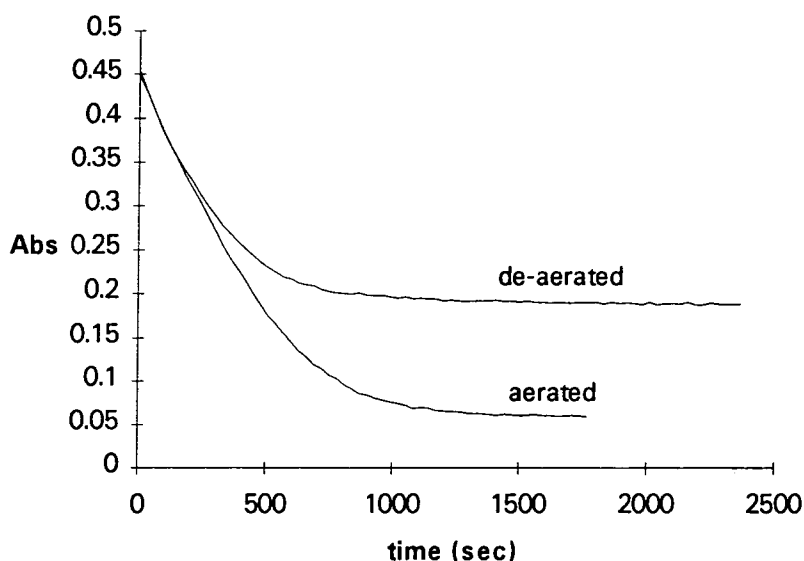
Figure 3.16

There was some difference between the two rates of decomposition, under otherwise identical conditions (Table 3.37).

	$10^3 \times k_{obs}$ (s^{-1})
Aerated	2.23 ± 0.02 (0.967)
	1.81 ± 0.02 (0.975)
	2.16 ± 0.02 (0.973)
De-aerated	3.64 ± 0.05 (0.918)
	3.34 ± 0.05 (0.930)

Table 3.37

However, the kinetic analysis correlation was so poor that little reliable distinction can really be made.

ii) pH 4.0

This was briefly examined, SNAP decomposition in buffer alone being compared in aerated and de-aerated solution (Table 3.38).

	10^3 x k_{obs} (s^{-1})
Aerated	4.44 ± 0.03 (0.960)
	4.40 ± 0.03 (0.955)
	4.71 ± 0.03 (0.961)
De-aerated	4.39 ± 0.03 (0.964)
	5.60 ± 0.04 (0.952)
	5.78 ± 0.05 (0.945)
	5.59 ± 0.06 (0.928)
	5.49 ± 0.10 (0.918)

Table 3.38

It can be seen that the correlations were all poor and that little difference can be seen between the two solutions. With M4PO at 4 x 10^{-3} M in-cell (1:10) the same sequence of events could be seen, as with pH 7.0 i.e. a higher final baseline indicating some product in de-aerated solution which disappeared upon aeration. As previously, this disappeared over 2 - 3 days.

Scans done show slight differences in the u.v. spectra for the aerated and de-aerated solutions, as shown in Figures 3.17 and 3.18, at the end of the reactions.
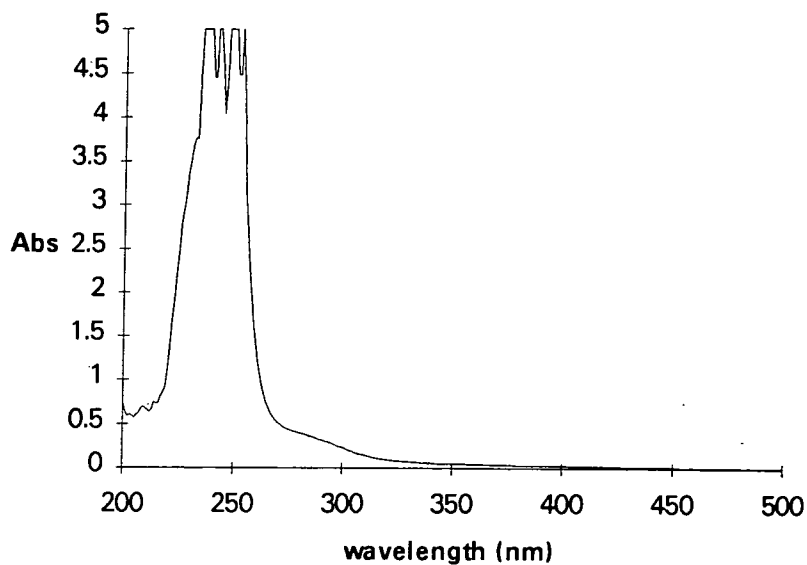
Aerated Solution

Figure 3.17
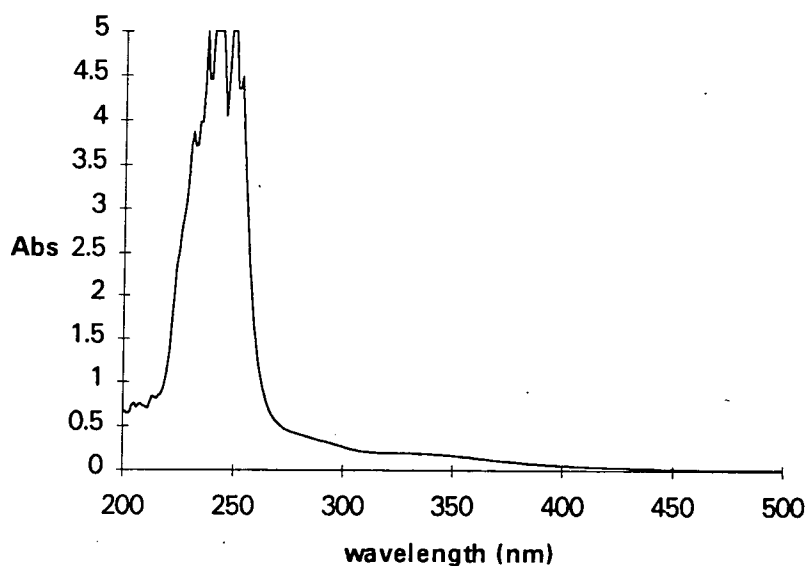
De-aerated Solution

Figure 3.18

The decrease in the observed rate of decomposition for SNAP with M4PO at high concentration may indicate that there is some role for free-radicals in initiating, or contributing to, SNAP decomposition. However, the change is small and may be spurious. Further investigation did not appear to offer any prospects of an insight into SNAP decomposition, because of the erratic nature of the kinetics.

3.10 Hemin and Haemoglobin as NO Detectors

3.10 1. Introduction

It is known that NO will react with free coordination sites of iron complexes of widely varying structures to form a nitrosyl derivative[17, 18].

The ability of NO to bind to such sites has important implications in biology, as the formation of such nitrosyl complexes may result in activation or inhibition of enzyme systems with iron prosthetic groups (see Chapter 1). One well-studied example is the binding of NO to deoxyhaemoglobin, this having a much greater affinity than oxygen or carbon monoxide[19] (equation 3.2).

$$HbFe(II) \ + \ NO \ \rightleftharpoons \ HbFe(II)(NO)$$

Equation 3.2

When the iron centre is oxidised in the presence of oxygen, methaemoglobin (MetHb) is formed, as well as nitrite and nitrate (equation 3.3).

$$HbFe(II)(NO) \ + \ O_2 \ \longrightarrow \ HbFe(III)$$
Methaemoglobin
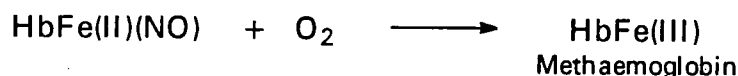
Equation 3.3

Unlike oxygen, NO binds to both iron (II) and iron (III) porphyrins (oxygen only binds to the Fe (II) state). In erythrocytes NO will be rapidly converted into nitrite/ nitrate and thus removed, the MetHb being reconverted to Hb by an enzyme, methaemoglobin reductase. Importantly, coordinated NO may display both electrophilic and nucleophilic properties, due to transfer of electron density within the metal-NO bond to formally give bound NO^+ or NO^- (cf. free NO, a free-radical and a poor electrophile/nucleophile). Thus *in vivo*, such metal complexes may be vital as nitrosating agents, since NO itself is not a nitrosating species. An example is shown below in Figure 3.19.

$^-O_2CCH_2CH_2$ $\quad$ $CH_2CH_2CO_2^-$

Me— $\quad$ —Me

NO

Fe

—Me

Me
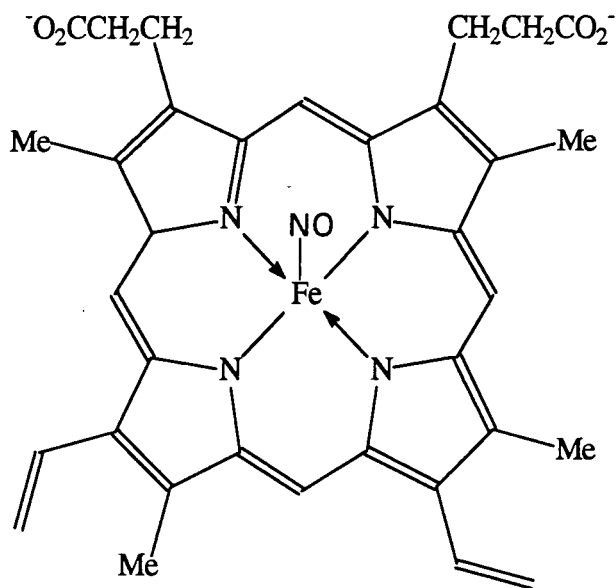
Diagram of a NO-Haem Complex

Figure 3.19

It was hoped to use hemin (or later, haemoglobin) as an efficient trap for NO, generated as a S-nitrosothiol (e.g. SNAP) decomposed, using the spectral changes as NO binds to the Fe(II) site in the porphyrin ring as the method of detection.

3.10.2. Hemin

Solubility problems were found with the hemin in DGA/NaOH buffer pH 7.4. This was overcome by dissolving hemin in a small amount of sodium hydroxide solution, to form a brown/black solution, then 1.0 ml of this was added to the 50 ml buffer to give a 2×10^{-5} M solution. (The pH only changed from 7.42 → 7.53.)

It was necessary to keep the hemin in the Fe(II) form, by reduction with sodium dithionite ($Na_2S_2O_4$). This proved problematic. It was found that hemin was <u>very</u> sensitive to atmospheric oxygen, as was the sodium dithionite itself. The latter had to be freshly prepared and added in excess as at an equivalent with hemin most was used up with traces of oxygen in the solution and had no effect on the hemin. Leaving a sample exposed to the air caused a <u>rapid</u> decline of both excess dithionite and hemin Fe(II) spectral areas, but just allowing dithionite to stand caused deterioration. See Figure 3.20.
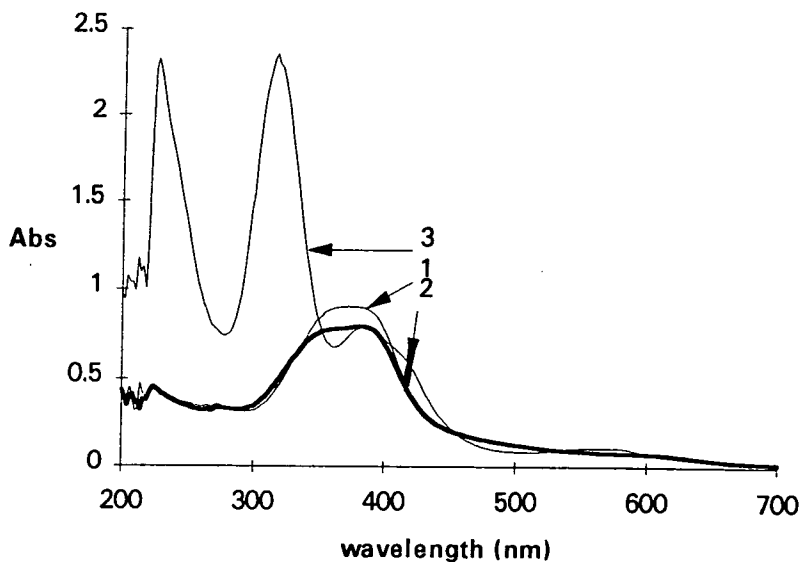
Figure 3.20   1 = Hemin alone   2 = Hemin + dithionite (1:1)

3 = Hemin + dithionite in excess

The trace for 3 shows that in a sealed cuvette, the excess dithionite causes a change in the spectrum. The peak at 315nm however is due to excess dithionite and it is only that part of the spectrum above 370nm which corresponds to hemin in the Fe(II) form. (The scan of dithionite alone at 1×10^{-3} M in-cell, shows that even at this high concentration there is no absorbance above 370nm. See Figure 3.21.)
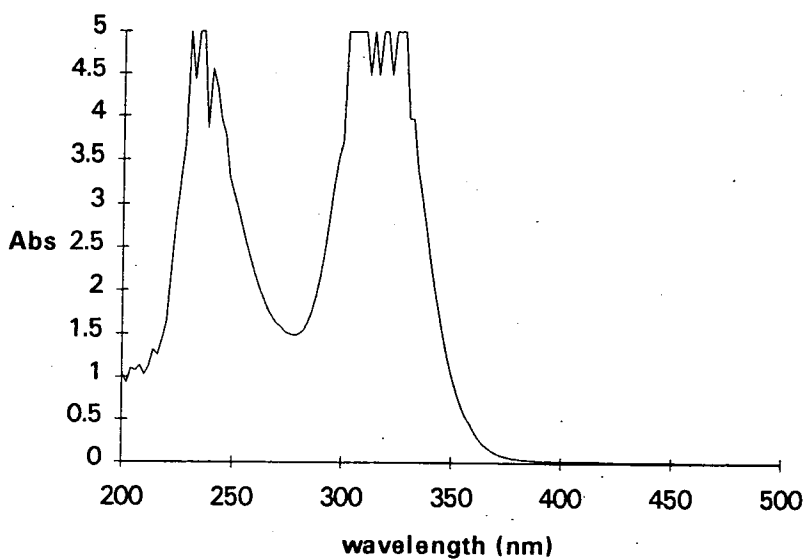
Figure 3.21

101

The buffer was de-aerated by sonication and vacuuming for ten minutes, followed by nitrogen being bubbled through it - this was repeated twice. It was then used to make all the solutions for testing hemin and dithionite further. The results are shown of hemin Fe(III) alone (2×10^{-5} M), dithionite alone (1×10^{-3} M) and hemin plus dithionite 2×10^{-5} M and 3×10^{-5} M respectively. It can be seen that there is a slight change upon reduction of the hemin from the Fe(III) form to the Fe(II) form. See Figure 3.22.
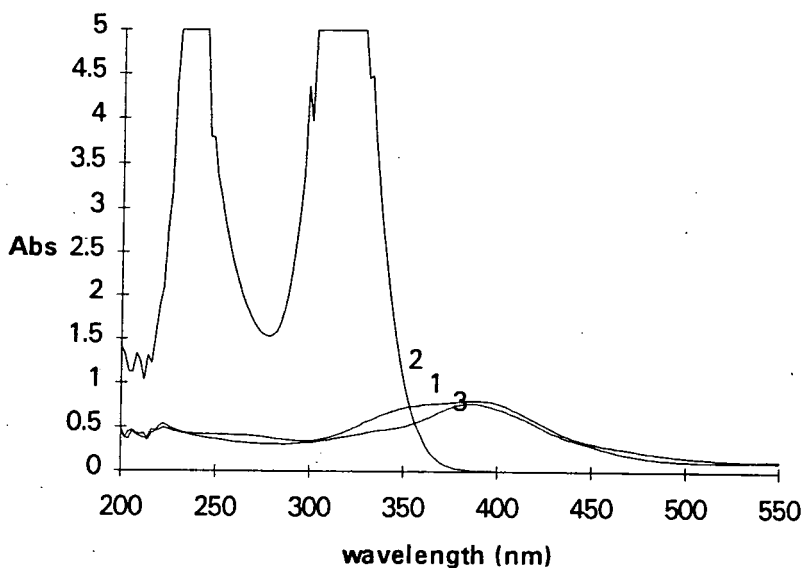
1 = Hemin Fe(III) alone   2 = Dithionite alone

3 = Hemin + dithionite

Figure 3.22

After standing 17 hours, covered very well with parafilm, the cell containing the hemin Fe(II) had reverted totally to the Fe(III) form, as indicated by the spectral change, i.e. 3 had become identical to 1.

Using de-aerated buffer (DGA/NaOH, pH 7.5) an attempt was made to see the effect of bubbling NO through the solutions of hemin Fe(III) and hemin Fe(II). NO was generated by the action of sodium nitrite solution upon ascorbic acid, the system being flushed through with nitrogen prior to use, which was also used subsequently as a carrier gas. Hemin Fe(III) was reduced with successive additions of sodium dithionite

102

solution before bubbling NO through. NO was also bubbled through de-aerated buffer alone and hemin Fe(III) solution. See Figure 3.23.
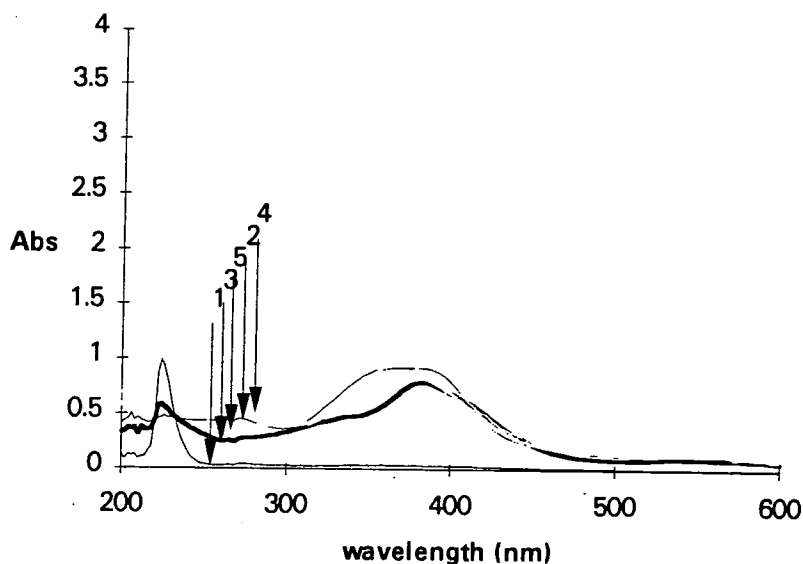
1 = NO gas in buffer alone   2 = Hemin in the most Fe^{2+} form

3 = Hemin Fe^{3+} form in buffer alone   4 = Hemin Fe^{3+} form + NO

5 = Hemin Fe^{2+} form + NO

Figure 3.23

Little difference could be seen between the peaks for NO/Fe(III)hemin and free Fe(III)hemin and similarly for NO/Fe(II)hemin and free Fe(II)hemin.

Using SNAP

With SNAP added to Hemin, at 4×10^{-4} M and 2×10^{-5} M respectively and recorded every sixty seconds for ten minutes; a small, rapid rise occurred in the 370nm region of the uv spectrum, followed by a slower decrease (de-aerated DGA/NaOH buffer, pH 7.5, Hemin as Fe(II)). This is shown in the traces below (Figure 3.24).
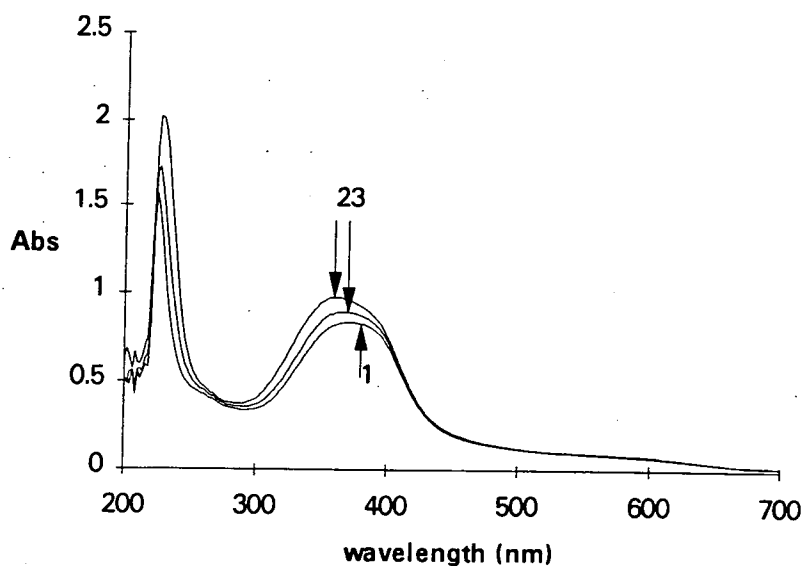
$$1 = 0 \text{ min} \quad 2 = 1 \text{ min}$$

$$3 = 10 \text{ min}$$

Figure 3.24

The exact nature of the change occurring here was not known.

This was repeated on a larger scale, but using aerated DGA/NaOH pH 7.5 buffer. HeminFe(III) at 2×10^{-5} M with 0.1 ml dioxan was scanned. The decomposition of SNAP in 0.1 ml dioxan added to the buffer alone (4×10^{-4} M in-cell) was multi-scanned every 30 seconds for 5 minutes. This was repeated, with the addition of hemin Fe(III) solution (2×10^{-5} M in-cell) with scanning every 45 seconds for 45 minutes. The actual pH for this mixture was 7.7. The scans seemed to indicate that no interaction *per se* was occurring between the hemin and SNAP, just superimposition of the two spectra, with decline due to SNAP decomposition. This is clearly shown in the superimposed traces in Figure 3.25.

1 = Hemin alone   2 = SNAP + Hemin (0 mins)

3 = SNAP + Hemin (after 45 mins)   4 = SNAP alone (0 mins)

5 = SNAP (after 150 secs)

Figure 3.25

The results seemed to indicate that hemin posed great difficulties in manipulation, especially if required for use in the Fe(II) form, due to its great sensitivity to air and the difficulty posed in trying to ensure the total exclusion of air.   Little if any interaction with NO could be detected when in the Fe (II) form, although this could be due to constraints imposed by apparatus and methodology.   Even when present as hemin Fe(III), NO still appeared not to react.   With SNAP, the same difficulties appeared to be true. It was decided to move on to using haemoglobin as a potential detector of NO generation from S-nitrosothiols, rather than attempt further work with the (technically difficult) production of thoroughly oxygen-free buffers and hemin Fe(II).

3.10.3. Haemoglobin

The haemoglobin was prepared as detailed in Appendix (B). Oxyhaemoglobin reacts with NO to give methaemoglobin and nitrate, as shown below in Figure 3.26.
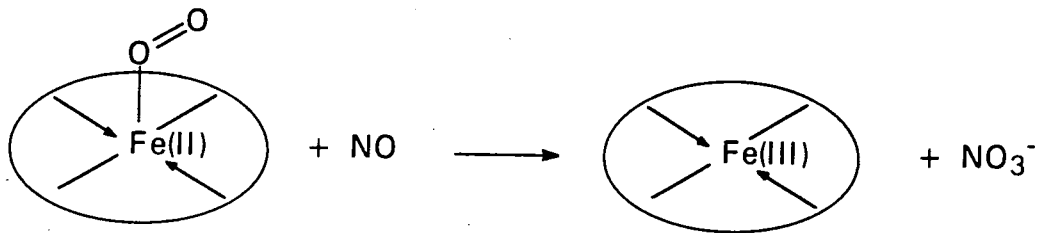
Figure 3.26

A scan of 6 μl of Hb solution, (used after thawing from freezer, shaking and keeping in the 'fridge between use) was taken in DGA/NaOH buffer, pH 7.5. (See Figure 3.27.)
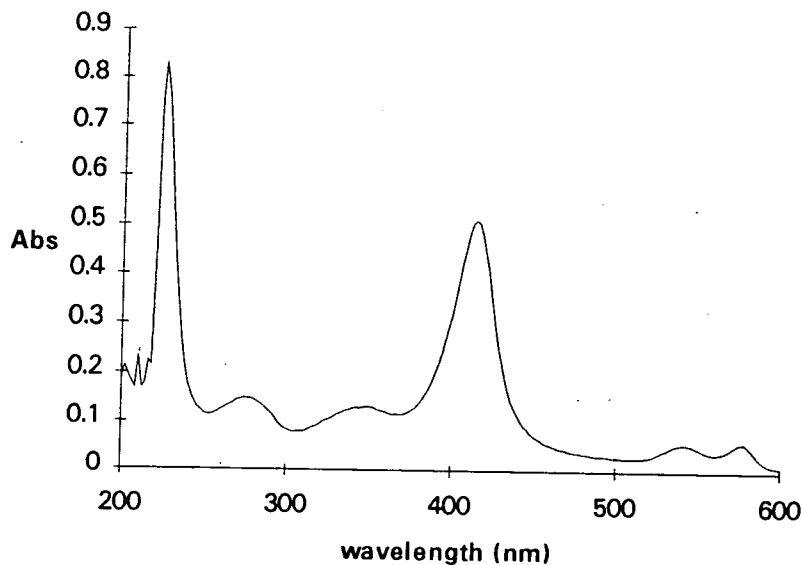
Figure 3.27

Note the peak around 420nm. A preliminary run was done in buffer de-aerated as previously for hemin. This gave a very poor resolution of change over 20 minutes, but a slight shoulder was detectable at 420nm.

The concentration of Hb had to be increased by an addition of 20 μl, after 10 μl Hb with SNAP still gave poor resolution of change. This quantity of Hb (20 μl) gave an absorbance maximum in the 420nm region of approximately 1.6 and corresponded to

a Hb concentration in-cell of 1.32×10^{-6} M. SNAP solution in de-aerated distilled water was used, to give an in-cell SNAP concentration of 1.5×10^{-5} M. The cell was flushed with nitrogen throughout all additions. This run indicated some change over one hour in the shoulder at 420nm, and an isosbestic point at 413nm.

Another run was performed as previously, with Hb at 1.32×10^{-6} M and SNAP at 1.5×10^{-5} M in DGA/NaOH buffer, pH 7.5, taking scans every 10 minutes for four hours. These are shown below in Figure 3.28.
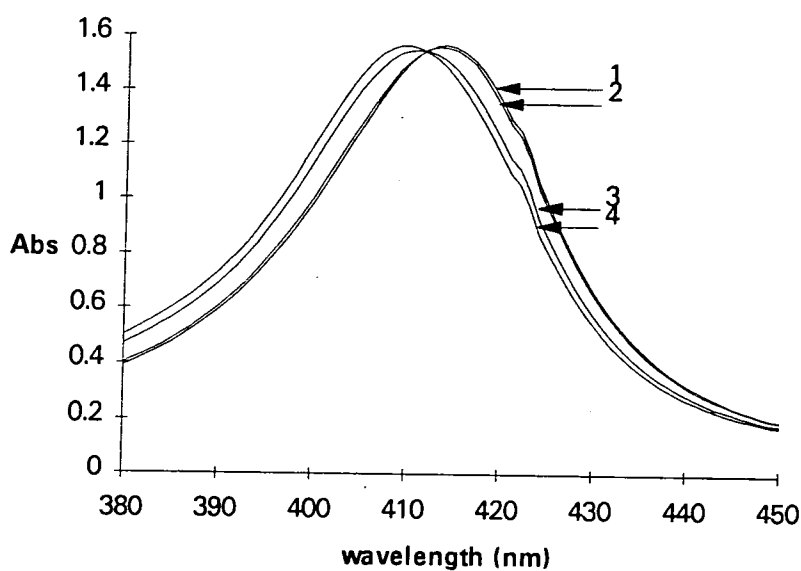
$$1 = 0 \text{ min} \qquad 2 = 10 \text{ min} \qquad 3 = 110 \text{ min} \qquad 4 = 240 \text{ min}$$

Figure 3.28

This showed that a decrease in absorbance at 421nm and/or an increase at 401nm would be suitable for measurement. Time drive runs were done at 421nm under the same conditions of buffer and reagents. However, both gave poor-fitting curves, whether for first order or for half order.

Example k_{obs} = 1.19×10^{-4} s^{-1} $\pm$ 0.01 (0.962), and
(First order) 0.95×10^{-4} s^{-1} $\pm$ 0.02 (0.954)

These were low values compared to the usual rate of decomposition of SNAP to be expected in DGA/NaOH pH 7.5 buffer. It could have been the case that the protein

was stabilising the SNAP and hence slowing its decomposition by some mechanism. Altering the stoichiometry of Hb to SNAP to 1:20 then 1:100 (Hb kept at 1.32×10^{-6} M in-cell) did not produce any better results, indeed the traces became disjointed. It was decided to abandon this work using hemin and haemoglobin, as it was proving far more complicated and time-consuming than expected. This was disappointing, given the investment in time required to produce the pure haemoglobin. However, new areas had opened with the discovery of trace metal catalysis of S-nitrosothiol decomposition.

3.11 Summary

The whole series of work performed had produced many puzzling results, most of which can be explained in terms of trace quantities of catalytic copper(II) ions, present as contamination in the distilled water and the various buffers used. The quantity of NaOH used in the latter makes a significant and variable contribution. The Griess reagent work indicated that nitrite is a product of SNAP decomposition, possibly to as much as 100% and certainly 90%, independent of pH and buffer type.

The variations in SNAP decomposition with buffer can be resolved as being due to intrinsic copper, with factors such as buffer type and pH affecting both its actual concentration and its availability, via chelation and complex formation. The general observation that decomposition is greatest at approximately neutral pH is a reflection of this _and_ the complexing ability of the S-nitrosothiol itself, in terms of its charge state.

Although unfortunately not explored fully, there is some indication that the presence of disulphide can have an effect upon S-nitrosothiol decomposition. Also, there seems to be the possibility that photolytic decomposition may augment, or be a complicating factor in, the copper catalysed decomposition. However, the lack of success with spin trapping reagents seems to indicate that this is only a minor aspect

of S-nitrosothiol decomposition in aqueous solutions. The complex nature of the reaction is indicated by the lag period between SNAP decomposition and pH decline and the fact that proton production does not appear to be simple in its stoichiometry.

References

1. J.P. Griess, *Philos. Trans. R. Soc.,* (London), 1864, **154**, 667

2. B. Saville, *Analyst*, 1958, **83**, 670

3. M. Feelisch, *J. Card. Pharm.*, 1991, **17** (3), 525

4. S.C. Askew, St. Andrews University, personal communication

5. S.C. Askew, St. Andrews University, personal communication

6. S. Oae, K. Shinhama, *Org. Prep. Proc. Int.*, 1983, **15** (3), 165

7. L. Field, R.V. Dilts, R. Ravichandran, P.G. Lenhart, G.E. Carnahan, *J. Chem. Soc., Chem. Comm.*, 1978, 249

8. R.S. Matthews, Durham University, personal communication

9. D.N. Cuthbert, R.B. Webber, in *A Modern Approach To Chemistry*, Intertext Books, London, 1969, Vol. 2, 119

10. M.J. Perkins, in *Essays In Free-Radical Chemistry*, Chem. Soc. Special Publ. No. 24, 1970, 97

11. E.G. Janzen, *Accts. Chem. Rev.*, 1971, **4**, 31

12. P.D. Bartlett, T. Funahashi, *J. Am. Chem. Soc.*, 1962, **84**, 2596

13. P. Graceffa, *Biochim. Biophys. Acta.*, 1988, **954** (2), 227

14. S.M.N.Y.F. Oh, D.L.H. Williams, *J. Chem. Soc., Perkin Trans. 2*, 1991, 685

15. D. Barton, W.D. Ollis, in *Comparative Organic Chemistry*, Ed. I.O. Sutherland, 1969, Vol. 2, 315

16. E.G. Janzen, R.V. Shetty, S.M. Kunanec, *Can. J. Chem.*, 1981, **59**, 756

17. V.S. Sharma, R.A. Isaacson, M.E. John, M.R. Waterman, M. Chevion, *Biochemistry*, 1983, **22**, 3897

18. Y. Henry, C. Durocq, D. Servent, C. Pellat, A. Guissani, *Eur. Biophys. J.*, 1990, **20**, 1

19. T.G. Traylor, V.S. Sharma, *Biochemistry*, 1992, **27**, 2847

Chapter 4

Decomposition of S-Nitrosothiols
By Metal Ions

4.1. Introduction

A puzzling and confused picture had developed, over many experiments, of the decomposition of S-nitrosothiols (principally SNAP). At a seminar to describe these and other results, a suggestion was made that metal ions in trace amounts might be responsible. This was acted upon initially by determining the effect on SNAP decomposition in phosphate buffer pH 7.4, made with a) tap water and b) distilled water, of the addition of ethylene diamine tetra-acetic acid (EDTA).

EDTA was used as a chelating agent as it has a high affinity for metal ions such as iron, copper, etc. It forms a hexadentate ligand around the ion, sequestrating it from the solution and thus preventing its involvement in other reactions (Figure 4.1).

$$\text{HOOCH}_2\text{C} \quad \text{CH}_2\text{COOH}$$
$$\text{HOOCH}_2\text{C} \diagdown \diagup \diagdown \diagup \text{CH}_2\text{COOH}$$
$$\text{N} \qquad \text{N}$$
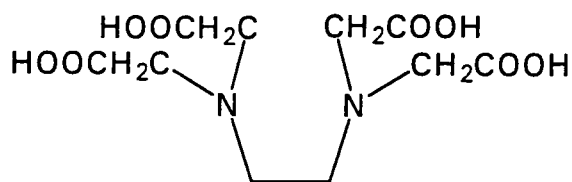
Figure 4.1

Although it is not particularly soluble, sufficient could be dissolved to achieve an in-cell concentration in excess of the intrinsic copper ion concentration. In both cases, <u>no</u> decomposition was observed by measuring absorbance at 340nm, unlike the known rapid decomposition in buffer alone.

4.2. The Effects of Various Metal Ions

The effects of various metal ions in solution in distilled water were next examined. As the SNAP stock solution was generated in dilute sulphuric acid, the metal salts chosen were sulphates wherever possible. A variety of metals were chosen - calcium, nickel, cobalt, chromium (III), copper (II), magnesium, silver, iron (III), zinc, manganese (II) and mercury (II).

Some difficulties were experienced with the solubility of the salts involved which entailed choosing a more soluble salt e.g. nitrate, and distilled water was used to minimise this and obviate problems that might have arisen from precipitation reactions in buffer solutions.

A solution of SNAP in dioxan was used as a stock solution - this enabled rapid addition and mixing of the SNAP with the cell contents yet produced a dioxan concentration in-cell of only 4%.

For metals such as zinc, manganese, magnesium, chromium, cobalt and nickel, there was only a slight decomposition which in fact matched that shown by SNAP in distilled water alone. However, pronounced decomposition occurred with copper (II) ions. Some slight decomposition was also noticed with silver ions, (greater than the slight decline to be expected in distilled water) yet this was far less than that noted with tap water.

It appeared possible therefore that traces of metal ions (particularly copper (II)) in the water supply could be responsible for SNAP decomposition.

Experiments performed with Hg^{2+} in distilled water showed that an extremely fast decomposition of SNAP took place - too rapid to be observed on our time scale. Total decomposition occurred at a stoichiometric ratio of 2:1 SNAP:Hg^{2+}. However, virtually no decomposition took place at a ratio of 50:1 - yet clear decomposition was observed with Cu^{2+} at this concentration (SNAP in all cases was 5 x 10^{-4} M in-cell).

From these results, the reaction with mercury (II) ions appeared to be non-catalytic in nature. Confirmation of the catalytic nature of the reaction of SNAP with Cu^{2+} was given by the following experiment. SNAP at 5 x 10^{-4} M in-cell was added to varying in-cell concentrations of Cu^{2+} and distilled water. The results showed an increasing decomposition rate with increasing Cu^{2+} concentration, while virtually no decomposition occurred with distilled water (Figure 4.2).
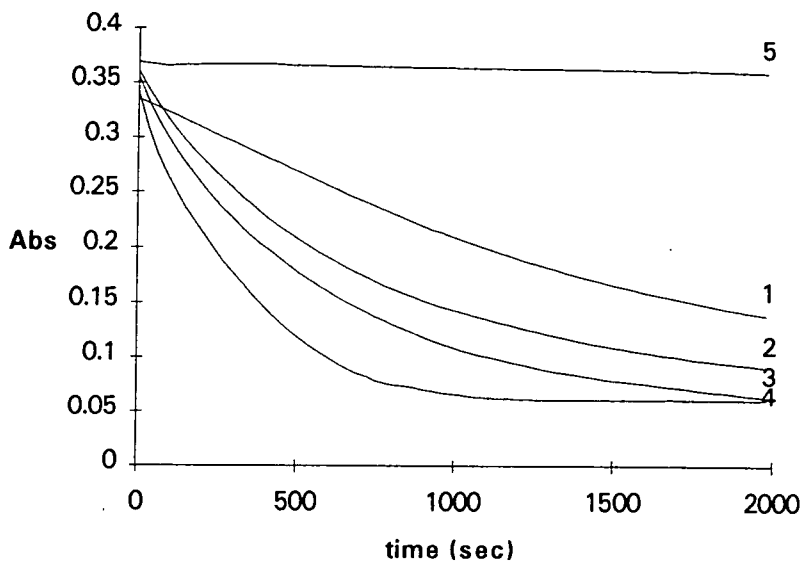
1 = SNAP + Cu 1 x 10^{-5} M 2 = SNAP + Cu 5 x 10^{-5} M
3 = SNAP + Cu 1 x 10^{-4} M 4 = SNAP + Cu 5 x 10^{-4} M
5 = SNAP in distilled water alone

Figure 4.2

Confirmation of the non-catalytic nature of the reaction between Hg^{2+} and SNAP was given by repeating the previous experiment using Hg^{2+} over the same range of concentrations (Figure 4.3).
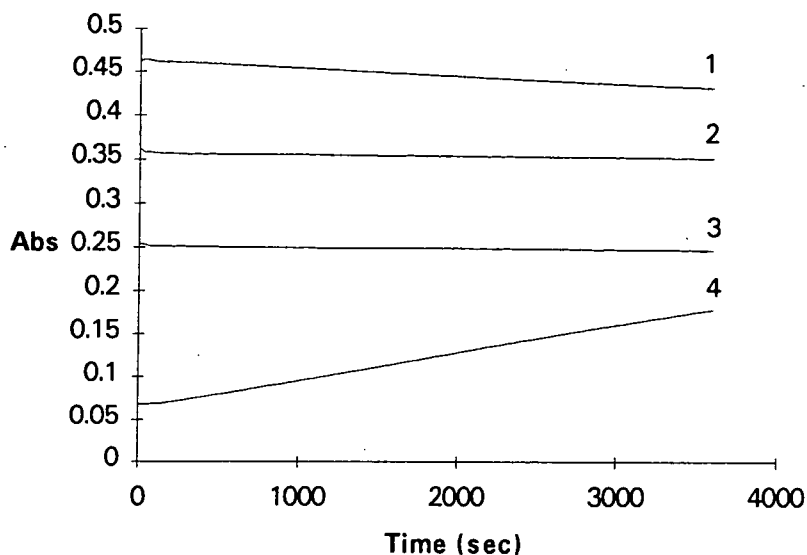
1 = SNAP alone (5 x 10^{-4}M)   2 = SNAP + Hg^{2+} (1 x 10^{-5} M)
3 = SNAP + Hg^{2+} (1 x 10^{-4} M) 4 = SNAP + Hg^{2+} (5 x 10^{-4} M)

Figure 4.3

It was confirmed that the reaction was extremely fast and that disappearance of SNAP was directly linked to the stoichiometric ratio of Hg^{2+}, there being no subsequent decomposition. With excess Hg^{2+}, the formation of a secondary reaction product, after initial total decomposition of the SNAP, was confirmed. The absorbance increase at 340nm was shown not to be due to re-formation of SNAP by scanning the various solutions over the 700 - 200nm range. The characteristic 340nm S-nitrosothiol peak was only present at low Hg^{2+} concentration. At high Hg^{2+} concentration a new species was being formed, probably a complex between excess Hg^{2+} and the initial reaction products (see Figure 4.4). The nature of this putative complex was not further explored.
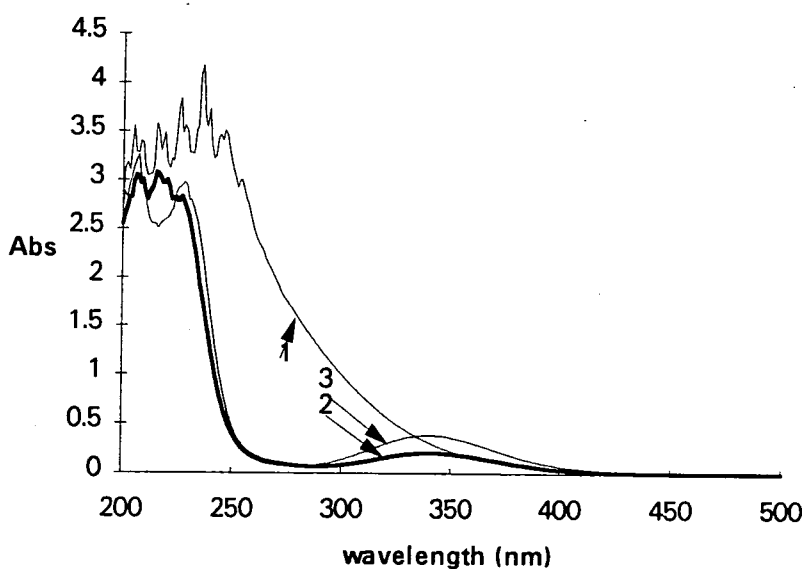
1 = Scan of trace 4, Fig. 4   2 = Scan of trace 3, Fig. 4
3 = Scan of trace 2, Fig. 4

Figure 4.4

The presence of Cu^{2+} in the water supply producing catalytic decomposition was confirmed by the decomposition of SNAP (at 5×10^{-4} M) in "old" distilled water (source being the old still supply), "new" distilled water (source being the newly introduced ion-exchange) and ordinary laboratory tap water. Analysis of the various water supplies was also performed with flame spectrometry. The results are shown below in Figure 4.5.
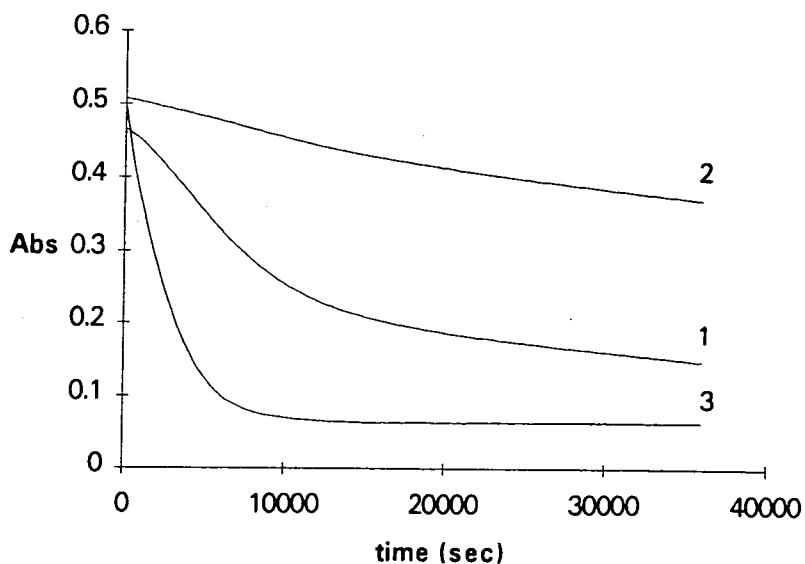
1	=	"old" distilled water	0.059 ppm Cu^{2+}
2	=	"new" distilled water	0.006 ppm Cu^{2+}
3	=	tap water	0.198 ppm Cu^{2+}

Figure 4.5

The decomposition of SNAP in distilled water with Cu^{2+} at high concentration was checked and found to be rather poor in terms of reproducibility.

SNOG

The same experiments were performed for comparison with another stable S-nitrosothiol, SNOG. The exact procedure was repeated, even using dioxan:water (1:3) as stock solvent for both SNAP and SNOG despite the fact that SNOG, unlike SNAP, is readily water soluble. The results are summarised below.

The differences between the two compounds were pronounced:

1. SNOG did not decompose in distilled water, while SNAP did so slowly but distinctly.

2. At high Cu^{2+} concentration SNAP readily decomposed but SNOG was still unaffected.

3. With Hg^{2+} in equivalent amounts, both were extremely rapidly decomposed, but SNOG did not form a secondary reaction complex leading to a slow recovery of

116

absorbance at 340nm. However, SNOG was decomposed by Hg^{2+}, like SNAP, on a stoichiometric basis. This highlights the different mechanisms that must exist between the Hg^{2+} and Cu^{2+} reactions.

The importance of buffer type was illustrated when citrate/NaOH buffer was chosen for further work with Cu^{2+} catalysis. It was found that no catalysis by copper occurred at pH 5.5 and pH 4.4 for treble concentration citrate buffer. This was considered to be due to chelation of the Cu^{2+} ions by the (tri)carboxylate groups of the citrate. Other buffers also were found to produce no SNAP decomposition with Cu^{2+}, e.g. TRIS/HCl and also Imidazole/HCl. In both cases complex formation was presumably to blame, as both gave distinct blue colourations when Cu^{2+} was added. With N-2-hydroxyethylpiperazine-N'-2-ethanesulphonic acid (HEPES)/NaOH, a pale blue colloidal precipitate was formed (at pH 7.4) i.e. copper hydroxide. A mono-carboxylate would not be expected to chelate Cu^{2+} in such a fashion and this was found to be the case - acetate buffer at treble concentration ($\simeq$ 0.2M) did not eliminate Cu^{2+} catalysis. Used with SNOG at 1×10^{-3} M and Cu^{2+} at 1×10^{-3} M it was shown that SNOG did decompose slowly and consistently, but less so at lower pH i.e. either the SNOG was more stable to Cu^{2+} catalysis at lower pH, or the Cu^{2+} was less available. The decomposition became marked at even higher pH (all in treble concentration acetate buffer). It may be that the availability of the Cu^{2+} ion is the major factor in these results.

It was apparent that the reaction of SNOG had changed in the presence of acetate buffer, compared to distilled water. SNAP was still rapidly decomposed (compared to SNOG) but SNOG itself was now relatively unstable. It was noted that in the case of SNOG in pH 5.5 acetate buffer (but not in the case of SNAP) a blue colouration was present in the cell at the end of the run - there was a distinct increase in absorbance at wavelengths >500nm. This may be due to complexation of Cu^{2+} with components of the reaction and may account for the sigmoidal shape of the SNOG decomposition curve, which itself may be indicative of a complex reaction system taking place. The

study of this particular reaction was difficult therefore due to the possibility of secondary reactions/complexations taking place.

4.3 SNAP decomposition with varying Cu(II) ion concentration

A series of experiments was performed with SNAP at 5×10^{-4} M in dioxan/water (25%) decomposing in treble concentration acetate buffer pH 4.6 with varying concentrations of added copper (II) ions. The results are shown below in Table 4.1.

$10^4 \times Cu^{2+}$ concentration (M)	$10^3 \times k$ (s^{-1})	$10^3 \times$ Mean (s^{-1})
15	10.71 ± 0.13 10.04 ± 0.08 10.22 ± 0.11	10.32
10	7.89 ± 0.23 9.10 ± 0.38 7.14 ± 0.19	8.04
5	5.23 ± 0.17 6.81 ± 0.23 5.44 ± 0.12	5.83
3	3.78 ± 0.02 4.67 ± 0.01 5.78 ± 0.02	4.54
1	2.33 ± 0.01 3.27 ± 0.07 $2.20 \pm 0.$	2.6
0.5	1.58 ± 0.03 1.46 ± 0.02 1.65 ± 0.03	1.56
0.1	0.49 ± 0 0.29 ± 0 0.43 ± 0.01	0.40

Table 4.1

In all cases, SNAP concentration = 5×10^{-4} M in-cell. Reaction was > 95% complete in all cases.

It can be seen that the amount of error tends to decrease with decreasing levels of copper. The results when plotted give no indication of linearity except possibly at the lowest Cu^{2+} concentrations (Figure 4.6).
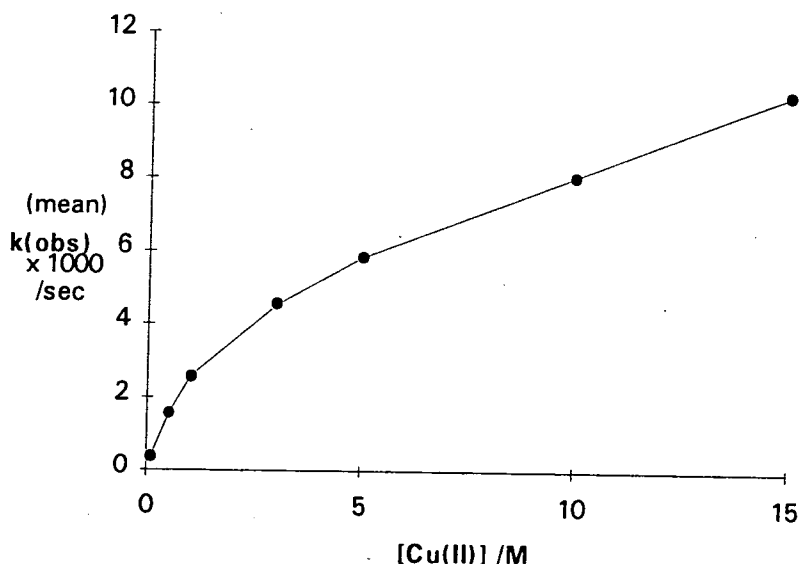
Figure 4.6

It is here that copper would be acting catalytically - perhaps at higher levels more complex reactions are taking place. The linearity is made more apparent by the fact that the k_{obs} value would not be expected to reach 0 (i.e. the origin) as some decomposition might be expected to occur at even lower Cu^{2+} concentrations, and even spontaneously in the total absence of copper due to, say, photolytic effects of the measuring process or thermal decomposition. The shape of the curve indicates that the decomposition rate decreases at higher Cu^{2+} concentrations, but unfortunately no measurements were taken at even higher concentrations to determine where saturation occurred (the curve is reminiscent of Michaelis-Menten kinetics).

A series of runs were performed the following day to fill in a gap in the curve at 7.5×10^{-4} M Cu^{2+}. This resulted in high values for k_{obs}, very much out of line with

previous ones. When a fresh solution of SNAP was made up and the runs re-performed, the mean value for k_{obs} had halved i.e. fresh solution produced significantly slower decomposition (see Table 4.2 below).

10^3 x k_{obs} "old" (s^{-1})	10^3 x Mean (s^{-1})	10^3 x k_{obs} "new" (s^{-1})	10^3 x Mean (s^{-1})
10.79 ± 0.09		4.93 ± 0.04	
11.45 ± 1.55	10.46	6.51 ± 0.06	5.48
9.15 ± 0.44		5.01 ± 0.06	

Table 4.2

The values obtained with freshly prepared SNAP were a better fit to first order kinetics than the mature solution values, although still not perfectly fitting the rest of the data. This seemed to be confirmation of the subjective feeling that old solutions of SNAP gave "odd" results when used after being left overnight. It was presumed that a product of decomposition (possibly disulphide ?) was responsible for such an effect.

This effect was confirmed by "maturing" a SNAP solution (25% dioxan/water) in aluminium foil in the dark at room temperature for two days then comparing it to identical fresh solution under the same conditions as above (see Table 4.3 below).

10^3 x k_{obs} "new" (s^{-1})	10^3 x Mean (s^{-1})	10^3 x k_{obs} "old" (s^{-1})	10^3 x Mean (s^{-1})
5.34 ± 0.02		9.47 ± 1.0	
6.00 ± 0.03	6.05	8.99 ± 0.79	9.29
6.82 ± 0.04		9.41 ± 0.92	

Table 4.3

The same trends were repeated, i.e. the fresh SNAP solution gave excellent first order kinetics fit while the mature solution produced poor fits and an overall faster

decomposition rate. This highlighted the need to use freshly-prepared solutions in all cases, to ensure reproducibility of results.

4.4. pH/Buffer dependence

An attempt was made to correlate the catalytic effect of Cu^{2+}, with change of buffer and/or change of pH on SNAP and if possible to extend this to other S-nitrosothiols.

An analysis of some of the buffers used previously was performed, for the presence of copper. This gave the following results, as in Table 4.4 below. In all cases, (3 x) indicates treble the normal (i.e. standard) concentration of the buffer.

Solution	Cu^{2+} content (ppm)
KH_2PO_4 (3 x) pH 5.9	0.78
KH_2PO_4 (3 x) pH 7.0	0.102
KH_2PO_4 (3 x) pH 7.8	0.102
D.G.A. (3 x) pH 5.9	0.105
Phthalate (3 x) pH 5.9	0.199
Distilled water	0.008

Table 4.4

A 1×10^{-4} M Cu^{2+} concentration is equivalent to 6.355 ppm i.e. the intrinsic copper represents approximately 1.5 - 3% of added copper at 1×10^{-4} M but 15 - 30% of the lowest level of added copper.

4.4.1 SNAP

A series of runs with SNAP at 5×10^{-4} M in 25% dioxan/water and Cu^{2+} at 1×10^{-4} M were performed in several buffers. The results were very variable (see Table 4.5).

Phosphate (3 x) buffer (KH_2PO_4/NaOH)

pH	Cu^{2+} concentration		
	1×10^{-4} M $10^4 \times k_{obs}$ (s^{-1})	5×10^{-5} M $10^4 \times k_{obs}$ (s^{-1})	1×10^{-5} M $10^4 \times k_{obs}$ (s^{-1})
7.8	20.4 ± 0 22.2 ± 0.1 24.1 ± 0.01	17.1 ± 0	4.9 ± 0.5 5.4 ± 0.4
7.0	39.8 ± 0.9 35.4 ± 0.5	28.4 ± 0.2 30.5 ± 0.1 30.1 ± 0.1	6.1 ± 0 7.5 ± 0
5.9	Poor	Poor	10.8 ± 0.4 7.2 ± 0.1 6.8 ± 0.1

Table 4.5

The general trend, as far as could be seen, was that the rate of decomposition increased, for a given pH, with increasing concentration of copper ions. For a given copper (II) ion concentration, the rate of decomposition increased as the pH decreased from 7.8 → 5.9. It may be the case that it is the effective concentration of copper that is being seen, i.e. as the pH increases, less copper is available for catalytic purposes as it is rendered unavailable by complexation (e.g. with OH$^-$ ions). Certainly, in buffer alone it was noticeable that the very low (but not negligible) concentration of intrinsic copper had little effect on SNAP decomposition except at the lowest pH, when it became more pronounced.

When other buffer systems were tried, decomposition took place very slowly, (presumably due to complexation of the copper ions) e.g. with DGA/NaOH and phthalate/NaOH buffer. Addition of EDTA to buffer caused complete prevention of decomposition in all cases.

An analysis was made of other buffers previously used. The results obtained were as shown in Table 4.6. All buffers were at treble the standard concentration.

Buffer		Cu^{2+} content (ppm)
TRIS/Maleate	pH 7.4	0.093
TRIS/HCl	pH 7.4	0.033
Acetate	pH 3.6	0.050
Acetate	pH 4.6	0.076
Acetate	pH 5.4	0.124

Table 4.6

It can be seen that a significant source of Cu^{2+} ions in all these buffers must be the sodium hydroxide (laboratory reagent grade) which had been used to produce them. This is understandable as the sodium hydroxide was the least pure reagent used (on cost grounds). The copper ions available for the decomposition reaction will be a function of pH, not sodium hydroxide content however, as complexation effects should greatly outweigh very small additional copper contributed via additional sodium hydroxide.

4.4.2 SNOG

With 5×10^{-4} M SNOG in treble concentration phosphate buffer, pH 7.0, Cu^{2+} at 1×10^{-4} M, a noticeable induction period (15 mins) occurred before a very slow decomposition took place. At pH 7.8, a rapid decomposition took place before

decomposition took place. At pH 7.8, a rapid decomposition took place before levelling off at a high absorbance, a clearly atypical result. At pH 5.9, a slow, steady decline in absorbance at 340 nm took place. None were amenable to analysis, the trend for increasing rate of decomposition with lower pH was <u>not</u> observed.

4.4.3 SNAC

With SNAC in identical conditions, a very rapid decomposition occurred at pH 7.8, before levelling off at a high absorbance. At pH 7, rapid decomposition took place, again with a relatively high level of final absorbance, while at pH 5.9, the reaction appeared to go to completion over a longer period of time.

4.4.4 SCYS

With S-nitroso-cysteine (SCYS) under identical conditions, decomposition was too rapid to be measured at pH 7.8 and 7.0. At pH 5.9, the merest final trace of reaction was visible. Whereas the buffer alone also had decomposed the SCYS too rapidly to be measured, curiously at this pH a distinct, sigmoidal decomposition took place over approximately 10 minutes. This appeared to show that there was no general trend for reactivity with Cu^{2+} but that SCYS was far more reactive than any other studied so far, and seemed to indicate the importance of N-acetylation in conferring stability on the S-nitrosothiol with respect to copper ions.

4.4.5 SNOCAP

With captopril S-nitrosothiol (SNOCAP) under identical conditions, no decomposition was observed at any pH. SNOCAP thus showed a surprising stability.

4.4.6 SMAA

With S-nitroso-mercaptoacetic acid (SMAA) under identical conditions, at pH 7.8 and 7.0, an initial rapid decline over the first one or two minutes was followed by a slow,

pronounced, while the effect of buffer alone, (which previously produced no decomposition) was to give a sigmoidal decomposition curve. These complex decompositions were not amenable to analysis.

4.4.7 STLA

With S-nitroso-thiolactic acid (STLA) under identical conditions, at all pHs there were very rapid, consistent declines, as shown in Table 4.7

TLA in PO_4 (3 x) pH 7.0, 5×10^{-4} M, 1×10^{-4} M Cu			
	k_{obs} (s^{-1})	Correl.	Mean k_{obs} (s^{-1})
TLACU01	0.0143	(0.937)	
02	0.0134	(0.982)	0.014 ± 0.0005
03	0.0143	(0.974)	
TLA in PO_4 (3 x) pH 5.9, 5×10^{-4} M, 1×10^{-4} M Cu			
	k_{obs} (s^{-1})	Correl.	Mean k_{obs} (s^{-1})
TLACU04	0.0047	(0.987)	
05	0.0046	(0.989)	0.0046 ± 0.0002
06	0.0044	(0.986)	
TLA in PO_4 (3 x) pH 7.9, 5×10^{-4} M, 1×10^{-4} M Cu			
	k_{obs} (s^{-1})	Correl.	Mean k_{obs} (s^{-1})
TLACU07 08 09	NOT ANALYSABLE (2nd order ?)		

Table 4.7

The results for STLA were found to be excellent (in terms of fit to first order kinetics) for pH 7.0 and pH 5.9, but broke down at pH 7.9. The results further support the view that catalysis is fastest at neutral pH and that complex kinetics occur at higher pH.

4.5. N-acetylation as a stabilising structure

It was decided to confirm the stabilising effect of N-acetylation with regard to copper-induced decomposition by examining the relative stability of S-nitroso-penicillamine (SPEN) compared to S-nitroso-N-acetylpenicillamine (SNAP), particularly as the former had not been studied previously. To facilitate a valid comparison, both were generated from Analar grade racemates, in treble concentration phosphate buffer pH 7.0, both in 25% dioxan/water mixtures. Both were 5×10^{-4} M in-cell, with a Cu^{2+} concentration in cell of 5×10^{-5} M (Table 4.8).

	k_{obs} (s^{-1})	Mean (s^{-1})
10^2x SNAP (s^{-1})	2.04, 2.02, 2.00, 1.97, 2.05	0.020 ± 0.0003
SPEN	0.267, 0.277, 0.275, 0.277, 0.284 0.287, 0.276, 0.273, 0.281, 0.282	0.278 ± 0.0006

Table 4.8

In all cases, reasonable to very good fits to first order kinetics were obtained. It can be seen that under these specific conditions, SPEN is approximately fourteen times more reactive than SNAP.

4.6 Esterification as a stabilising/destabilising structure

An attempt was made to check on whether esterification of the carboxylate group could have an effect upon the rate of decomposition of some of these S-nitrosothiols.

4.6.1 Work with phosphate buffer

A comparison was made between SCYS and S-nitroso-ethylcysteine (SECYS) 5×10^{-4} M in phosphate buffer, treble concentration pH 7.0, with copper at 1×10^{-4} M in-cell.

The work was performed on the stopped flow attachment on the Shimadzu spectrophotometer. A brief check was made of SNAC at the same time but this was really too slow for the machine (see Table 4.9).

Compound	k_{obs} (s^{-1})	Mean (s^{-1})
S-nitroso-ethylcysteine	3.62 $\pm$ 0.15, 3.86 $\pm$ 0.09 3.82 $\pm$ 0.10, 3.84 $\pm$ 0.04 3.65 $\pm$ 0.05, 3.46 $\pm$ 0.06 3.38 $\pm$ 0.08, 3.61 $\pm$ 0.43 3.84 $\pm$ 0.08	3.68 $\pm$ 0.17
(S-nitroso-N-acetylcysteine)	4.02 x 10^{-4} $\pm$ 0.17	
S-nitroso-cysteine	0.638 $\pm$ 0.017, 0.641 $\pm$ 0.013 0.677 $\pm$ 0.014, 0.655 $\pm$ 0.022 0.690 $\pm$ 0.016, 0.661 $\pm$ 0.017 0.682 $\pm$ 0.022	0.663 $\pm$ 0.019

Table 4.9

It can be seen that SECYS is approximately 5 - 6 times as reactive as SCYS, which in turn is several orders of magnitude more reactive than SNAC. A check was made on S-nitroso-mercaptoacetic acid (SMAA) under identical conditions (see Table 4.10).

	10^3 x k_{obs} (s^{-1})	10^3 x Mean (s^{-1})
SMAA	4.43 $\pm$ 0.10 4.04 $\pm$ 0.26 4.24 $\pm$ 0.36	4.24 $\pm$ 0.16

Table 4.10

It can be seen that this is considerably slower than SECYS or SCYS in decomposing, but an order of magnitude faster than SNAC.

With EDTA, all these S-nitrosothiols showed great stability (over 30 minutes).

Under identical conditions, methylmercaptopropionic acid (MMP) and mercaptopropionic acid (MPA) S-nitrosothiols were tested and it was found that while the ester form did not decompose at all over 45 minutes, the free acid did slowly decompose.

Further work was done with the S-nitrosothiols of 3-mercaptopropionic acid (SMPA) and its ester, methylmercaptopropionic acid (SMMP). The two compounds were very stable in the presence of EDTA and also in buffer alone (no yellow species etc. was found.). In phosphate buffer, treble strength pH 7.0 with 1×10^{-4} M copper, at 5×10^{-4} M SMPA showed a slow decomposition over 45 minutes (absorbance half gone at this stage). The reaction occurred with a good fit to first order kinetics.

$10^4 \times k_{obs}$ (s^{-1}) = 2.37; 1.67; 3.80; 3.54   Mean = 2.85×10^{-4} s^{-1} $\pm$ 1.0

The ester form (SMMP) showed no decomposition.

4.6.2 Peculiar reaction of SMMA

Further to this, a comparison was made between mercaptoacetic acid S-nitrosothiol (SMAA) and its methyl ester (SMMA), under the same conditions of buffer, pH and copper. As an initial check, SNAC, SCYS, SECYS, SMAA and SMMA were monitored in buffer as previously, using EDTA in place of extraneous copper ions. All showed either no decline over 30 minutes or very slow decline in the case of the most reactive S-nitrosothiols. However, with SMMA, the absorbance declined to half its value in ten minutes, then increased. Clearly a different product was being formed. The fact that a new product was being formed was also indicated by the formation of a yellow colour in the cell. This showed a distinct peak at approximately 290nm. When repeated using buffer alone, after 1 hour a distinct shoulder at

approximately 340nm had developed (but with no absorbance peak at 540nm, i.e. not re-formation of the S-nitrosothiol).

After 16 hours this shoulder had resolved into a distinct peak at about 340nm as shown in Figure 4.7.
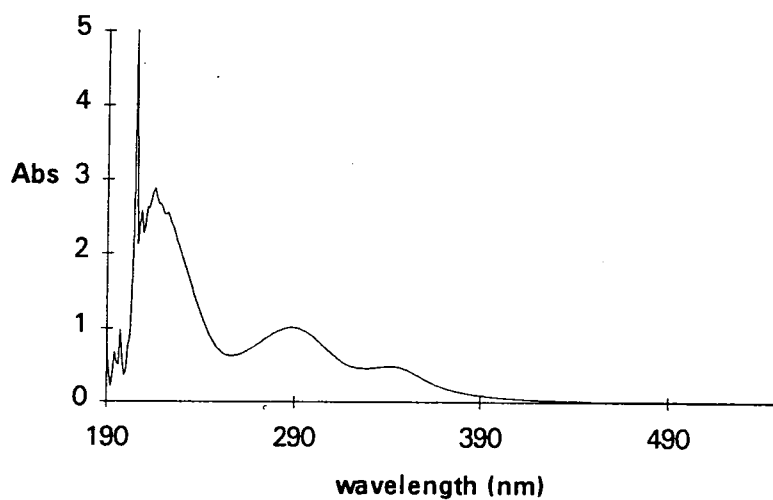
Figure 4.7

The SMMA with EDTA only showed a slight shoulder after this length of time cf in buffer alone after one hour.

When repeated with added copper (5 x 10^{-5} M in-cell, SMMA at 5 x 10^{-4} M in-cell as before) over 30 minutes, the initial SNO peak at 335nm changed to a peak at 350nm and more slowly developed another peak at 290nm, as shown in Figure 4.8.
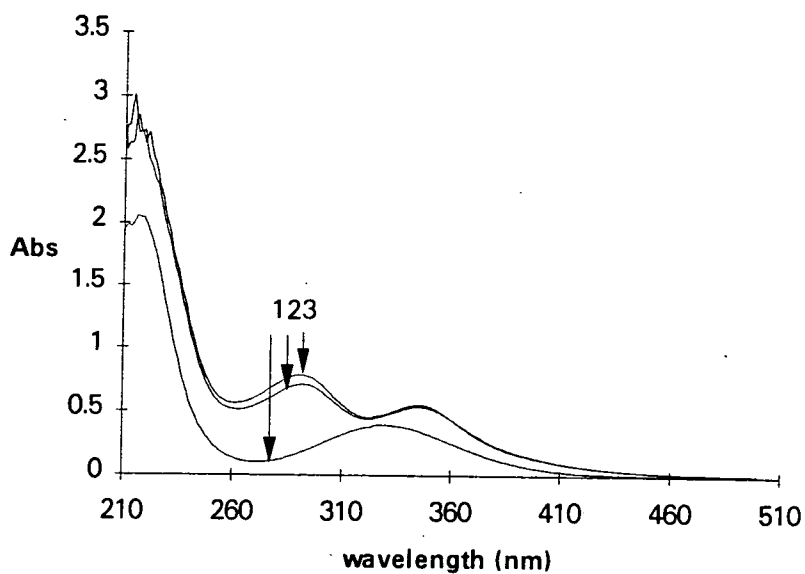
1 = After 0 mins   2 = After 15 mins   3 = After 30 mins

Figure 4.8

After 16 hours this had resolved into twin peaks as shown in Figure 4.9
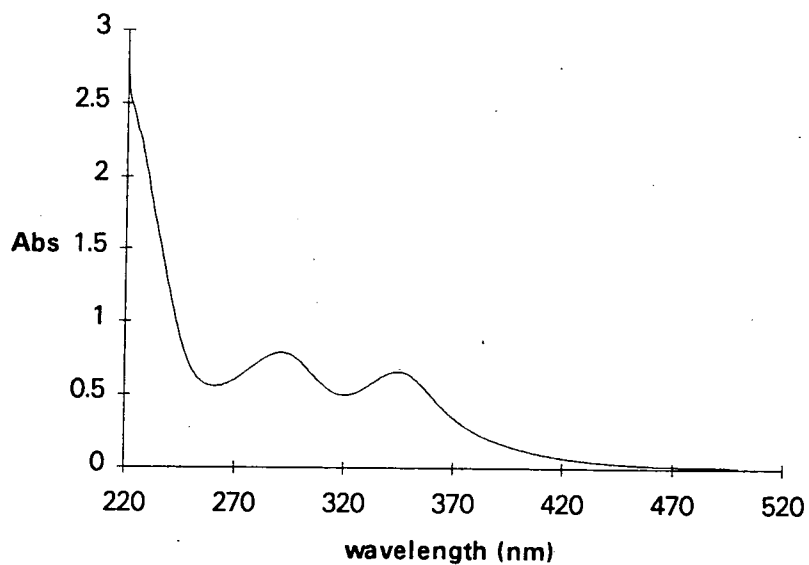
Figure 4.9

With EDTA, over 20 minutes a peak at 288nm was formed, (Abs = 0.982 after 18 minutes) with no shoulder at 350nm. With copper ions at 1×10^{-4} M in-cell, twin peaks form at 344nm (Abs = 0.649) and 294nm (Abs = 0.653).

The formation of the peak at approximately 290nm was measured at 288nm until completion. It was found that the trace obeyed excellent first order kinetics, k_{obs} = $2.09 \times 10^{-2}\,s^{-1} \pm 0$.

At higher copper concentration, i.e. 5×10^{-4} M in-cell, SMMA as before, over 30 minutes, yet another reaction occurred. The scan seemed to indicate two slight shoulders at 290nm and 350nm superimposed on a spectrum similar to that of a normal disulphide decomposition product. Other methyl esters of S-nitrosothiols do not give these effects, i.e. decomposition appears to be the same as for the free acid analogue (so far as is known). It would appear that the S-nitrosothiol of methyl mercaptoacetic acid reacts, in the presence of buffer at pH 7.0 but in the absence of copper, to form a new compound with a distinct absorbance peak *ca.* 290nm. In the presence of very low concentrations of copper (II) ions this product is initially formed but over considerable time some new product is formed with a distinct absorbance peak at 350nm. At higher copper concentrations this 350nm compound is formed first and later the 290nm compound develops. Possibly an equilibrium situation exists, with slow interconversion between the two. Finally, at high copper concentrations decomposition via a "normal" pathway takes place, and is additional to these reactions. See Chapter 5 for a further, complementary analysis of this reaction.

4.7 SMAA decomposition examined

An analysis of the decomposition of S-nitroso-mercaptoacetic acid (SMAA) in acetate buffer (treble concentration) at pH 5.0 with various concentrations of copper ions was performed. It was hoped that buffer interference would be minimal as the carboxylate group was common. The system gave fairly good reproducible traces on the stopped

flow attachment. In all cases SMAA was 5×10^{-4} M in-cell. As well as in a variety of copper concentrations, the SMAA was added to buffer alone and buffer plus EDTA. No decomposition was apparent with EDTA but a <u>very</u> slow decomposition occurred in buffer alone. This was difficult to measure accurately, but was taken as 8.7×10^{-5} s^{-1} $\pm$ 0.4. The concentration of copper ions was taken over the range 1×10^{-5} M to 1×10^{-2} M in-cell. The results were as shown in Table 4.11.

$[Cu^{2+}]$ /M	$10^2 \times k_{obs}$ (s^{-1})	$10^2 \times$ Mean (s^{-1})
1×10^{-5}	2.89 $\pm$ 0.10 2.89 $\pm$ 0.14 2.79 $\pm$ 0.11 2.73 $\pm$ 0.12	2.83 $\pm$ 0.07
5×10^{-5}	2.04 $\pm$ 0.08 1.87 $\pm$ 0.14 1.93 $\pm$ 0.12 1.78 $\pm$ 0.11	1.91 $\pm$ 0.09
1×10^{-4}	2.08 $\pm$ 0.12 1.86 $\pm$ 0.13 1.81 $\pm$ 0.11 1.70 $\pm$ 0.11	1.86 $\pm$ 0.14
5×10^{-4}	1.60 $\pm$ 0.09 1.75 $\pm$ 0.08 1.77 $\pm$ 0.07 1.52 $\pm$ 0.09	1.66 $\pm$ 0.10
1×10^{-3}	1.69 $\pm$ 0.17 1.73 $\pm$ 0.15 1.61 $\pm$ 0.16 1.54 $\pm$ 0.15	1.64 $\pm$ 0.07
5×10^{-3}	1.93 $\pm$ 0.19 2.01 $\pm$ 0.20 2.06 $\pm$ 0.22 1.88 $\pm$ 0.19	1.97 $\pm$ 0.07
1×10^{-2}	2.01 $\pm$ 0.29 1.89 $\pm$ 0.24	1.95 $\pm$ 0.06

Table 4.11

The results when plotted graphically seemed to indicate higher catalytic activity at low (catalytic) concentrations and a puzzling <u>decrease</u> in reactivity at higher concentrations (see Figure 4.10). The first order "quality" of the data curves could have been better

however and the possibility of random behaviour at these higher concentrations cannot be ruled out.

k_{obs} (mean) x 100 sec^{-1}

[Cu^{2+}] x 10^{-5} /M
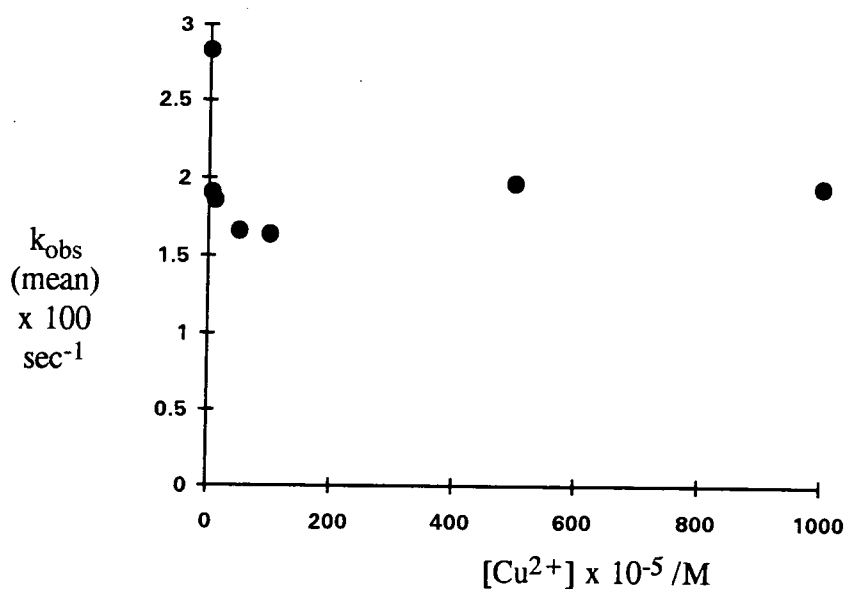
Figure 4.10

4.8 Stopped flow analysis of S-nitroso-cysteine decay

The decomposition of L-cysteine S-nitrosothiol (SCYS) over a wide range of copper (II) concentration was examined at pH 7.0 in KH$_2$PO$_4$/NaOH buffer, treble concentration, with the S-nitrosothiol at 5 x 10^{-4} M in-cell concentration. The results are shown below in Table 4.12.

Table 4.12

SCYS in PO$_4$ (3 x) pH 7.0, 5 x 10^{-4} M : 1 x 10^{-4} M Cu			
	k_{obs} (s^{-1})	Correl.	Mean k_{obs} (s^{-1})
6CYSCU7	0.157 ± 0.002	(0.981)	
6	0.137 ± 0.001	(0.974)	
5	0.151 ± 0.001	(0.989)	0.137 ± 0.001
4	0.138 ± 0.001	(0.984)	
3	0.138 ± 0.002	(0.972)	
2	0.136 ± 0.001	(0.989)	
1	0.137 ± 0.003	(0.938)	

Table 4.12 continued

SCYS in PO_4 (3 x) pH 7.0, 5×10^{-4} M : 7.5×10^{-5} M Cu			
	k_{obs} (s^{-1})	Correl.	Mean k_{obs} (s^{-1})
5CYSCU1	0.071 ± 0.002	(0.911)	
2	0.070 ± 0.002	(0.901)	
3	0.071 ± 0.002	(0.905)	0.072 ± 0.003
4	0.069 ± 0.002	(0.902)	
5	0.072 ± 0.002	(0.897)	
6	0.077 ± 0.002	(0.902)	

SCYS in PO_4 (3 x) pH 7.0, 5×10^{-4} M : 5×10^{-5} M Cu			
	k_{obs} (s^{-1})	Correl.	Mean k_{obs} (s^{-1})
4CYSCU1	0.068 ± 0.003	(0.889)	
2	0.067 ± 0.003	(0.890)	
3	0.068 ± 0.002	(0.898)	0.070 ± 0.004
4	0.072 ± 0.003	(0.890)	
6	0.076 ± 0.002	(0.895)	

SCYS in PO_4 (3 x) pH 7.0, 5×10^{-4} M : 4×10^{-5} M Cu			
	k_{obs} (s^{-1})	Correl.	Mean k_{obs} (s^{-1})
3CYSCU2	0.071 ± 0.002	(0.899)	
3	0.070 ± 0.002	(0.904)	
4	0.072 ± 0.002	(0.899)	0.072 ± 0.002
6	0.074 ± 0.002	(0.896)	
7	0.071 ± 0.003	(0.899)	

SCYS in PO_4 (3 x) pH 7.0, 5×10^{-4} M : 2.5×10^{-5} M Cu			
	k_{obs} (s^{-1})	Correl.	Mean k_{obs} (s^{-1})
2CYSCU2	0.066 ± 0.002	(0.912)	
3	0.064 ± 0.002	(0.906)	
4	0.058 ± 0.002	(0.911)	0.062 ± 0.003
5	0.061 ± 0.002	(0.916)	
7	0.059 ± 0.002	(0.908)	

SCYS in PO_4 (3 x) pH 7.0, 5×10^{-4} M : 1×10^{-5} M Cu			
	k_{obs} (s^{-1})	Correl.	Mean k_{obs} (s^{-1})
1CYSCU1	0.028 ± 0.000	(0.984)	
3	0.033 ± 0.000	(0.983)	
4	0.036 ± 0.000	(0.985)	0.034 ± 0.004
6	0.035 ± 0.000	(0.982)	
7	0.038 ± 0.000	(0.978)	

SCYS in PO_4 (3 x) pH 7.0, 5×10^{-4} M : Alone in buffer			
	k_{obs} (s^{-1})	Correl.	Mean k_{obs} (s^{-1})
0CYSCU2	0.025 ± 0.001	(0.848)	
3	0.035 ± 0.002	(0.826)	0.031 ± 0.005
4	0.032 ± 0.0016	(0.850)	

The results gave a graph which appeared to indicate <u>some</u> linearity at low copper concentrations, but above 4×10^{-5} M this ceased. The curves were quite reproducible for any given concentration, and a reasonable fit to first order kinetics, including those done in buffer alone. (See Figure 4.11).

$$10^5 \times [Cu^{2+}] \; / \; mol \; l^{-1}$$
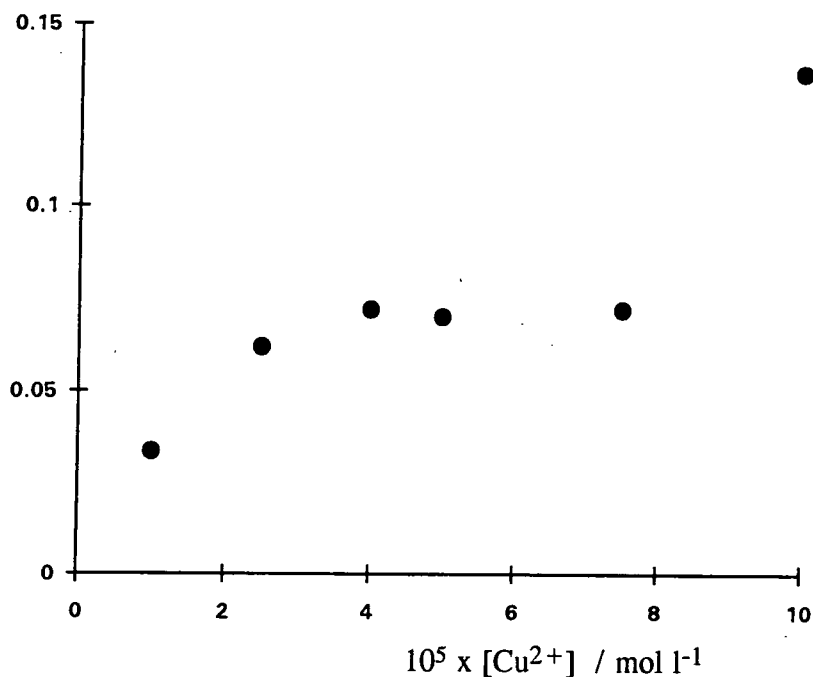
Figure 4.11

This work was repeated, care being taken to perform at least six runs per concentration. The results are shown in Table 4.13

Table 4.13

SCYS alone in buffer PO$_4$ (3 x) pH 7.0, 5×10^{-4} M			
	k_{obs} (s^{-1})	Correl.	Mean k_{obs} (s^{-1})
2CYSCU1	0.097 ± 0.002	(0.920)	
3	0.114 ± 0.003	(0.903)	
4	0.096 ± 0.002	(0.916)	0.094 ± 0.011
5	0.094 ± 0.002	(0.932)	
7	0.096 ± 0.002	(0.919)	
8	0.079 ± 0.002	(0.935)	
9	0.082 ± 0.002	(0.914)	

Table 4.13 continued

SCYS in PO_4 (3 x) pH 7.0, 5 x 10^{-4} M, 1 x 10^{-5} M Cu			
	k_{obs} (s^{-1})	Correl.	Mean k_{obs} (s^{-1})
3CYSCU4	0.134 $\pm$ 0.001	(0.966)	
5	0.130 $\pm$ 0.001	(0.961)	
6	0.126 $\pm$ 0.001	(0.980)	0.130 $\pm$ 0.004
7	0.136 $\pm$ 0.001	(0.964)	
8	0.125 $\pm$ 0.002	(0.967)	
10	0.126 $\pm$ 0.001	(0.969)	

SCYS in PO_4 (3 x) pH 7.0, 5 x 10^{-4} M, 2.5 x 10^{-5} M Cu			
	k_{obs} (s^{-1})	Correl.	Mean k_{obs} (s^{-1})
4CYSCU2	0.169 $\pm$ 0.001	(0.975)	
3	0.167 $\pm$ 0.001	(0.974)	
4	0.165 $\pm$ 0.001	(0.971)	
5	0.168 $\pm$ 0.001	(0.969)	0.169 $\pm$ 0.003
6	0.173 $\pm$ 0.001	(0.967)	
7	0.173 $\pm$ 0.001	(0.967)	
8	0.168 $\pm$ 0.001	(0.972)	
9	0.168 $\pm$ 0.001	(0.972)	
10	0.171 $\pm$ 0.001	(0.971)	

SCYS in PO_4 (3 x) pH 7.0, 5 x 10^{-4} M, 5 x 10^{-5} M Cu			
	k_{obs} (s^{-1})	Correl.	Mean k_{obs} (s^{-1})
5CYSCU1	0.270 $\pm$ 0.002	(0.968)	
2	0.275 $\pm$ 0.002	(0.964)	
3	0.287 $\pm$ 0.002	(0.967)	
4	0.267 $\pm$ 0.002	(0.966)	0.276 $\pm$ 0.006
5	0.280 $\pm$ 0.002	(0.967)	
7	0.281 $\pm$ 0.002	(0.962)	
8	0.277 $\pm$ 0.002	(0.961)	
9	0.275 $\pm$ 0.002	(0.968)	
10	0.273 $\pm$ 0.002	(0.961)	

Other runs were performed at concentrations higher than 5 x 10^{-5} M for copper, but although these gave good, consistent traces, the kinetics were widely different from first order, whereas at these lower concentrations the fit to first order was good, as is shown by the correlation coefficients and the low value for standard deviation in each cohort at any given concentration. The Cu^{2+} concentration in the buffer alone was

calculated to be 0.16 x 10^5 M from the results of previous analysis. The results are plotted in Figure 4.12.

10^5 x [Cu (II)] (M)
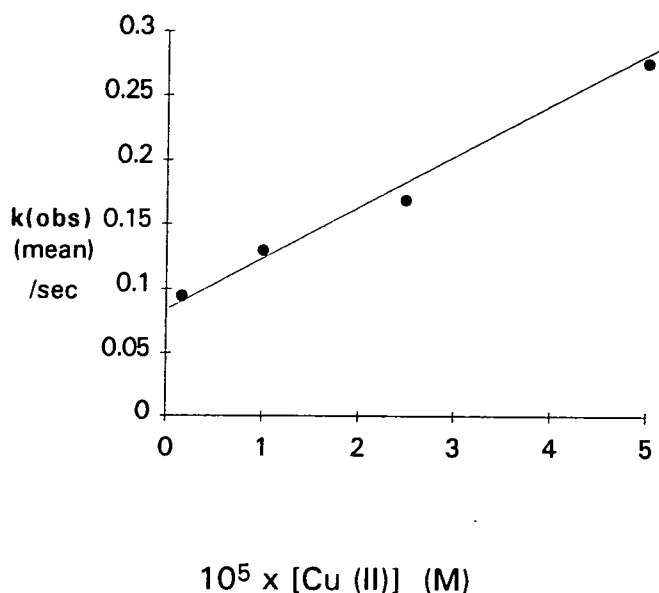
Figure 4.12

It will be noted that there is a clearer distinction between k_{obs} (mean) for each concentration of copper in the last work, much more in line with what might be expected. Furthermore, it will be noted that a distinct difference exists between the k_{obs} (mean) for any pair of values at a given copper concentration. The reason for this is not apparent, as the same procedures were followed for both experiments. The linear nature of results at low Cu^{2+} concentration is more apparent also.

The obvious further line of enquiry would be to vary the SCYS concentration while maintaining copper concentration (at a low level such as 1 x 10^{-5} M) in order to obtain a value for k with respect to SCYS, but time did not allow this. Further work is required also on other S-nitrosothiols with regard to copper catalysis, ensuring that only concentrations of copper below 5 x 10^{-5} M are used.

4.9 SUMMARY

4.9.1 Introduction

The various attempts to determine the parameters governing the decomposition of SNAP and other S-nitrosothiols had proved very frustrating. It was with a definite degree of chagrin therefore that the source of this problem proved to be so simple (with hindsight) namely trace quantities of metal ions in the water supply, specifically copper (II) ions. However, the picture is not quite as simple as this, as previous experimental work had shown that, at least in the case of SNAP, thermal and/or photo effects can also play a part in the decomposition. Refluxing a solution of SNAP in dry methanol in the dark rapidly produces the disulphide[1], while allowing SNAP to stand in pure dioxan in sunlight causes similar decomposition. Concentrations of copper would be expected to be negligible in both solvent systems, by their nature.

Most of the experimental work performed previously, that proved so puzzling, can now be explained in terms of metal ion (copper (II)) catalysis. It must be stated that the list of metal ions tested was not exhaustive and there may be other metal ions, untested, which have some catalytic decomposition effect upon S-nitrosothiols. Thus no rare earth metals were tested and some transition metal ions were omitted. Of the latter that were tested, many exist in several other valence states, often less stable in solution and these may have catalytic ability. Two that were obvious candidates were Fe^{2+} and Cu^+ ions, especially the latter given the known catalytic ability of Cu^{2+} ions. Both have subsequently been shown to be catalytic - Fe^{2+} ions have a slight effect[2] and Cu^+ ions have a far greater catalytic effect than Cu^{2+} ions[3]. Unfortunately time did not permit the setting up of the involved experimental conditions (rigorous exclusion of oxygen from apparatus and solutions).

Similar time constraints applied to the results with Hg^{2+} ions. Although there are references to the reaction of Hg^{2+} ions with all manner of S-derived compounds[4, 5] including R-SNO compounds[6] it does not seem to be the case that the kinetics have been examined for various R-SNO compounds. These should be amenable to stopped

flow kinetic analysis, given their speed and the fact that any products do not appear to interfere with measurement of absorbance decline at 340nm.

4.9.2 Buffer solutions

The work on buffer solutions, performed primarily with SNAP, can be explained to a large extent by the presence in all solutions of intrinsic copper (II) ions. The copper analyses carried out demonstrated that the distilled water used in the laboratory was of poor quality (from an old still). Also, copper was present in all buffer solutions prepared, to a greater or lesser extent, depending on the nature of the constituents. The largest source was probably the sodium hydroxide pellets used to make many of the buffers, as shown by the increasing copper (II) content of acetate buffer with increasing pH (increasing sodium hydroxide concentration) and between TRIS/Maleate/NaOH buffer pH 7.4 and TRIS/HCl buffer pH 7.4. These buffers represented therefore a significant addition to the background copper present in the water. The availability of the copper (II) ions is complicated, however, by the effect of pH change on the structure of the copper/ligand complex[7, 8].

The other complicating factor will be the effect of the buffer salt constituents themselves upon the copper ions. Some buffer constituents such as DGA, HEPES, TRIS and Maleate would be expected to chelate the copper ions, (although how successfully will depend upon molecular structural factors) as has been demonstrated for some of them e.g. citrate, imidazole, DGA, as illustrated in Figure 4.13 below.

Maleate   DGA
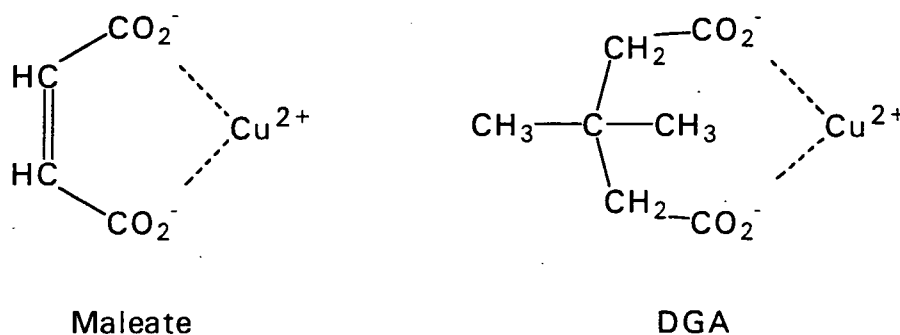
Figure 4.13

With others, such as phosphate, the solubility product of copper phosphate will probably be a factor.

Thus the decomposition kinetics of any particular S-nitrosothiol would be expected to depend upon a multiplicity of factors such as buffer type and concentration, copper concentration inherently present, pH, etc. This would lead to the situation that was actually observed, where the kinetics were difficult to measure consistently. The appearance of half order kinetics, indicative (often) of free-radical kinetics could be taken to be an artifact, but may have some basis for rationalisation in terms of the actual reactions mechanism(s).

4.9.3 Copper-induced decomposition

The experimental work seems to have proven that copper (II) ions are responsible for the general decomposition of the S-nitrosothiols that have been observed under various conditions. Supporting this is the fact that in every case where decomposition was observed, addition of EDTA at a concentration in excess of the known/anticipated copper ion concentration produced complete (or in the case of the most reactive S-nitrosothiols, virtually complete) reduction in decomposition. Also, addition of copper (II) ions to the particular solution increases the rate of decomposition significantly.

Copper may form five, six or seven-membered ring systems with compounds containing nitrogen and sulphur, e.g. S-nitrosothiols, as shown in the following possible structures (Figure 4.14).

A
5 - membered ring

B
6 - membered ring

C 6 - membered ring
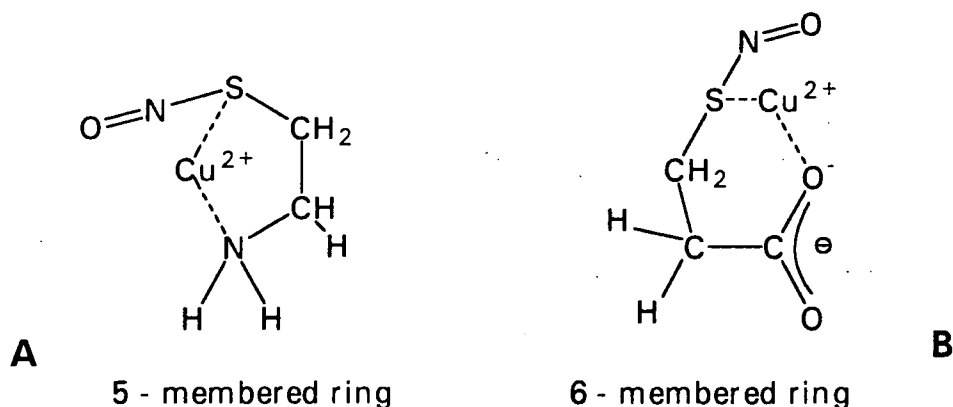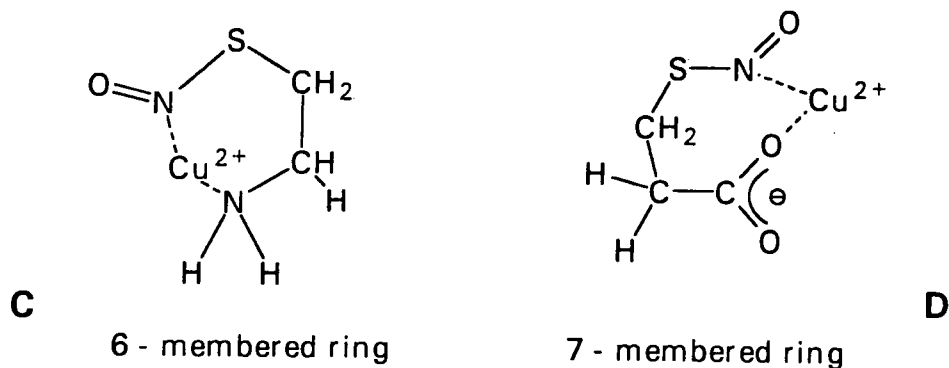
D 7 - membered ring

Figure 4.14

If this <u>is</u> the case for the S-nitrosothiol compounds, then it might be expected that

A) six-membered ring systems would be more likely to form as they are more energetically favoured, and this in turn would mean that RSNO compounds of this type would be more easily decomposed.

B) The possession of a free NH_2 moiety in the molecular structure would ensure a greater rate of decomposition, as copper ions would be more easily held than if this function was combined.

C) Esterification might lead to a reduction in the rate of decomposition as the acetate anion could not be formed. (At the pHs employed in all this work, the free acetate function would be to all intents 100% ionised.)

4.9.4 Structure and reactivity

i) Introduction

The preliminary work that has been performed has suggested some answers. It is
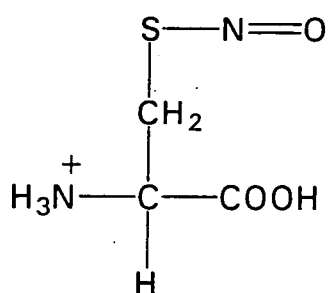
Low pH form of SCYS
Figure 4.15

known that all S-nitrosothiols examined are very stable in acidic solution (<pH 2) whether in water or buffer. At low pH all amine groups would be protonated and an acetate group would be in the molecular form, so neither would readily help to combine with copper (II) ions,

141

which might also be less readily chelated if in the hexa aqua form (see Figure 4.15).

The optimum pH for catalysis by copper (II) ions to occur therefore would be around pH 7, when the COOH group is totally ionised and the $^+NH_3$ group is becoming de-protonated. This does seem to give credence to the view that the copper (II) ions are exercising their effect via chelation by the <u>amine</u> and the nitrogen or the sulphur atoms of the SNO group on one side <u>or</u> the <u>carboxylate anion</u> and the nitrogen or the sulphur atoms of the SNO group on the other, or a combination of both.

ii) SNAP and SPEN
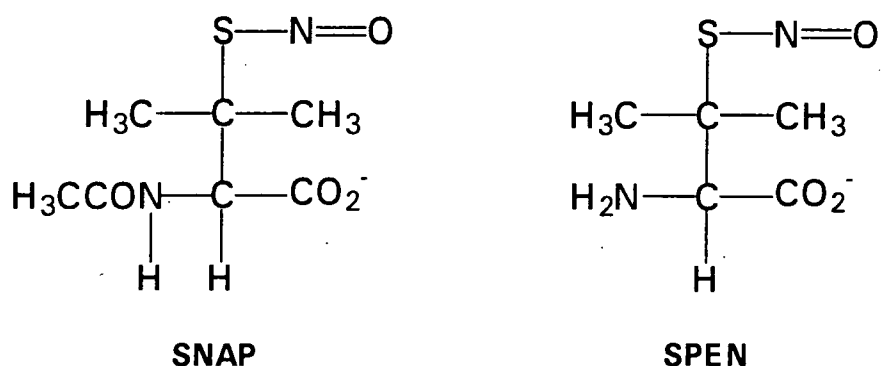
Figure 4.16

It was found that SPEN was approximately fourteen times more reactive than SNAP under identical conditions (see Figure 4.16). This seems to indicate the importance of the NH_2 group in the decomposition process, since the effectiveness of the amine group for binding Cu(II) ions will be greatly decreased by its acetylation, due to the electron-withdrawing effect of the acetyl moiety delocalising the nitrogen lone pair.

iii) Importance of a free amine group

Figure 4.17

142
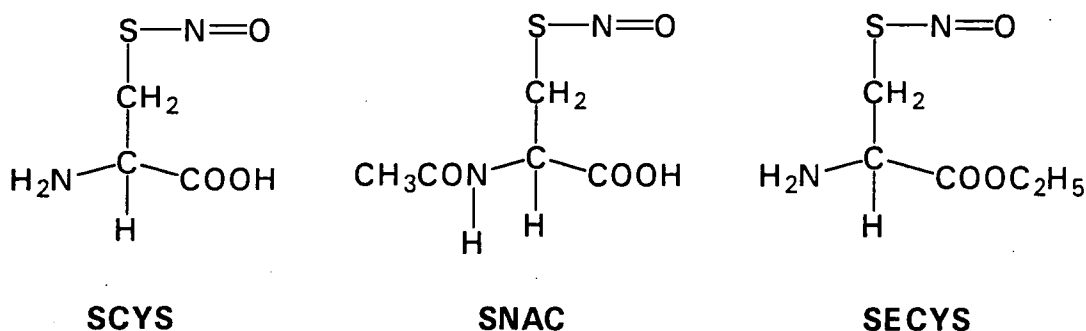
Confirmation was given in this work about the importance of a free NH_2 group, as it was clearly shown that SCYS is approximately one thousand times more reactive than SNAC (although this figure is open to question in terms of its magnitude, the absolute reactivity difference is not). (See Figure 4.17). However, it was found that the ester is even more reactive than cysteine itself (by approximately five times). This would tend to indicate that there may be competition between the amine and carboxylate functions for chelation (and subsequent reaction) of copper. Furthermore, although both lead to subsequent decomposition, (as the total absence of an amine group does not prevent copper ion catalysis of an S-nitrosothiol), the k_{obs} figures indicate that the decomposition is very much mediated via the amine function and that a free carboxylate function is very much slower, thus acting as a (competitive) hindrance to the overall rate of decomposition. This could be confirmed by:-

A)   testing the reactivity of the ethyl ester of SNAC - it should be extremely unreactive. This chemical was unavailable and no attempt was made to synthesise it.

B)   testing the reactivity of the ethyl/methyl ester of SPEN - it should be even more reactive than SPEN itself. This chemical was also unavailable and an attempt to synthesise a simpler thiol ester failed - if it had been successful, the SPEN ester was going to be synthesised next. Although two alternative preparative methods were discovered in the literature[9, 10], no time was available to perform the syntheses.

C)   testing the compounds shown below in Figure 4.18.
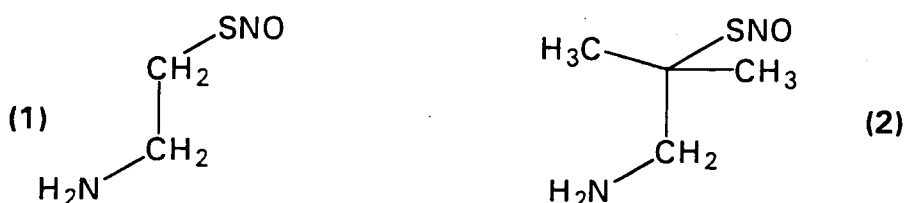
Figure 4.18

Both should be extremely reactive in the presence of copper (II) ions, with compound (1) being at least as reactive as ethyl cysteine SNO, and probably more so as there would be less steric hindrance, while (2) should be marginally less reactive (and green in colour). Compound (2) was not available but while compound (1) (cysteamine) was available, time had run out for further experimental work before its use could be considered.

It was noted that SCYS was about twice as reactive as SPEN, which possibly may be due to steric hindrance (caused by the bulky methyl groups attached to the SNO carbon) affecting the initial formation of the copper-S-nitrosothiol complex. However, other values for SCYS have been lower than this, approximating to the same value of k_{obs} as SPEN, so this is highly debatable.

iii) Simple free acids and esters

| SMAA | SMMA | SMPA | SMMP |

STLA
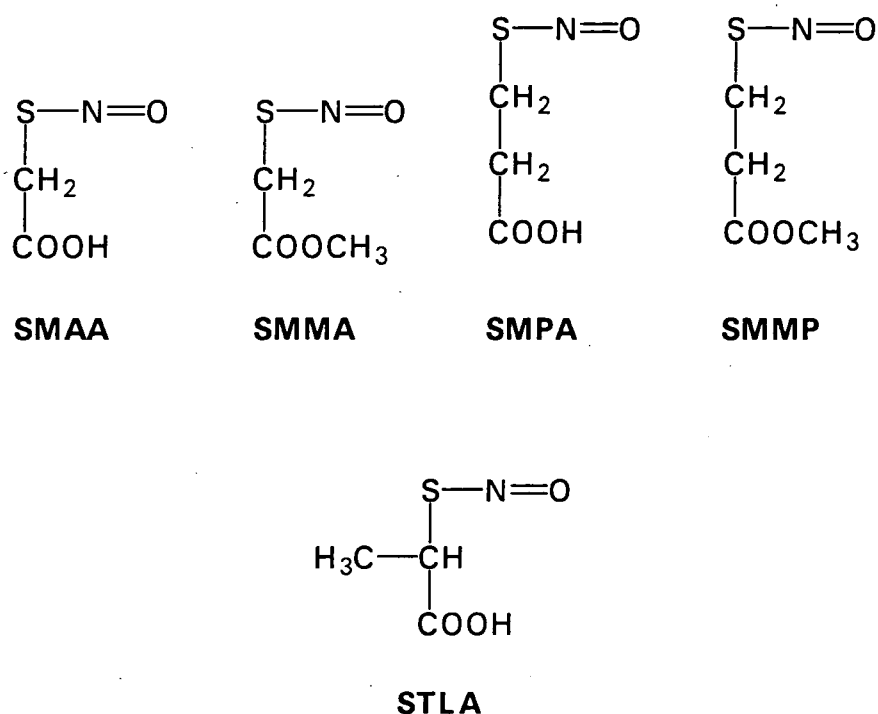
Figure 4.19

As expected, the simple free acids were much less reactive than those compounds containing an amine function. (See Figure 4.19.) Some evidence was produced to suggest that a compound capable of forming a seven-membered ring structure with copper (SMPA) was much less reactive than one producing a six-membered structure, but this was not definitely shown as unfortunately the buffers used were different, although identical conditions prevailed in all other respects. Much more substantive was the fact that the esters were distinctly unreactive compared to the corresponding acid, as might be expected. SMMA is a special case in that it appears to undergo unique reactions unconnected with copper catalysis. An attempt was made to synthesise isobutyrate-2-thiol from 2-bromo isobutyric acid with a view to producing the S-nitrosothiol (SMIBA) shown in Figure 4.20 (it was unavailable otherwise).
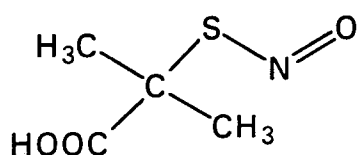
Figure 4.20   **SMIBA**

This would have been used to investigate whether a tertiary carbon atom attached to the SNO group

A) was responsible for the green coloration of such compounds.

B) did have an effect upon k_{obs} by comparison with SMAA and STLA.

Unfortunately, although several methods were attempted (see experimental section) it could not be synthesised.

iv) Miscellaneous

SNOCAP

$$S-N=O$$

NH₂ on the structure...

The chemical structure diagram shows:

H—C(NH₂)(COOH)—(CH₂)₂—C(=O)—NH—CH(CH₂—S—N=O)—C(=O)—NH—CH₂—COOH
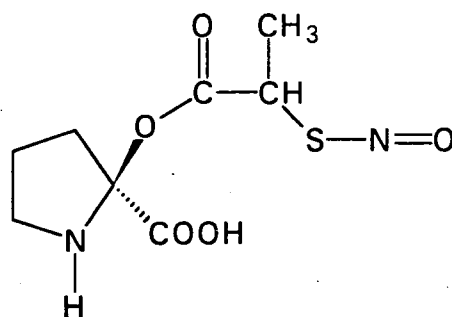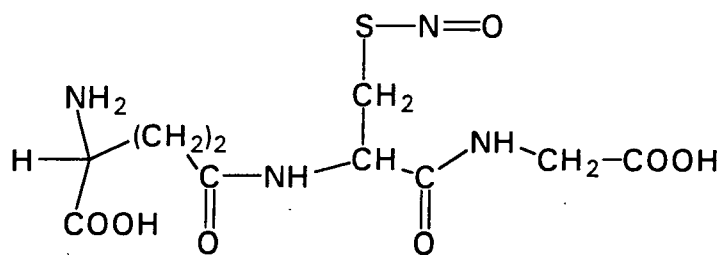
SNOG

Figure 4.21

The anomalous unreactivity of the above compounds, (Figure 4.21) which are relatively unreactive and yet contain an amide or imine function can be explained as follows. In the case of SNOG, which is a tripeptide of glutamate/cysteine/glycine, the amine is effectively combined as in N-acetyl cysteine, while the carboxylate group is effectively removed by formation of a peptide linkage with the amine of the glycine. The two reactive sites are thus removed and this (coupled with the steric hindrance produced by the bulky glutamate and glycine residues on either side of the cysteine SNO moiety) ensure that SNOG is remarkably stable.

Similarly, SNOCAP is very unreactive because the nitrogen is in a ring system as a secondary amine and the carboxylate function is kept *trans* to the SNO group by the ring, which inhibits copper complex formation. Paradoxically, both of these compounds would have worked as vasodilatory agents, via release of NO in biological systems. It is clear that their breakdown and release of NO in biological situations must be mediated via enzymic systems and <u>not</u> be metal ion mediated. In fact, the biological reactivity of S-nitrosothiols has been shown to bear little relation to their chemical reactivity[11]. The most obvious example of this is SNOG, which is chemically relatively unreactive, yet has important biological roles e.g. anti-platelet aggregation[12].

4.9.5 Decomposition at varying copper concentrations

The results of the limited work done with cysteine and mercaptoacetic acid S-nitrosothiols were inconclusive. With SCYS, there appeared to be a reasonable linearity at low copper concentrations, indicating a first order dependence on Cu^{2+} ion, but this rapidly deteriorated and appeared to plateau. Also, despite rigorous adherence to reproducing identical conditions, there was a wide spread in k_{obs} values obtained for a given copper concentration. With SMAA, there appeared to be a decline in k_{obs} with increasing copper ion concentration, which levelled off. No attempt was made to vary S-nitrosothiol concentration at constant copper concentration and little conclusion can be drawn from this work except to say that the effects are oddly variable.

4.10 Conclusion

It would appear that in the catalytic decomposition of S-nitrosothiols by copper (II) ions, two coordination sites are possible. These are

a) at SNO and NH_2 and

b) at SNO and COO^-.

There is the obvious possibility that copper could coordinate at either the sulphur or the nitrogen atom in the RSNO group (see Figure 4.22).
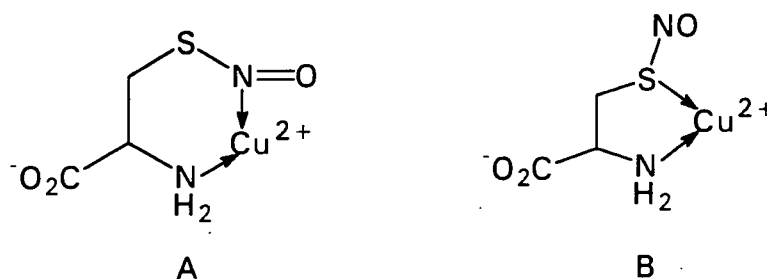
Figure 4.22

However, being a borderline hard acid, Cu^{2+} is known to coordinate better at nitrogen rather than sulphur[8], so it is much more likely that the actual coordination will be as shown in A, particularly as this would entail a six-membered ring structure for the complex. Furthermore, it probably is easier to envisage subsequent NO loss from such a complex, producing the observed decomposition.
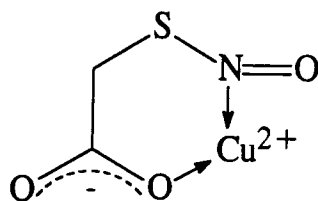
Figure 4.23

In the case of the S-nitrosothiols of carboxylate derivatives e.g. mercaptoacetic acid, the copper (II) ion would be expected to bind as shown in Figure 4.23.

The copper would also be expected to be complexed by the carboxylate anion. This would have the effect of reducing the copper available for binding as shown and would result in decreased decomposition. Such complexation was noted also with buffers such as citrate/NaOH. Decomposition would be expected to be faster with a six-membered ring structure than with a seven-membered ring structure (cf. SMAA and SMPA), as was observed.

Although the fundamentals of the reaction(s) of S-nitrosothiols in aqueous solution appear to have been determined, more work is required and it would be useful to test other compounds to discover more exactly the parameters affecting the catalysis by copper (II) ions. Structures to be tested could include:

A) longer chain analogues of cysteine, to see how this affected catalysis e.g. homocysteine. It would be expected that this would be less reactive, if the idea of a six-membered ring structure as the most reactive complex was correct.

B) esters of various compounds, e.g. NAP and PEN, as previously mentioned.

C) a range of compounds varying in the nature of the carbon atom adjacent to the SNO group (primary, secondary and tertiary) to see if the increased bulkiness did increase reactivity via steric hindrance e.g. S-nitroso-cysteine (primary), S-nitroso-3-methyl-cysteine (secondary) and S-nitroso-penicillamine (tertiary).

By using low concentrations of copper ($< 1 \times 10^{-5}$ M) the kinetics should be consistent and more amenable to analysis, allowing the order(s) with respect to RSNO and Cu^{2+} to be determined. In turn, this may allow some hypothesis to be developed regarding the nature of the Cu^{2+}/S-nitrosothiol reaction complex. In fact, a recent paper[13] has described a Cu^{2+}/penicillamine complex, with a structure as shown below in Figure 4.24. Such complexes may have relevence to aspects of the mechanism of S-nitrosothiol decomposition by Cu^{2+} ions. Other questions which remain to be answered include whether NO is released directly or as NO^+, if disulphide is the only other reaction product and whether copper bonds via the nitrogen or the sulphur of the SNO group, albeit with the former being more likely.
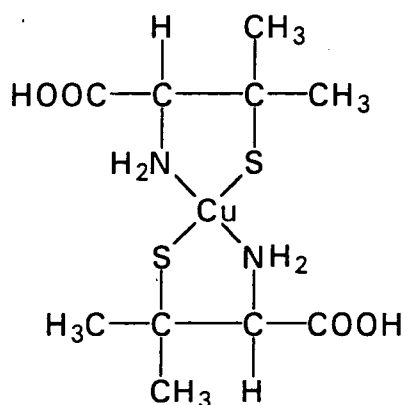
Figure 4.24

References

1. L. Field, R.V. Dilts, R. Ravichandran, P.G. Lenhert, G.E. Carnahan, *J. Chem. Soc., Chem. Comm.*, 1978, 249

2. S.C. Askew, St. Andrews University, personal communication

3. D.J. Barnett, Durham University, Ph.D. thesis

4. V.V. Morchan, F.M. Tulypa, E.Y. Baibarova, *Zh. Neorg. Khim.*, 1979, **24**, 2557

5. L. Sacconi, F. Mani, A. Bencini, in *Comprehensive Coordination Chemistry*, Vol. 5, 1070

6. B. Saville, *Analyst*, 1958, **83**, 670

7. B.J. Hathaway, in *Comprehensive Coordination Chemistry*, 1987, Vol. 5, 682

8. B.J. Hathaway, in *Comprehensive Coordination Chemistry*, 1987, Vol. 5, 594

9. G.R. Ramage, ICI Ltd., British Patent No. 591381, 1947

10. S.M. Kupchan, T.J. Giacobbe, I.S. Krull, A.M. Thomas, M.A. Eakin, D.C. Fessler, *J. Org. Chem.*, 1970, Vol. 35, 3539

11. W.R. Matthews, S.W. Kerr, *J. Pharm. Exp. Ther.*, 1993, **267**, 1529

12. M.W. Radomski, D.D. Rees, A. Dutra, S. Moncada, *Br. J. Pharmacol.*, 1992, **107**, 745

13. A. Hanaki, H. Sago, *Chem. Lett.*, 1994, 109

Chapter 5

Transnitrosation

1. Thiolate Anion Attack on a S-nitrosothiol

2. Direct Nitrosation of a Substrate by a S-nitrosothiol

3. Investigation of MMA reaction with SNAP

5.1 Thiolate Anion attack on a S-nitrosothiol

5.1.1 Introduction

Early work had been performed on SNAP and cysteine solutions in water, with added aliquots of sodium hydroxide solution. SNAP in distilled water was found to be very stable (over 30 minutes, as the pH of the solution was e.g. 4.0). However, when mixed with an equivalent of cysteine in a dilute solution of sodium hydroxide (pH 9.4), it decayed quite rapidly, the new pH of the solution being 8.9. It was observed that the colour of the solution changed from green to red to colourless. This could be interpreted now as the extremely rapid formation of cysteine-S-nitrosothiol (red), followed by its slower decay (to colourless products) as shown in Figure 5.1.
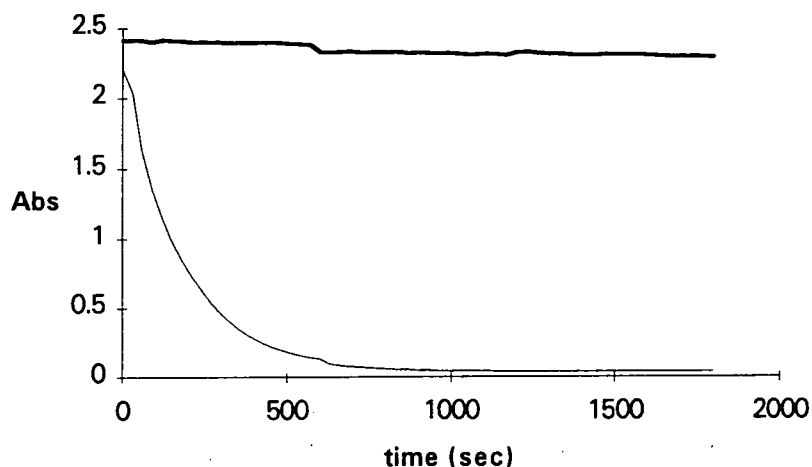
Figure 5.1

It was felt therefore that this possible transnitrosation should be examined more closely.

It would be required that the rate of reaction would be measured by observing the decay at 335-340nm of the SNO moiety of the S-nitrosothiol as it was attacked by the thiolate anion (RS⁻). If it occurred, this would be pH dependent, as with increasing pH more RS⁻ would be formed and hence the rate of decay of the R-SNO compound would increase.

Unfortunately, the product formed would also be an S-nitrosothiol and would therefore have an absorbance maximum in the 335-340nm region.

It was felt that this problem could be circumvented as follows. The attacking thiolate anion could be generated from a simple thiol carboxylic acid, such as mercaptoacetic acid (HS-CH$_2$-COOH, (MAA)). This has pK$_a$ values of 3.5 (COOH) and 10.3 (SH)[1]. If sodium hydroxide was added to it in excess of that required to totally neutralise the carboxylate group, the thiol would act as its own buffer (under pseudo first order conditions) to vary the final pH. SNAP, being green, has a small (ε = 15 mol^{-1} l cm^{-1}) absorbance maximum at 590nm, whereas the red S-nitrosothiols have a maximum at 540nm approximately.

There is very little overlap between these two regions at 600nm, and this was chosen as the wavelength for detecting decrease in absorbance due to the decomposition of the SNO group of SNAP. In order to make the absorbance as large as possible, a concentrated solution of SNAP was required - for an absorbance of only 0.27 at 600nm, a 2 x 10^{-2} M SNAP solution was necessary. As the reaction was extremely quick (alkaline MAA solution added to the green aqueous SNAP solution turned red immediately) stopped flow would be required i.e. a 4 x 10^{-2} M SNAP solution as stock. As SNAP is insoluble in water at this level, a 40% dioxan/water solution was used to solubilise the SNAP. MAA was present at 0.8M in aqueous sodium hydroxide solution. Altering the sodium hydroxide content slowly up from 0.8g (the theoretical equivalent needed to neutralise the MAA carboxylate group) would increase the final, reaction pH.

5.1.2. SNAP and Mercaptoacetic Acid (MAA)

All solutions were made with thoroughly deoxygenated solvents (water and dioxan) to avoid oxidation of the thiol in alkali, and were wrapped in aluminium foil to exclude light, aiding stability. The stopped-flow tubing etc. was also wrapped in aluminium

foil. The results were all excellent first order kinetics and very consistent, at all pH values, as shown in Table 5.1 below.

k_{obs} (Mean) (s^{-1})	Runs	NaOH added (g)	pH
$7.1 \times 10^{-3} \pm 0.2$	6	0.84	6.5
1.16 ± 0.06	12	0.869	9.8
2.94 ± 0.11	12	0.892	9.9
6.28 ± 0.14	6	0.920	10.1
11.71 ± 0.33	15	0.958	10.2
16.18 ± 0.30	12	0.999	10.76
22.3 ± 0.31	13	1.049	10.9
29.2 ± 0.40	9	1.093	11.06
35.2 ± 0.83	13	1.149	11.10
42.51 ± 0.55	14	1.207	11.36
47.2 ± 0.60	14	1.250	11.46
51.7 ± 1.40	14	1.282	11.55
56.62 ± 1.35	14	1.337	11.60
62.84 ± 0.93	14	1.401	11.70
69.3 ± 0.85	21	1.431	11.7

Table 5.1

The pH was measured by adding aliquots of each solution together, but this became difficult to measure at higher pH, possibly as the pH meter was getting beyond its range, or the concentrated alkali solution affected it. It was not possible to proceed beyond 1.43g, as beyond this level phase separation occurred in the MAA/SNAP/dioxan/water system when mixed. A graph of k_{obs} (mean) against pH showed a distinct curve (Figure 5.2), but this trend was much more accurately shown by a graph of k_{obs} (mean) against NaOH added (g), Figure 5.3.
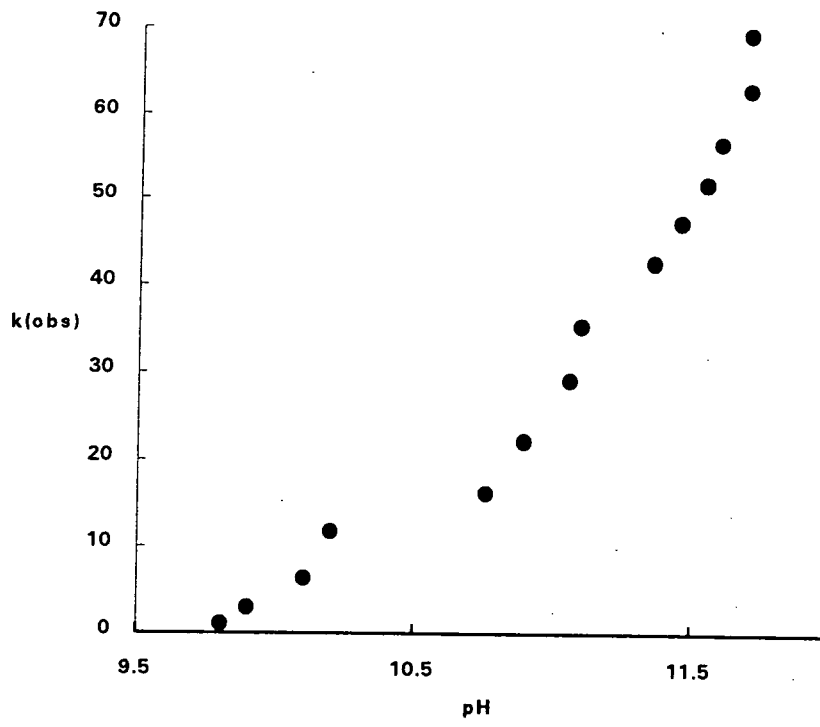
Figure 5.2
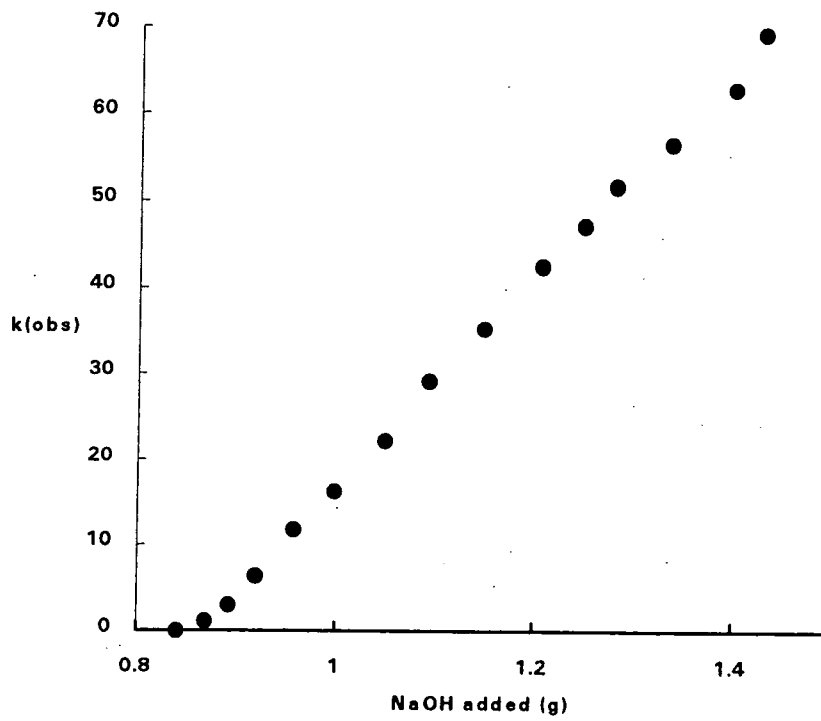
Figure 5.3

In the latter the increase in k_{obs} can be seen to reflect very accurately addition of NaOH. Although the inherent weakness of the system (its high concentration) precluded taking the pH to > 12 (due to NaOH solubility/phase problems), the sigmoidal nature is apparent. Thus it can be said that thiolate anion (RS^-) is the attacking species on R'SNO as its concentration will increase with increasing pH until the thiol is present as 100% RS^-, around pH 12 and above.

Unfortunately, the system does not have any great flexibility and measurement of a series of SNAP/thiol reactions is limited by the requirement for a carboxylate compound of high relative stability (i.e. the simple thiol derivatives of acetic and propionic acids).

5.2.3 Effect of additional thiol

In the proposed reaction

$$SNAP + MAA^- \rightleftharpoons NAP^- + SMAA$$
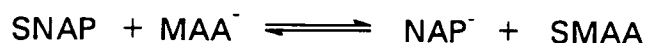
the effect of additional NAP i.e. free thiol, should be to compete with MAA^- in attacking SNAP, hence producing a reduction in k_{obs} (mean) at any given pH. To test this, SNAP and MAA in borax buffer, treble concentration, pH 10.8 were reacted together at a 1:1 equivalence (2×10^{-2} M in-cell) and the k_{obs} values obtained. This was then repeated under identical conditions, with the addition of NAP to the TGA solution at the same equivalence. The curves corresponded extremely well in all cases to second-order kinetics as shown in Tables 5.2.   **Tables 5.2**

SNAP + MAA		SNAP + MAA+NAP	
k_{obs} (mol l^{-1} s^{-1})		k_{obs} (mol l^{-1} s^{-1})	
15.06	(0.993)	10.65	(0.991)
14.83	(0.993)	10.38	(0.992)
15.32	(0.994)	10.36	(0.991)
14.75	(0.994)	10.22	(0.991)
14.39	(0.991)	10.02	(0.991)
16.19	(0.990)	11.05	(0.991)
Mean $= 15.09 \pm 0.57$		Mean $= 10.45 \pm 0.33$	

The results show a very significant difference, with a distinct drop in k_{obs} (mean) in the presence of NAP, as expected. Although these results point to support for thiolate anion attack on RSNO, there was a pH difference of approximately 0.3 units between the two solutions during the reaction and this may account for the observed effect.

5.1.4 Possible use of absorbance maximum differences to detect transnitrosation

One way to measure the transnitrosation would be to use two compounds whose extinction coefficients (ε values) differed widely at the 340nm absorbance maximum. If these were sufficiently different, transnitrosation could be measured by watching the fall at 340nm of the high ε RSNO compound as it was attacked by the thiolate anion of the other compound, producing another RSNO compound of lower ε value.

Several S-nitrosothiols were tested for stability and ε value in 0.1M HCl. Stability was measured as the decline from maximum absorbance at 335nm with time in DGA/NaOH treble concentration pH 7.4 buffer. The ε values were calculated from the maximum absorbance achieved over time when a 1×10^{-3} M equivalent of thiol was nitrosated by a 1.1×10^{-3} M equivalent of $NaNO_2$ in 0.1M HCl, typically (Table 5.3).

Thiol	[RSH]	S-nitrosothiol Abs_{max} (mean)		ε_{335} mol^{-1} l m^{-1}
Glutathione	1×10^{-3}	0.906	(335nm)	906
MAA	1×10^{-3}	0.66	(331nm)	660
MMA	1×10^{-3}	0.78	(331nm)	780
TLA	1×10^{-3}	0.685	(335nm)	685
NAC	5×10^{-4}	0.47	(335nm)	940
NAC	1.5×10^{-3}	1.430	(335nm)	953
CAPT	1.5×10^{-3}	1.59	(335nm)	1060
CYST	2.7×10^{-2}	2.00	(336nm)	741

Table 5.3

In terms of stability and difference in ε values, the best two examples were SNOG and SNOCAP. Using 1.5×10^{-3} M solutions of each, a 0.25 absorbance unit drop was potentially available. Both the compounds are quite soluble (more so than SNAP) and therefore should be able to be used in (say) treble concentration alkali buffers such as Borax/NaOH. SNOG and cysteine S-nitrosothiol (SCYS) by comparison have less than a 0.1 Abs. unit difference at 335nm at the same in-cell concentration. When both systems were tried, at the physiological pH 7.4 in DGA/NaOH buffer, no discernible reaction appeared to take place, even between SNOG and captopril, over two hours. This appears to refute the possibility of transnitrosation occurring between these biological compounds at physiological pH 7.4, by non-enzymic means. However, it could be that the sensitivity of the system was not sufficient to detect this.

5.2 Direct Nitrosation of a Substrate by a S-nitrosothiol?

5.2.1 Introduction

The view that a NO donor in a biological system could donate directly a NO group to another compound e.g. a thiol, haem group or protein has yet to be substantiated. An attempt was made to ascertain whether a S-nitrosothiol could donate a NO group directly to a compound. N-methylaniline was chosen as the model substrate because much is known about its reactivity with a wide variety of nitrosating agents in many solvent systems[2]. The experiments were performed at pH 7.4 (physiological pH), using a buffer system (DGA/NaOH) that does not contain any compound that might itself react with NO in a competitive reaction. SNAP was initially chosen as it is known to be a stable solid which can be prepared in a pure state. The proposed sequence was as shown below, it being known that NMA is nitrosated at the amine group, giving a yellow species, N-nitroso-N-methylaniline (NMANO) (Equation 5.1).
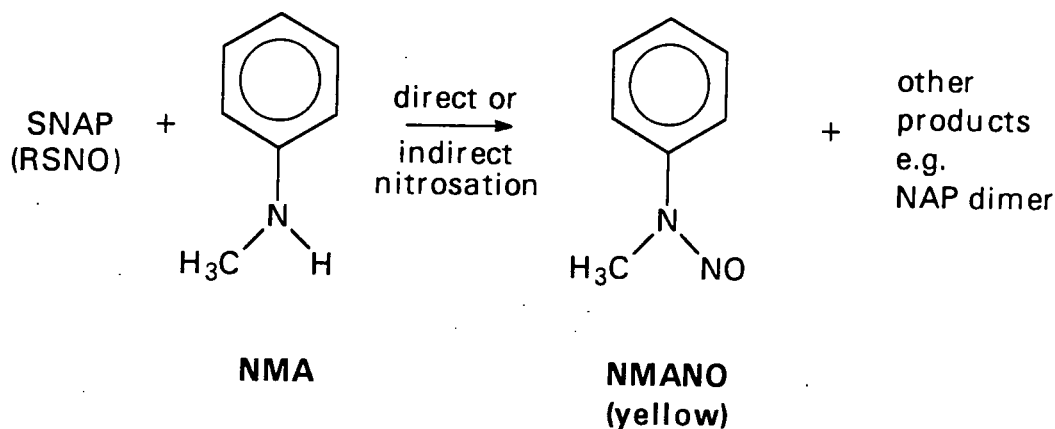
Equation 5.1

NMA was freshly distilled and kept refrigerated. It dissolved easily in both pH 4.0 and 7.4 buffers (DGA). A scan showed that introducing one crystal of $NaNO_2$ into NMA in pH 4.0 buffer produced a huge absorbance change at 260nm (Figure 5.4).
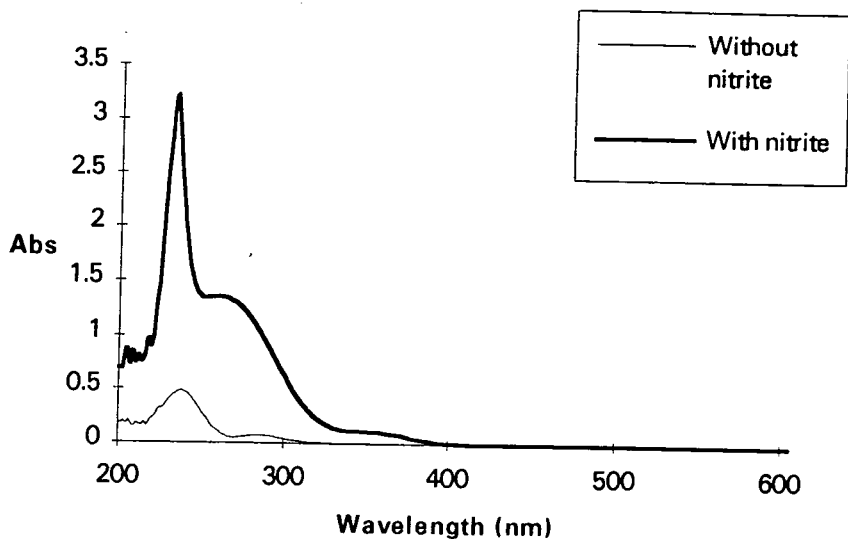
Figure 5.4

When compared to $NaNO_2$ in buffer alone, the region with the greatest change (26x) was at 270nm. When SNOG was added to the buffer, and NMA in buffer introduced, no reaction occurred (pH 4.0). Upon adding one crystal of $NaNO_2$, a huge absorbance at 270nm was noted i.e. no transnitrosation had occurred with SNOG at pH 4.0.

5.2.2. SNAP and N-methylaniline (NMA)

In DGA/NaOH buffer, pH 7.4, SNAP and NMA (both 4×10^{-4} M) produced a rapid rise at 270nm. The kinetics were excellent half order.

When the same buffer was thoroughly deoxygenated, very little or no reaction occurred with SNAP. Upon agitating the buffer in air and re-using, the SNAP again produced a marked rise in absorbance at 270nm. This effect was regularly reproducible, although bubbling air into the deoxygenated cell in the course of the reaction produced only an extremely slight rise in absorbance (Figure 5.5).
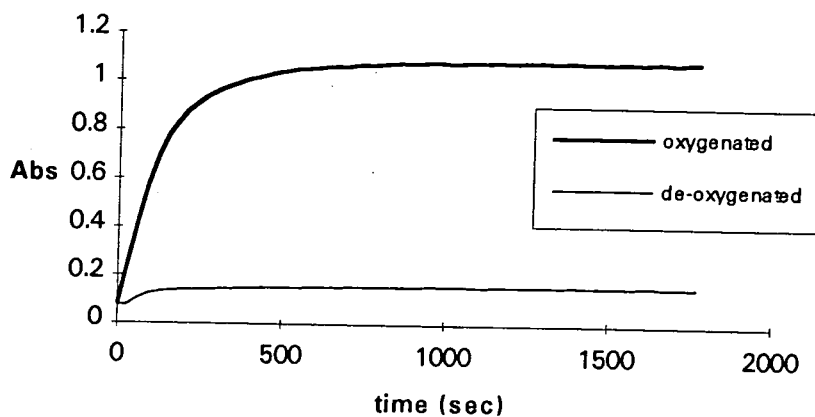
Figure 5.5

A conversion to NMANO of approximately 80% occurred, as measured by the difference between the λ_{max} absorbance for the reaction and that given by the nitrosation of NMA by excess sodium nitrite in acid.

These results indicated that the nitrosation of NMA cannot take place directly i.e. by direct attack on the NMA of the RSNO. As the presence of oxygen is a prerequisite for reaction, several steps must be involved (Scheme 5.1).
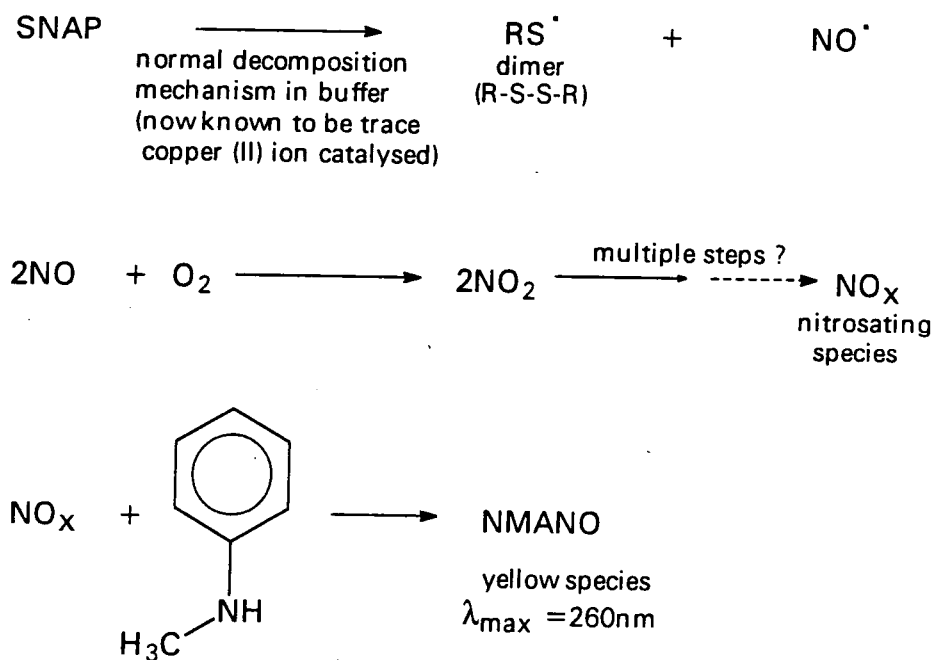
Scheme 5.1

161

The kinetics of the trace seemed to fit first order kinetics as well - direct transnitrosation would give second order kinetics as NMA + SNAP were at equivalent concentrations.

5.2.3 Effect of varying SNAP and NMA

An attempt was made to determine the order of reaction with respect to SNAP and NMA. NMA was kept at 1.5×10^{-2} M, with SNAP varied from 1×10^{-4} M to 7×10^{-4} M, under the same buffer conditions. However the NMA absorbance was impossibly high, preventing the NMANO appearance being measured. Diluting the NMA solution to 2×10^{-4} M brought the absorbance to manageable levels, (as shown by $NaNO_2$ nitrosation) but this dictated a SNAP concentration of 1×10^{-5} M as a maximum ! This was attempted, but the SNAP was too dilute to produce any effect. Finally, it was decided to alter SNAP:NMA ratios just slightly to try to discern any trend (See Table 5.4).

[NMA] (mol l⁻¹)	Example	[SNAP] (mol l⁻¹)	Mean k_{obs} Abs$^{1/2}$ s⁻¹	Correl.	Runs
2×10^{-4}	4nma03	2×10^{-4}	$1.42 \times 10^{-3} \pm 0.19$	(0.997)	4
4×10^{-4}	4nma09	2×10^{-4}	$1.50 \times 10^{-3} \pm 0.17$	(0.995)	5
6×10^{-4}	4nma14	2×10^{-4}	$1.60 \times 10^{-3} \pm 0.09$	(0.994)	4
2×10^{-4}	4nma19	4×10^{-4}	$1.26 \times 10^{-3} \pm 0.21$	(0.998)	4
2×10^{-4}	4nma23	6×10^{-4}	$1.12 \times 10^{-3} \pm 0.20$	(0.993)	3

Table 5.4

All the plots seemed to give very good half order curves, but a wide range of values were present. There was much overlap in values and a better and more worthwhile analysis was found by merely examining the curves (Figures 5.7 - 5.11). It can be seen that with increasing NMA and constant SNAP the same rate of reaction occurs, with a low total absorbance (approximately 0.5 abs). With increasing SNAP at constant NMA, the rate of reaction was again approximately the same but the total absorbance increase is greater with each SNAP concentration i.e. $0.5 \rightarrow 1.3$. Thus increasing SNAP concentration over NMA does not appear to increase the rate of

NMANO formation, but provides more available NO_x for nitrosation of NMA up to 100% conversion, in competition with loss of NO to competitor reactions e.g. nitrite formation.
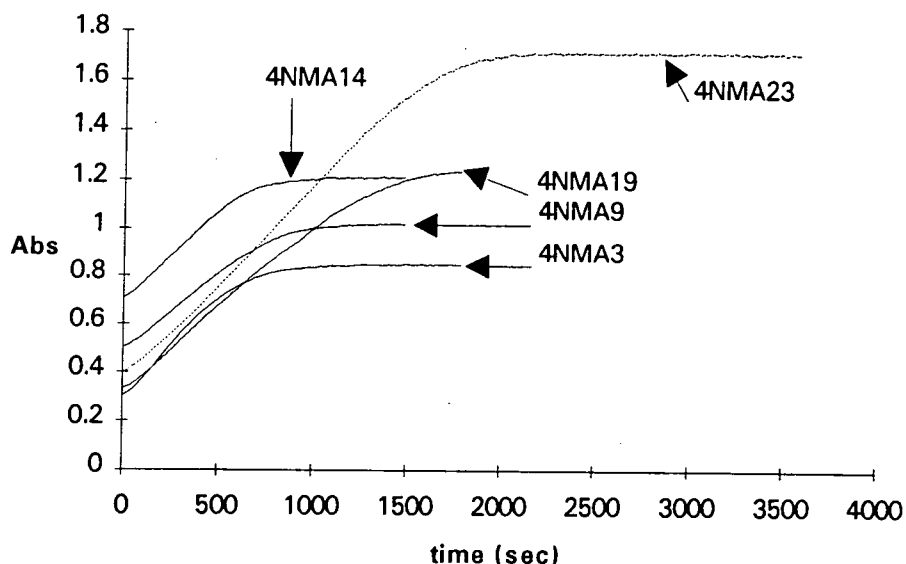
Figures 5.7 - 5.11

5.2.4 Use of other S-nitrosothiols

The work was repeated, under identical conditions as those used with SNAP, for those S-nitrosothiols that were available in the solid form i.e. SNOG and SNAC. With SNOG, no reaction occurred, over a prolonged period. With the crude SNAC solid preparation, no reaction occurred at first, but after approximately 30 minutes, an increase in absorbance at 270nm developed. This had the same form as that with SNAP. It is known that the crude solid SNAC decomposes suddenly, after variable periods in buffer (see Chapter 3), for unknown reasons. The sudden onset of SNAC decomposition would then produce the observed effect. These results indicate that any nitrosation must depend on the stability of the RSNO compound in the buffer. SNAP is thus ideal for use in this respect, being sufficiently unstable in buffer to produce an immediate effect, yet being stable enough to be produced in the solid form.

5.3 Investigation of MMA reaction with SNAP

5.3.1 Introduction

This work was a sideline of an initial investigation into the possible transnitrosation of thiols by S-nitrosothiols (see earlier). The anomalous production of a yellow species was noted while investigating the transnitrosation of thiols by SNAP, easily visible as a green to red colour change. It had been discovered that when methylmercaptoacetic acid (MMA) solution in buffer (Borax/NaOH pH 10.0) was added to a solution of SNAP in the same buffer, the green colour of SNAP was discharged and momentarily a red colour was produced. Unlike other thiols however (including thiols with an esterified carboxylic acid group), this rapidly changed to a yellow colour. It was found that in order to produce a reasonably strong yellow colour, the SNAP solution had to be quite concentrated, i.e. 2×10^{-3} M in-cell, while the MMA solution had to be considerably stronger than this, e.g. 0.1M in-cell.

A series of scans were performed at 60 second intervals of the reaction between SNAP (1×10^{-3} M) and MMA (0.1M) in Borax/NaOH buffer, pH 10.0, and compared with SNAP and MMA alone in buffer.

The MMA spectrum was confined below 320nm and it could be seen that upon mixing there was the immediate formation of the S-nitrosothiol of MMA, as shown by the change from the characteristic 590nm peak for SNAP to the 543nm peak for SMMA (i.e. a green to red colour change). Over the next minute the SMMA disappeared, with the concomitant production of a substance with an absorbance maximum at 413nm. This was maximal after two minutes then slowly disappeared, the red colour changing to yellow then slowly to colourless over several hours.

5.3.2 Investigation

Keeping the SNAP at 1×10^{-2} M in-cell and varying the concentration of MMA, it was found that under identical conditions a maximum value for the absorbance at 410nm could be obtained (Table 5.5).

10^2 x [MMA] (M)	1	2	2.5	3	4	5	6	7	10	20
Abs$_{max}$ @ 410nm	1.18	0.55	0.75	0.98	1.42	2.05	1.69		1.13	0.28
(repeated for a shorter range to confirm [MMA])				1.30	1.49	1.51	1.36	1.20		

Table 5.5

It was found that the best stoichiometric ratio for maximum production was 1:5 (SNAP:MMA). If MMA was kept at the 5 x 10^{-2} M concentration and the concentration of SNAP varied e.g. 0.5 x 10^{-2} M and 2 x 10^{-2} M, the absorbance maximum at 410nm fell from 1.6 to 0.4 and went from 1.6 to off-scale, respectively.

The yellow species did not extract into ether or other organic solvents such as chloroform. Upon addition of acid, the solution became colourless, the yellow colour being restored upon the addition of alkali. This process was not repeatable indefinitely - the reformed yellow colour rapidly deteriorated, as if some decomposition always took place. The reaction was not buffer dependent - the same species formed in $NaHCO_3$/NaOH buffer, pH 10.2.

To test the necessity for the presence of SNAP, a solution of MMA (5 x 10^{-2} M) in DGA/NaOH pH 4.0 buffer was partially nitrosated by the addition of $NaNO_2$ sufficient for 1 x 10^{-2} M MMA only (theoretically - the actual percentage nitrosation of MMA at pH 4.0 would be much less than 20%). A pink colour developed over 5 minutes and upon addition and dissolving of one NaOH pellet, a yellow colour slowly appeared (Abs$_{max}$ 410nm) as the pH rose to 9.8. When 0.1M HCl was used in place of buffer and the nitrosation carried out as before, a deep red colour was produced. Upon addition and dissolving of a weighed quantity of NaOH, sufficient to be just in excess, the pH rose to 8.6 and a very deep yellow colour was produced.

It was found, at a qualitative level, that other thiols such as thiolactic acid (TLA), cysteine, cysteine methyl ester (CME), mercaptoacetic acid (MAA), mercaptopropionic acid (MPA) and its methyl ester (MMP) did not produce a new species after initial transnitrosation. These experiments showed that quantitative work might be problematical due to the large pH changes produced in buffers when the high concentrations needed for pseudo first-order kinetics were employed. Carboxylic acid derivatives of thiols were used to ensure water solubility, but these obviously affected buffer pH.

Thus with SNAP and MMA in Borax/NaOH buffer pH 10.0 (1×10^{-2} M and 2×10^{-1} M in-cell, respectively), the actual reaction mixture pH was approximately 8.7 ! However, measuring the disappearance of the SNAP absorbance maximum at 590nm, using stopped flow spectrophotometry gave very good pseudo first order kinetics, indicating how rapid the formation of SMMA was, <u>before</u> formation of the yellow species.

$$k_{obs} = 3.19, 3.21, 2.94, 2.85, 2.71, 3.02, 3.24, 2.74, 3.08, 2.88, 2.90, 2.87, 2.98$$

$$\text{Mean} = 2.97 \pm 0.16 \text{ s}^{-1}$$

5.3.3 Summary

From the results it can be deduced that the role of SNAP is merely to nitrosate the MMA and that buffer type is irrelevant. The amount of yellow species formed depended upon the original SMMA concentration, but there may be an equilibrium which is shifted away from the yellow species formation by the presence of excess free thiol, hence the maximal production, measured at 410nm, when the SNAP:MMA ratio is 1:5. The results are summarised below in Scheme 5.2.

$$\text{SNAP} \quad + \quad \begin{array}{c} \text{CH}_2\text{S}^- \\ | \\ \text{COOCH}_3 \\ \text{(colourless)} \end{array} \quad \xrightarrow[\substack{\text{anion attack} \\ \text{on SNAP}}]{\text{thiolate}} \quad \begin{array}{c} \text{CH}_2\text{SNO} \\ | \\ \text{COOCH}_3 \\ \text{(red)} \end{array}$$

$$\begin{array}{c} \text{CH}_2\text{SNO} \\ | \\ \text{COOCH}_3 \end{array} \quad + \quad \begin{array}{c} \text{CH}_2\text{S}^- \\ | \\ \text{COOCH}_3 \end{array} \quad \longrightarrow \quad \begin{array}{c} \textbf{yellow species} \\ \text{Abs}_{max} = 410\,\text{nm} \end{array}$$
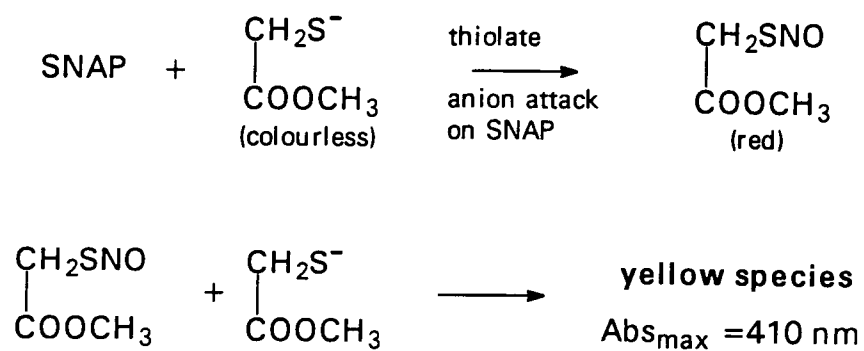
Scheme 5.2

The presence of the ester is crucial, as thioglycolic acid does not form a yellow species. The elucidation of structure and mechanism of formation of this unstable yellow complex remains to be achieved.

References

1. E.E. Reid, in *Organic Chemistry of Bivalent Sulphur*, Chemical Publishing, New York, 1958, Vol. 1, 470

2. D.L.H. Williams, in *Nitrosation*, Cambridge University Press, Cambridge, 1988, 95 (and references therein).

Chapter 6

Experimental Details

6.1. Experimental methods

Much of the work was performed using standard UV/visible spectrophotometry, with a variety of machines and stopped-flow spectrophotometry, although adaptations of these were also used.

1.1 UV/Visible Spectrophotometry

Many measurements were carried out using the Perkin Elmer Lambda 2 and later the more modern Shimadzu UV-2101PC spectrophotometers. Solutions for reaction were made up and thermostatted in a water bath at 25°C, which also supplied the thermostatting water for the cell-holder of the spectrophotometer in the case of the Lambda 2 machine. Care was taken to ensure free-flow by periodic cleaning of water bath and tubing to remove algae and other detritus. The Shimadzu had a Peltier-effect attachment (PCC + Controller) which utilised air current as a cooling agent, was very accurate and removed the need for water bath thermostatting in the machine. In a typical run, a small volume (e.g. 0.1 ml) of reactant (e.g. SNAP in methanol) would be pipetted into a 1 cm pathlength quartz cell using a previously calibrated Gilson pipette dedicated to the purpose. Further reactants would be added from another calibrated Gilson (e.g. 2.4 ml buffer) so that turbulence ensured thorough mixing. The machine would be already set to start immediately, with an identical reference cell already present. In this way the time lag between mixing the reactants and first data capture would be only a few seconds. The difference in absorbance between sample and reference cells would be measured against time.

Some work was also carried out using a simple UV/visible spectrophotometer, the Philips PU8725, notably the work on nitrite production/S-nitrosothiol decomposition using the Griess method. Unlike the other machines used, this did not have a dedicated PC and software, absorbance measurements being noted manually.

1.2 Stopped-Flow Spectrophotometry

Reactions that took place on a faster time-scale (completed in under 30 seconds) were measured using a Hi-Tech Scientific SF-3 series stopped flow spectrophotometer e.g. work done on transnitrosation of thiol by S-nitrosothiol in alkaline solution. This is shown in diagrammatic form in Fig 6.1.

Later work (e.g. on copper catalysis of S-nitrosocysteine decomposition) was performed on a stopped-flow attachment to the Shimadzu UV/visible spectrophotometer, the Hi-Tech SFA-12 Rapid Kinetics Accessory. This had the same basic design as shown above, but on a "mini" scale. One difference was that a specially designed quartz cuvette was attached to the syringe drivers by an "umbilical" tube which not only provided for entry of the reaction solutions, mixing in the cuvette and subsequent exit, but also provided thermostatting from a separately attached water bath.

In both cases, the principle of operation was that two reaction solutions were stored in reservoirs which fed two identical driver syringes. Care was taken that concentration changes (i.e. a halving) were allowed for when mixing the solutions, especially if comparison was required with other systems. The two syringe pistons were linked so that equal volumes were expelled from each upon commencement of a run. The solutions present in the thermostatted sections of tubing were therefore equally mixed prior to filling a third syringe, whose emerging piston acted as a switch to halt flow and simultaneously trigger the measurement of the reaction in the cell. This was done by passing a monochromatic beam of selected wavelength through the cell. The change in the intensity of the beam as the reaction proceeded was converted to an electrical signal and was expressed as a voltage change through biasing of the standing voltage. This allowed amplification of the voltage change alone instead of the entire standing voltage with superimposed small voltage change. This voltage change thus directly reflected the progress of the reaction in the cell. The traces

Monochromatic Light Source

Data Collection & Analysis

Detector & Photomultiplier

Waste

OP

MP

Stop & Trigger

S3

S1

S2

P

A

R

B

R

R - reservoirs

S1,S2,S3 - syringes

P - piston

MP - mixing point

OP - observation point

A & B - reaction solutions
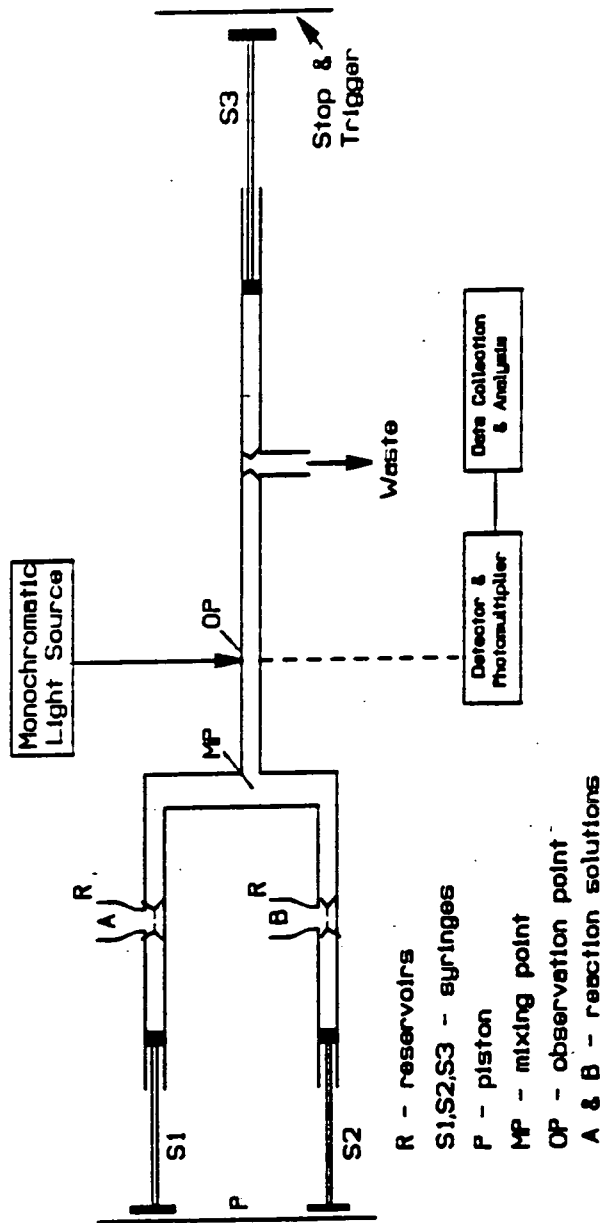
Figure 6.1

produced were analysed using a kinetic analysis program supplied by Hi-Tech running on an Apple IIe microcomputer. In the case of the Shimadzu, they were analysed using the First-Order Rate Constant Evaluation program (FORCE) written by Mr C. Greenhalgh and adapted by him for use in Microsoft Windows environment from its original form for use with Perkin Elmer software on the Lambda 2.

1.3 pH Measurement

These were carried out using a PTI-6 Universal digital pH meter, with an accuracy taken to be $\pm$ 0.05 pH units, although probably better.

1.4 Analysis

Metling points were determined using a recently serviced melting point apparatus. N.M.R. was performed using the department's Bruker 250 MHz instrument, care being taken with all deuterated solutions to minimise contact with atmospheric water vapour, but especially with sodium hydroxide solution and sulphuric acid solution. Analysis of water and buffer solutions for trace quantities of copper were performed on the department's Perkin Elmer 5000 Atomic Absorption spectrometer, by Mr R. Coult. Elemental analysis was performed on samples using the department's Carlo Erba Elemental Analyser by Mrs J Dostal.

1.5 Kinetic Analysis

The reactions were often observed through the disappearance of the absorbance due to the S-nitroso group in the 330 - 340nm region, although other wavelengths for particular reaction monitoring were also used. Throughout much of the work, understanding was hampered by inconsistent or even irreproducible reaction progression in the worst cases, or the kinetics were not amenable to analysis with a very high coefficient of correlation. For a first-order reaction, R $\rightarrow$ P, where R is the

reactant and P the product, the rate of disappearance of reactant (or appearance of product) can be given by equation 6.1

$$-\frac{dR}{dt} = \frac{dP}{dt} = k[R] \qquad 6.1$$

where k = a constant

Upon integration this gives the first-order rate constant k_0 (equation 6.2)

$$k_0 = \frac{1}{t} \ln \frac{[R]_0}{[R]_t} \qquad 6.2$$

where $[R]_0$ and $[R]_t$ are concentrations of reactant R at time = 0 and time = t respectively.

Assuming that the Beer-Lambert law is obeyed by the solution i.e. $A = \varepsilon\, c\, l$ where

    A = absorbance ε = molar extinction coefficient

    c = concentration (molar)   l = pathlength (cm)

Then for a standard 1 cm cell

$A_0 = \varepsilon_R[R]_0$ i.e time = 0   6.3

$A_t = \varepsilon_R[R]_t + \varepsilon_P[P]_t$ i.e time = t   6.4

where $[R]_t$ is the concentration of reactant R at time = t and $[P]_t$ is concentration of product P at time = t.

(In practice, a wavelength is chosen where absorbance of reactant is maximal while absorbance of any product is negligible, ideally.)

But $[P]_t = [R]_0 - [R]_t$, so equation 6.4 can be written

$A_t = \varepsilon_R[R]_t + \varepsilon_P[R]_0 - \varepsilon_P[R]_t$ 6.5

At reaction completion (infinity), A_t becomes A_∞

and since $[P]_\infty = [R]_0$, $A_\infty = \varepsilon_P[P]_\infty = \varepsilon_P[R]_0$

i.e. $A_t - A_\infty = \varepsilon_R[R]_t - \varepsilon_P[R]_t$

$$\therefore [R]_t = \frac{(A_t - A_\infty)}{(\varepsilon_R - \varepsilon_P)} \qquad\qquad 6.6$$

Also, $A_0 = \varepsilon_R[R]_0$

and $A_\infty = \varepsilon_P[P]_\infty = \varepsilon_P[R]_0$

so $A_0 - A_\infty = \varepsilon_R[R]_0 - \varepsilon_P[R]_0$

$$\therefore [R]_0 = \frac{(A_0 - A_\infty)}{(\varepsilon_R - \varepsilon_P)} \qquad\qquad 6.7$$

Therefore

$$k_0 = \frac{1}{t}\ln\frac{(A_0 - A_\infty)}{(A_t - A_\infty)} \qquad \text{from inserting 6.6 and 6.7 into 6.2}$$

This can be rearranged to give the form suitable for a graph

$$\ln(A_t - A_\infty) = -k_0 t + \ln(A_0 - A_\infty)$$

Plotting $\ln(A_t - A_\infty)$ against time should give a straight line of slope $-k_0$, the observed rate constant.

For some reactions, notably the work using Griess reagents and SNAP in buffers, a manual calculation was made of $\ln(A_t - A_\infty)$ and a calculator used to obtain the best-fit slope of the graph. For most work however, the kinetics programs, which use a more sophisticated method, were used.

The half-order kinetics that were observed have already been discussed.

Analysis of data for half-order kinetics was calculated manually as no program was available.

For all reactions, whether manually calculated or program-analysed, a minimum 90% of reaction time was used for analysis, with infinity values of > 10 half-lives.

6.2 Chemical methods

All laboratory reagents used were purchased commercially and were of Analar grade with the exception of some buffer salts, acids and sodium hydroxide solution, which were standard laboratory grade. Buffers were made according to the directions and concentrations given in Dawson *et al*[1]. Reference to "treble concentration" buffer indicates that the concentration of buffer salts was three times that referred to as the standard concentration in this book.

2.1 S-nitrosothiol synthesis

These were often generated *in situ* before use by dissolving the thiol at the calculated weight for the required concentration in dilute mineral acid. A 1.1 times stoichiometric equivalent of sodium nitrite was then added to the flask and the sealed solution given several minutes to react completely. The solution would be used at room temperature but protected from sunlight with aluminium foil, being freshly prepared for use when required.

Some of the more stable S-nitrosothiols were produced in the solid state.

i) SNAP

SNAP was prepared according to the method of Field *et al*[2] with some variations. Sodium nitrite and N-acetyl-D,L-penicillamine (NAP) were weighed out in a 2:1 ratio, the sodium nitrite being dissolved in water while the NAP was dissolved in warmed methanol/HCl, to which was added concentrated sulphuric acid. This was stirred to dissolve the NAP before cooling in ice to the point where NAP was about to precipitate. The sodium nitrite was then added to the aluminium foil covered flask over several minutes and the sealed flask allowed to stir continuously for 45 minutes. It was then filtered with a Buchner funnel and washed with ice-cold distilled water

several times before being damp-dried with air on the Buchner. It was then dried by high-vacuuming at room temperature and stored in the freezer.

ii) SNAP dimer

SNAP dimer was also prepared according to Field's method by boiling SNAP in methanol under reflux for one hour then using a rotary evaporator to remove the solvent, leaving the white dimer behind.

iii) SNOG

Several attempts were made to synthesise the S-nitrosothiol of glutathione (SNOG) in a pure, dry powder form using different methods. One was an adaptation of a method by Means et al[3]. Equivalent quantities of 0.5 mmolar glutathione and sodium nitrite were dissolved in 0.1 ml cold water and 0.05 ml of 11.7M HCl was added. After 2-3 minutes this was frozen in dry ice/acetone and scraped onto a sintered glass funnel surrounded by a liquid nitrogen "packing" in another, plastic, funnel. The frozen mixture was then washed with 0.1 ml quantities of absolute ethanol cooled in dry ice/acetone. The residue was then high-vacuumed for several hours. Unfortunately, although deep red in colour, the viscous liquid did not dry out to form a powder.

Another attempt was made using glutathione stirred in dry ether surrounded by a dry ice/acetone bath, through which was passed dry nitrogen gas. Subsequently, a mixture of NO_2 and NO, generated from the action of concentrated sulphuric acid on sodium nitrite, was added to the nitrogen stream. The NO_2 and NO (brown) condensed to form N_2O_3 (blue) in the ether. After 2½ hours the ether/N_2O_3 were removed from the dry ice/acetone bath and connected to a high vacuum pump. Only traces of pink powder were found, in the immediate vicinity of the N_2O_3 entry.

Repeating the experiment with dry CH_3CN and dry tetrachloromethane produced a similar failure, due no doubt to the lack of solubility of the glutathione.

A further attempt was made by producing pure liquid N_2O_3 itself and then adding glutathione directly to it, the N_2O_3 being generated as before, but condensed out directly in a dry ice/acetone bath. The mixture was stirred for 30 minutes, then the N_2O_3 high-vacuumed off at room temperature. However, a clear bright yellow syrup was left, which upon further vacuuming produced a sticky semi-solid. Obviously not SNOG, it was probably an NO_2/glutathione adduct. (A UV scan of the yellow substance showed it to be very different from glutathione, SNOG etc.)

Finally, SNOG was prepared in high yield and a pure form following the method of Hart[4]. Glutathione (2.5 mmol) was dissolved in 8.0 ml of water containing 0.43 ml concentrated HCl. 2.5 mmol of sodium nitrite was added to the stirred solution, over 45 minutes, in an ice bath, the flask being covered in aluminium foil. 10 ml of Analar acetone was then added to the solution, which was further stirred for 15 minutes. A pink precipitate was produced, which was filtered on a Buchner and washed successively with ice cold water, acetone and ether respectively, then air dried on the Buchner before being high-vacuumed dry. The yield was 83%.

All the usual tests proved it to be high purity SNOG (>95%). The vital point in the preparation was the use of a small quantity of water - increasing this led to the inability to precipitate out the SNOG with acetone.

iv) SNAC

The same method was used to prepare a dry, albeit crude form of S-nitroso-N-acetylcysteine (SNAC). To 2 mmol each of NAC and sodium nitrite were added 1 ml of 2M HCl. The mixture was stirred in an ice bath for 5 minutes then 30 ml of acetone were added. An immediate <u>white</u> precipitate was produced with total disappearance of the red colour. This could not be re-nitrosated and was possibly the

NAC dimer. Upon repeating the method, but with the addition of 10 ml of 50:50 acetone/ether, no white precipitate formed and the red solution decreased in size. This was repeated, with a viscous deep red solution being left, before final shaking with two lots of dry ether and high-vacuuming to give a deep red solid. This was found to be approximately 40% pure SNAC.

v) SNOCAP

Another crude, dry, solid sample of S-nitrosocaptopril (SNOCAP), was obtained by following the method of Loscalzo *et al*[5]. A column of Dowex 50 x 8 - 100 resin pre-treated with HCl was washed with distilled water until no acid was detected with indicator paper. 1 mmol captopril and 1.1 mmol sodium nitrite were put in an aluminium foil covered flask with stirring and 2 ml of 2M HCl added. After 5 minute this was added to the foil covered column. The column was washed through with water into a large flask, the solution frozen (with rotation) in dry ice and the solid high vacuumed for 4 days to give a dry pink solid. This was 48% SNOCAP, stable if kept in a freezer.

Checks on purity estimations of molar extinction coefficients were made by dissolving an exact weight of thiol (sufficient to produce a 1×10^{-3} M final concentration) in 0.1M HCl, containing a 1.1 x equivalent of sodium nitrite, in a 100 ml flask. This was kept at 25°C in a water bath and made up to the mark with more acid. After 10 minutes samples were removed and the absorbance maxima at 335nm and 545nm were obtained. The samples of dry, solid S-nitrosothiols were weighed out as for theoretical 100% S-nitrosothiols and dissolved as above and their absorbances compared.

2.2 Attempts at thiol syntheses

Several attempts were made to synthesise thiols that would, when nitrosated, provide potentially useful comparative data on structure/activity relationships with regard to copper(II) ion catalysis.

i) Methyl thiolactate (MTL)

$$\underset{\displaystyle CH_3\overset{\textstyle |}{C}HCOOCH_3}{\overset{\textstyle SH}{}}$$
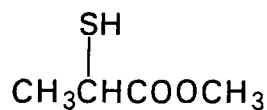
An attempt was made to synthesise this, to enable comparison between the reactivity of a carboxylate S-nitrosothiol and its ester. The method used was based upon the original one outlined by Sheehan et al[6], using 1,3-dicyclohexylcarbodiimide (DCC) as an intermediate. One-to-one equivalents of methanol and thiolactic acid (TLA) were stirred together with 1.0 equivalent of DCC in 80 ml of tetrahydrofuran. Little reaction seemed to occur, the thiol ester could not be identified. A literature search identified several other variants[7], including those where using 4-dimethylaminopyridine (DMAP) as a catalytic reaction intermediate was suggested[8, 9]. Another attempt was made using the method of Neises and Steglich[10], where thiolactate dissolved in dry CH_2Cl_2 had DMAP and methanol added at 0°C then DCC stirred in at room temperature and left for 3 hours. Urea was filtered off and the filtrate evaporated and purified. However, no thiol was found. It could have been that the thiol group was acting as its own ester-forming reagent. Time did not permit examining the effect of using great excess of dry methanol as solvent/reactant.

ii) 2-mercaptoisobutyric acid (MIBA)

$$HS\!-\!\overset{\displaystyle CH_3}{\underset{\displaystyle CH_3}{\overset{\textstyle |}{\underset{\textstyle |}{C}}}}\!-\!COOH$$
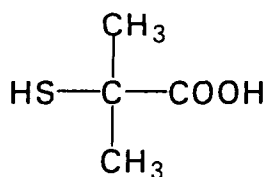
Some attempts were made to synthesise the above thiol so that the S-nitrosothiol could be investigated with regard to the effect of the tertiary carbon upon SNO reactivity with copper (II) ions in solution. Several methods were attempted, those

by Reid[11], Pan and Fletcher[12] and Mori[13]. With the former, bromoisobutyric acid (BIBA) was mixed with thiourea (50 mmol each) in 25 ml of water and heated with stirring for 3 hours. 6 g of NaOH in 10 ml of water were added and stirred and heated, all under nitrogen. The alkali was neutralised with HCl and the mixture extracted with ether, which upon drying and evaporation gave a pale yellow liquid at 64% yield. The Pan and Fletcher variation of this, using dimethyl sulphoxide (DMSO) as solvent, and stirring overnight at room temperature was tried, but with poor results. The Mori method involved refluxing 0.036 mol BIBA with 0.038 mol potassium ethylxanthogenate in 50 ml acetone for 7 hours. After overnight cooling, the acetone was removed by rotary evaporation and the residue stirred with 15 ml ethylene diamine under nitrogen in a 30°C water bath. The mixture was cooled and neutralised with ice/H_2SO_4 solution. The mixture was extracted into ether, dried and evaporated to give a yellow oil. The advantage of this method was that a much milder alkaline agent was used to liberate the thiol from the intermediate - thiols are particularly susceptible to oxidation when heated in strong alkali, hence the use of a nitrogen atmosphere.

In all cases, nitrosation of the product with $NaNO_2$/H_2SO_4 produced a red solution with absorbance maxima at 330nm and 560nm i.e. the product appeared to be the tertiary thiol. However, caution must be exercised, as the putative product was red, while experience with other tertiary S-nitrosothiols would suggest that it should be green. Initial attempts to purify the crude product, by recrystallisation from n-hexane failed, and no further time was available to achieve purification and further analysis.

6.3 Haemoglobin preparation

For the experimental work with haemoglobin, this had to be extracted from a pint blood sample (kindly donated by Professor D.L.H. Williams) using an established protocol[14]. Physiological saline used was made by dissolving 0.9g sodium chloride per 100ml of distilled water in one litre quantities, which were degassed by

vacuuming and sonication for 20 - 30 minutes. The solution was then bubbled with nitrogen gas for 10 minutes and kept at 4°C in a sealed flask prior to use.

6.3.1 Blood preparation   - for 100 ml

1. Centrifuge to remove plasma, 20 minutes at 3000 rpm. Make up to 160 ml with 0.9% saline after removing supernatant plasma. Mix gently by inversion. Centrifuge at 9000 rpm for 20 minutes. Remove supernatant with a Pasteur pipette on an air vacuum line. Resuspend to 160 ml as before, centrifuge and remove supernatant. Repeat 3 more times.

2. Add distilled water at 4°C, double the total red cell volume, (approximately 300 ml) to the cells. Stir for 45 minutes at 4°C then stand overnight to let cells lyse.

3. Centrifuge one hour at 9000 rpm. Remove and keep supernatant (of haemoglobin).

4. Remove proteins and membranes by adding ammonium sulphate at 209g/litre. Stir at 4°C for 30 minutes. Centrifuge at 9000 rpm for one hour and keep supernatant. To this add more ammonium sulphate at 200g/litre slowly with stirring. Stir at 4°C overnight.

5. The haemoglobin (Hb) plus ammonium sulphate precipitate is collected as a deep red semi-solid mass by centrifugation at 9000 rpm for 30 minutes. It is removed with a spatula into plastic 50 ml tubes and stored at -80°C.

N.B. Tubes were maintained in ice throughout all manipulations given above. Care and a delicate touch are needed to remove the very thin buff (white cell) layer during saline wash stages (all five). 30 ml plastic centrifuge tubes are useful (x6) for the initial stages, 250 ml large plastic pots for the ammonium sulphate stages.

6.3.2 Dialysis   - For 25 ml of mixture

The Hb/ammonium sulphate mixture has to be dialysed to remove proteins and phosphate. 1mM HEPES/NaCl (0.1M) pH 7.2 solution was made with 4 ml 500mM HEPES/NaOH buffer pH 7.2 plus 11.68g NaCl made up to 2 litre and stored at 4°C. 100mM HEPES/KCl (35mM) pH 7.4 solution was stored similarly.

1. Dilute the Hb/ammonium sulphate mixture to twice its volume with HEPES/NaCl pH 7.2 solution. Pour into two 18 inch lengths of 1 cm Visking tubing previously boiled twice in distilled water for 30 minutes. Before knotting ensure plenty of room is allowed for volume expansion (minimum of four inches of flat tubing after knotting).

2. Place filled tubing in 1 litre beaker, cover with HEPES/NaCl pH 7.2 solution (approximately 700 ml required). Change every 3 hours (i.e. 2 litre /day required), storing throughout in a fridge. Repeat for 5 days.

3. On the sixth day replace buffer with HEPES/KCl pH 7.4 solution (2 litres required).

4. Test for total Hb and dilute with HEPES/KCl buffer to give a 5% solution.

6.3.3 Sterilisation

The Hb solution must be sterilised immediately, prior to storing in a freezer, as otherwise quite rapid deterioration of the product will occur.

1. Filter the solution (which has been kept in a freezer prior to use) using a gravity with paper filter i.e. do not use the much faster Buchner filter, as the partial vacuum produced to speed filtration tends to scour oxygen from the OxyHb, and may cause excess production of Methaemoglobin (MetHb).

2. The coarsely filtered solution is then filtered using 0.22 μm Millipore filters. A 100 ml plastic syringe is used to force the Hb solution through the filters (one filter

is required per 25 ml aliquot, approximately, of Hb solution). The solution falls directly into sterile 25 ml screw-top tubes which are immediately sealed.

6.3.4 Calibration

This was carried out using standard Hb samples and Drabkin's solution, as obtained commercially, to produce a calibration curve. This fitted the Beer-Lambert very well. From this, the average absorbance for the prepared (unknown) Hb was equivalent to 9.374g Hb per 100 ml i.e. to produce a 5% solution required dilution by 1.875, with the previously prepared 0.0167M phosphate buffer. Upon checking again with Drabkin's, this gave the solution as being 4.76% Hb. Methaemoglobin (MetHb) was tested for using the phosphate buffer to dilute the Hb solution to 25%, then leaving it 10 minutes. Equal volumes of 10% KCN and 12% acetic acid were mixed (CARE!) in the fumes cupboard and one drop of the mixture added to the Hb/phosphate solution. The absorbance of the original Hb/phosphate solution at 635nm was compared with the absorbance of the cyanide/Hb/phosphate solution. This gave a MetHb concentration of 3.7% i.e. 1.06% OxyHb. The high value for the MetHb was probably due to the use of a Buchner filter to speed up filtration of the Hb solution prior to sterilisation by Millipore filter.

References

1. R.M.C. Dawson, D.C. Elliott, W.H. Elliott, K.M. Jones, in *Data For Biochemical Research*, Oxford Science Publications, 3rd Ed., 1990

2. L. Field, R.V. Dilts, R. Ravichandran, P.G. Lenhert, G.E. Carnahan, *J. Chem. Soc., Chem. Comm.*, 1978, 249

3. G.E. Means, J.W. Park, United States Patent No. 4900719, 1990, 1904

4. T.W. Hart, *Tet. Lett.*, 1985, **26**, 2013

5. J. Loscalzo, D. Smick, N. Andon, J. Cooke, *J. Pharm. Exp. Ther.*, 1989, **249**, 726

6. J.C. Sheehan, G.P. Hess, *J. Am. Chem. Soc.*, 1955, **77** (1), 1067

7. Y.S. Klausner, M. Bodansky, *Synth.*, 1972, **9**, 453

8. A. Hassner, V. Alexanian, *Tet. Lett.*, 1978, **46**, 4475

9. E.P. Boden, G.E. Keck, *J. Org. Chem.*, 1985, **50**, 2394

10. B. Neises, W. Steglich, *Angew. Chem. Int. Ed.*, 1978, **17**, 522

11. E.E. Reid, in *Organic Chemistry of Bivalent Sulphur*, Chemical Publishing, New York, 1958, Vol. 1, 452

12. H.L. Pan, T.L. Fletcher, *Chem. Ind.*, 1968, 546

13. K. Mori, Y. Nakamura, *J. Org. Chem.*, 1969, **34**, 4170

14. R. Hazelwood, Wellcome Research Laboratories, Beckenham, Kent, personal communication

APPENDIX (A)

The use of SNAP in experimental Physiology

A.1. Introduction

The S-nitrosothiols have a useful role to play in many aspects of physiological research, primarily as NO donators for vasodilation studies[1, 2, 3, 4]. The following work was performed while on a visit to the University of St Andrews, Scotland and illustrates such use.

A.2. Rat-tail artery vasodilation study

A 1 cm section of rat-tail artery was dissected out and set up for experimentation. This specific materal is chosen because it approximates to the calibre of artery that shows best response, but is still thick enough to allow reasonably easy manipulation. It was cannulated and provided with two flow systems of gassed (5% CO_2) and oxygenated (95%) Krebs/Ringer solutions. One flows through the artery lumen and is used to infuse injected SNAP. (See diagram of apparatus Figure A.1)

A solution of SNAP was made up in TRIS/HCl buffer, pH 7.5, with SNAP at various concentrations ranging from 1×10^{-7} M to 1×10^{-2} M. Tone was induced first in the artery using phenylephrine and the subsequent relaxation with SNAP observed. (The maximum achieved with any preparation has been 80%, usually 70%, the reason for this partial response being unknown[5].) The relaxation was measured from equilibrated tonic base line to tip of deflection, expressed as a percentage relaxation. The passage time of SNAP through the artery was 0.3 seconds. Paper speed was 1 cm/2 minutes. See diagram for typical traces (Figure A.2). The results are shown in Table A.1

Table A.1

Dose [SNAP] (M)	Relaxation %
1×10^{-7}	5.2
3.75×10^{-7}	13.9
5×10^{-7}	23.0
1×10^{-6}	33.7
5×10^{-6}	55.0
1×10^{-5}	58.8
1×10^{-4}	65.6
1×10^{-3}	72.0
1×10^{-2}	72.0
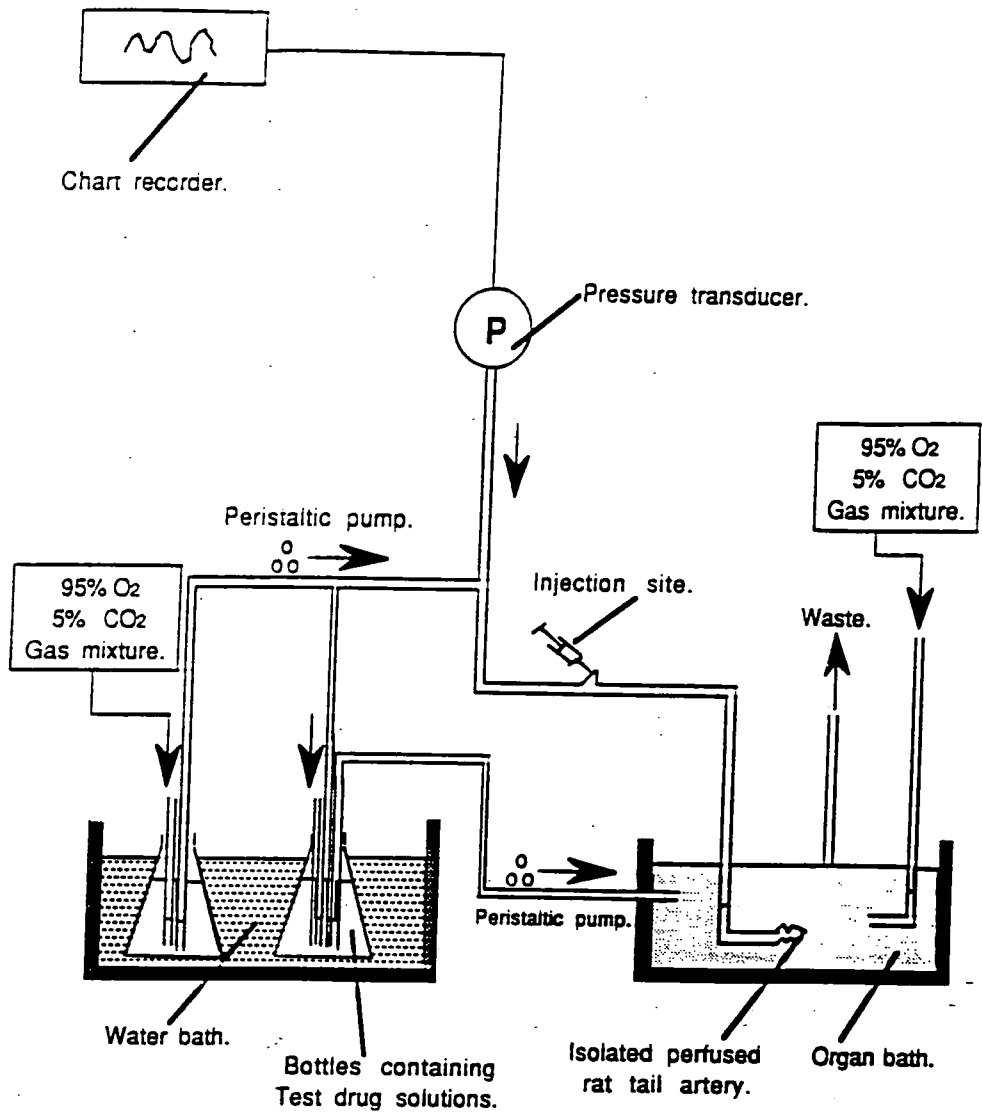
Figure A.1
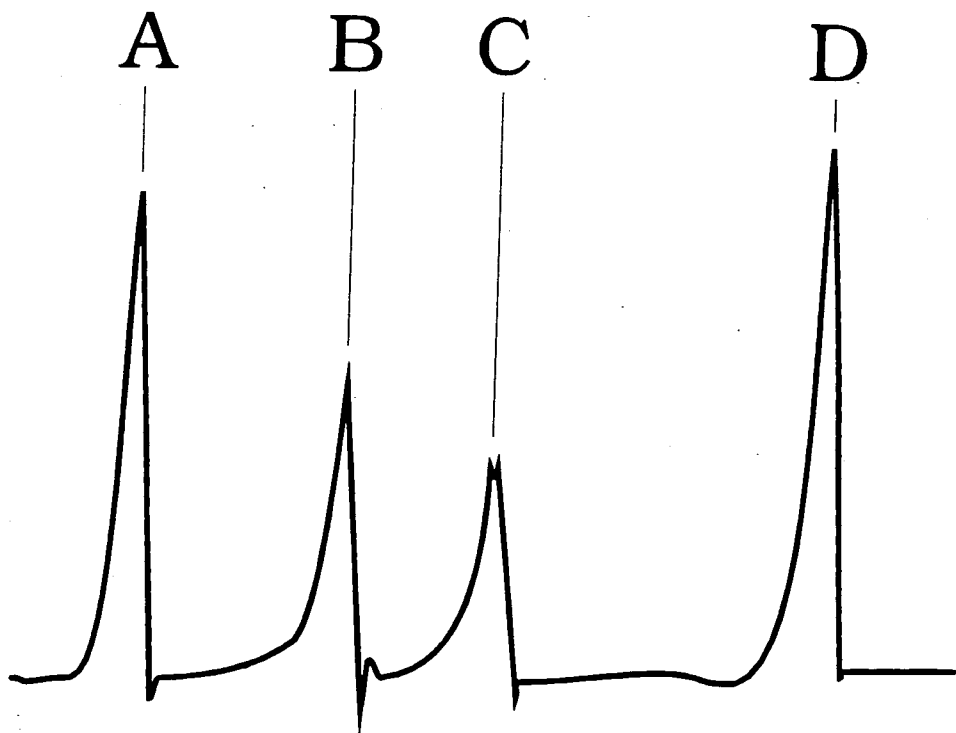
Traces obtained following injection of SNAP/buffer at various concentrations
$A = 5 \times 10^{-6}$ M SNAP, $B = 1 \times 10^{-6}$ M SNAP
$C = 5 \times 10^{-7}$ M SNAP, $D = 1 \times 10^{-5}$ M SNAP

Figure A.2

The results were plotted to give a log(dose) versus response curve (see Figure A.3)
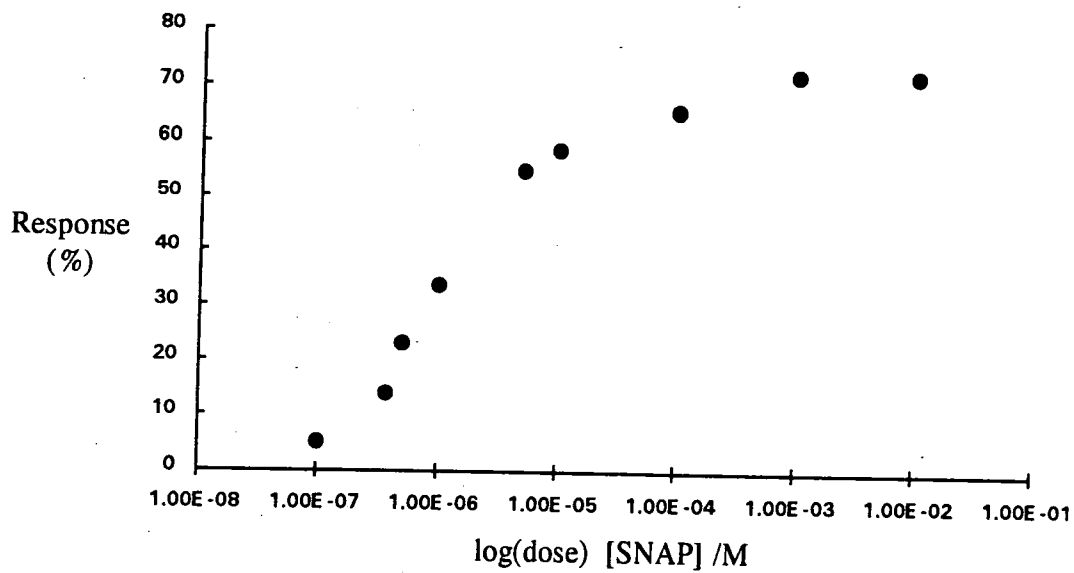
Figure A.3

A.3. Conclusion

From the results it can be seen that SNAP appears to produce a sigmoidal (pharmacological dose) response curve that is typical of a drug acting at a receptor site. That is, increasing drug concentrations result in an increasing response until a maximal stimulus is achieved when all receptors are being stimulated. In this instance, SNAP probably would be said to be acting as an "indirect agonist" i.e. acting through an intermediary and not directly activating the receptor responsible for the response[6].

The question of the exact mechanism of action of S-nitrosothiols and their possible role as endogenous species is still unresolved, as discussed in Chapter 1.

References

1. R.M. Clancy, S.B. Abramson, *Anal. Biochem.*, 1992, **204**, 365

2. R.D. Curran, F.K. Ferrari, P.H. Kispert, J. Stadler, D.J. Stuehr, R.L. Simmons, T.R. Billiar, *F.A.S.E.B.*, 1991, **5**, 2085

3. A. Jansen, J. Drazen, J.A. Osborne, R. Brown, J. Loscalzo, J.S. Stamler, *J. Pharm. Exp. Ther.*, 1992, **261**, 154

4. P.R. Myers, R.L. Minor, R. Guerra, J.N. Bates, R.G. Harrison, *Nature* (London), 1990, **345**, 161

5. S.C. Askew, personal communication.

6. in *Basic Pharmacology*, Ed. R.W. Foster, 2nd Ed., Butterworths, London, 1986, 338

APPENDIX (B)

Research Colloquia, Seminars, Lectures and Conferences

A requirement of the Board of Studies in Chemistry is that a postgraduate research thesis contains an appendix listing.

A) Details of the postgraduate induction course.

B) All research colloquia, seminars and lectures arranged by the Chemistry department during the period that the author was a postgraduate student, with an indication of those personally attended. Also, lectures organised by Durham University Chemical Society, with an indication of those personally attended.

C) All research conferences attended and papers and posters presented by the author.

B.1. First Year Induction Course, October 1990

The course consists of a series of one hour lectures on the services available in the department, familiarisation exercises etc.

1. Introduction, research resources and practicalities
2. Safety matters
3. Electrical appliances and hands-on spectroscopic services
4. Departmental computing
5. Chromatography and high pressure operations
6. Elemental Analysis
7. Mass spectrometry
8. Nuclear magnetic resonance spectroscopy
9. Glassblowing techniques

B.2. Research colloquia, seminars and lectures arranged by Durham University Chemistry department 1990-1993. (* denotes personal attendance, # denotes invited specially for the graduate training programme)

11.10.90   Dr. W.A. MacDonald, ICI, Wilton
Materials for the Space Age

* 24.10.90   Dr. M. Bochmann[#], University of East Anglia
Synthesis, Reactions and Catalytic Activity of Cationic Tritium Alkyls

26.10.90   Prof. R. Soulen[#], South Western University, Texas
Preparation and Reactions of Bicycloalkenes

* 31.10.90   Dr. R. Jackson[#], University of Newcastle-upon-Tyne
New Synthetic Methods: alpha - Amino Acids and Small Rings

* 01.11.90   Dr. N. Logan, University of Nottingham
Rocket Propellants

* 06.11.90   Dr. P. Kocovsky[#], University of Uppsala
Stereo-controlled Reactions Mediated by Transition and Non-transition Metals

07.11.90   Dr. G. Gerrard[#], British Petroleum
Raman Spectroscopy of Industrial Analysis

08.11.90   Dr. S.K. Scott, University of Leeds
Clocks, Oscillations and Chaos

* 14.11.90   Prof. T. Bell[#], SUNY, Stoney Brook, USA
Functional Molecular Architecture and Molecular Recognition

21.11.90   Prof. J. Pritchard, Queen Mary & Westfield College, University of London
Copper Surfaces and Catalysts

* 28.11.90   Dr. B. J. Whitaker[#], University of Leeds
Two-Dimensional Velocity Imaging of State-Selected Reaction Products

* 29.11.90   Prof. D. Crout, University of Warwick
Enzymes in Organic Synthesis

* 05.12.90   Dr. P.G. Pringle[#], University of Bristol
Metal Complexes with Functionalised Phosphines

13.12.90   Prof. A.H. Cowley, University of Texas
New Organometallic Routes to Electronic Materials

15.01.91   Dr. B.J. Alder, Lawrence Livermore Laboratories, California
Hydrogen in All Its Glory

17.01.91   Dr. R.P. Sarre, University of Nottingham
Comet Chemistry

* 24.01.91   Dr. P.J. Sadler, Birbeck College, University of London
Design of Inorganic Drugs: Precious Metals, Hypertension and HIV

30.01.91   Prof. E. Sinn[#], University of Hull
Coupling of Little Electrons in Big Molecules. Implications for the
Active Sites of (Metalloproteins and Other) Macromolecules

* 31.01.91   Dr. D. Lacey, University of Hull
Liquid Crystals

* 06.02.91   Dr. R. Bushby[#], University of Leeds
Biradicals and Organic Magnets

* 14.02.91   Dr. M.C. Petty, University of Durham
Molecular Electronics

* 20.02.91   Prof. B.L. Shaw[#], University of Leeds
Synthesis with Coordinated, Unsaturated Phosphine Ligands

* 28.02.91   Dr. J. Brown, University of Oxford
Can Chemistry Provide Catalysts Superior to Enzymes?

* 06.03.91   Dr. C.M. Dobson[#], University of Oxford
NMR Studies of Dynamics in Molecular Crystals

* 07.03.91   Dr. Markam, ICI pharmaceuticals
DNA Fingerprinting

24.04.91   Prof. R.R. Schrock, Massachusetts Institute of Technology
Metal-ligand Multiple Bonds and Metathesis Initiators

25.04.91   Prof. T. Hudlicky, Virginia Polytechnic Institute
Biocatalysis and Symmetry-Based Approaches to the Efficient Synthesis
of Complex Natural Products

20.06.91 Prof. M.S. Brookhart, University of North Carolina
Olefin Polymerisations, Oligomerisations and Dimerisations Using
Electrophilic Late Transition Metal Catalysts

* 29.07.91 Dr. M.A. Brimble, Massey University, New Zealand
Synthetic Studies Towards the Antibiotic Griseusin-A

* 17.10.91 Dr. J.A. Salthouse, University of Manchester
Son et Lumiere - a Demonstration Lecture

* 31.10.91 Dr. R. Keely, Metropolitan Police Forensic Science
Modern Forensic Science

06.11.91 Prof. B.F.G. Johnson#, Edinburgh University
Cluster-Surface Analogies

* 07.11.91 Dr. A.R. Butler, St. Andrews University
Traditional Chinese Herbal Drugs: a Different Way of Treating Disease

* 13.11.91 Prof. D. Gani#, St. Andrews University
The Chemistry of PLP Dependent Enzymes

* 20.11.91 Dr. R. More O'Ferrall#, University College Dublin
Some Acid-Catalysed Rearrangements in Organic Chemistry

28.11.91 Prof. I.M. Ward, IRC in Polymer Science, University of Leeds
The SCI Lecture: The Science and Technology of Orientated Polymers

* 04.12.91 Prof. R. Grigg#, Leeds University
Palladium-Catalysed Cyclisation and Ion-Capture Process

* 05.12.91 Prof. A.L. Smith, ex Unilever
Soap, Detergents and Black Puddings

* 11.12.91 Dr. W.D. Cooper#, Shell Research
Colloid Science: Theory and Practice

* 22.01.92 Dr. K.D.M. Harris#, St. Andrews University
Understanding the Properties of Solid Inclusion Compounds

* 29.01.92 Dr. A. Holmes#, Cambridge University
Cycloaddition Reactions in the Service of the Synthesis of Piperidine
and Indolizidine Natural Products

* 30.01.92 Dr. M. Anderson, Sittingbourne Research Centre, Shell Research
Recent Advances in the Safe and Selective Chemical Control of Insect Pests

12.02.92 Prof. D.E. Fenton[#], Sheffield University
Polynuclear Complexes of Molecular Clefts as Models for Copper Biosites

13.02.92 Dr. J. Saunders, Glaxo Group Research Limited
Molecular Modelling in Drug Discovery

* 19.02.92 Prof. E.J. Thomas[#], Manchester University
Applications of Organostannanes to Organic Synthesis

* 20.02.92 Prof. E. Vogel, University of Cologne
The Musgrave Lecture Porphyrins: Molecules of Interdisciplinary Interest

* 25.02.92 Prof. J.F. Nixon, University of Sussex
The Tilden Lecture Phosphaalkynes: New Building Blocks in Inorganic and Organometallic Chemistry

26.02.92 Prof. M.L. Hitchman[#], Strathclyde University
Chemical Vapour Deposition

05.03.92 Dr. N.C. Billingham, University of Sussex
Degradable Plastics - Myth or Magic?

* 11.03.92 Dr. S.E. Thomas[#], Imperial College
Recent Advances in Organoiron Chemistry

12.03.92 Dr. R.A. Hann, ICI Imagedata
Electronic Photography - an Image of the Future

* 18.03.92 Dr. H. Maskill[#], Newcastle University
Concerted or Stepwise Fragmentation in a Deamination-Type Reaction

07.04.92 Prof. D.M. Knight, Philosophy Department, University of Durham
Interpreting Experiments: the Beginning of Electrochemistry

13.05.92 Dr. J-C. Gehret, Ciba Geigy, Basel
Some Aspects of Industrial Agrochemical Research

15.10.92   Dr. M. Glazer & Dr. S. Tarling, Oxford University & Birbeck College, London
It Pays to be British - The Chemist's Role as an Expert Witness in Patent Litigation

20.10.92   Dr. H.E. Bryndza, Du Pont Central Research
Synthesis, Reactions and Thermochemistry of Metal (Alkyl) Cyanide Complexes and their Impact on Olefin Hydrogenation Catalysis

* 22.10.92   Prof. A. Davies, University College London
The Ingold-Albert Lecture The Behaviour of Hydrogen as a Pseudometal

28.10.92   Dr. J.K. Cockcroft, University of Durham
Recent Developments in Powder Diffraction

* 29.10.92   Dr. J. Emsley, Imperial College, London
The Shocking History of Phosphorus

04.11.92   Dr. T.P. Kee, University of Leeds,
Synthesis and Co-ordination of Silylated Phosphites

* 05.11.92   Dr. C.J. Ludman, University of Durham
Explosions, a demonstration lecture

* 11.11.92   Prof. D. Robins[#], Glasgow University
Pyrrolizidine Alkaloids: Biological Activity, Biosynthesis and Benefits

* 12.11.92   Prof. M.R. Truter, University College, London
Luck and Logic in Host-Guest Chemistry

18.11.92   Dr. Nix[#], Queen Mary College, London
Characterisation of Heterogenous Catalysts

* 25.11.92   Prof. Y. Vallee, University of Caen
Reactive Thiocarbonyl Chemistry

25.11.92   Prof. L.D. Quin[#], University of Massachusetts, Amherst
Fragmentation of Phosphorus Heterocycles as a Route to Phosphoryl Species with Uncommon Bonding

26.11.92   Dr. D. Humber, Glaxo Greenford
AIDS - The Development of a Novel Series of Inhibitors of HIV

* 02.12.92   Prof. A.F. Hegarty, University College, Dublin
              Highly Reactive Enols Stabilised by Steric Protection

* 02.12.92   Dr. R.A. Aitken[#], University of St. Andrews
              The Versatile Cycloaddition Chemistry of $Bu_3P.CS_2$

* 03.12.92   Prof P. Edwards, Birmingham University
              The SCI Lecture - What is a Metal?

  09.12.92   Dr. A.N. Burgess[#], ICI Runcorn
              The Structure of Perfluorinated Ionomer Membranes

  20.01.93   Dr. D.C. Clary[#], University of Cambridge
              Energy Flow in Chemical Reactions

* 21.01.93   Prof. L.Hall, Cambridge
              NMR - Window to the Human Body

* 27.01.93   Dr. W. Kerr, University of Strathclyde
              Development of the Pauson-Khand Annulation Reaction: Organo-cobalt
              Mediated Synthesis of Natural and Unnatural Products

* 28.01.93   Prof. J. Mann, University of Reading
              Murder, Magic and Medicine

  03.02.93   Prof. S.M. Roberts, University of Exeter
              Enzymes in Organic Synthesis

  10.02.93   Dr. D. Gillies[#], University of Surrey
              NMR and Molecular Motion in Solution

  11.02.93   Prof. S. Knox, Bristol University
              The Tilden Lecture Organic Chemistry at Polynuclear Metal Centres

* 17.02.93   Dr. R.W. Kemmitt[#], University of Leicester
              Oxatrimethylenemethane Metal Complexes

  18.02.93   Dr. I. Fraser, ICI Wilton
              Reactive Processing of Composite Materials

  22.02.93   Prof. D.M. Grant, University of Utah
              Single Crystals, Molecular Structure and Chemical-Shift Anisotropy

* 24.02.93   Prof. C.J.M. Stirling[#], University of Sheffield
              Chemistry on the Flat-Reactivity of Ordered Systems

* 10.03.93   Dr. P.K. Baker, University College of North Wales, Bangor
             Chemistry of Highly Versatile 7-Co-ordinate Complexes

* 11.03.93   Dr. R.A.Y. Jones, University of East Anglia
             The Chemistry of Wine Making

* 17.03.93   Dr. R.J.K. Taylor#, University of East Anglia
             Adventures in Natural Product Synthesis

* 24.03.93   Prof. I.O. Sutherland#, University of Liverpool
             Chromogenic Reagents for Cations

* 13.05.93   Prof. J.A. Pople, Carnegie-Mellon University, Pittsburgh, USA
             The Boys-Rahman Lecture Applications of Molecular Orbital Theory

  21.05.93   Prof. L.Weber, University of Bielefeld
             Metallo-Phospha Alkenes as Synthons in Organometallic Chemistry

* 01.06.93   Prof. J.P. Konopelski, University of California, Santa Cruz
             Synthetic Adventures with Enantiomerically Pure Acetals

  02.06.93   Prof. F. Ciardelli, University of Pisa
             Chiral Discrimination in the Stereospecific Polymerisation of Alpha
             Olefins

  07. 06.93   Prof. R.S. Stein, University of Massachusetts
             Scattering Studies of Crystalline and Liquid Crystal Polymers

  16.06.93   Prof. A.K. Covington, University of Newcastle
             Use of Ion Selective Electrodes in Ion Chromatography

  17.06.93   Prof. O.F. Nielsen, H.C. Ørsted Institute, University of Copenhagen
             Low Frequency IR and Raman Studies of Hydrogen Bonded Liquids

  13.09.93   Prof. A.D. Schlüter, Freie Universität Berlin, Germany
             Synthesis and Characterisation of Molecular Rods and Ribbons

  13.09.93   Dr. K.J. Wynne, Office of Naval Research, Washington, USA
             Polymer Surface Design for Minimal Adhesion

  14.09.93   Prof. J.M. DeSimone, University of North Carolina, Chapel Hill, USA
             Homogenous and Heterogenous Polymerisations in Environmentally
             Responsible Carbon Dioxide

28.09.93   Prof. H. Ila, North Eastern Hill University, India

            Synthetic Strategies for Cyclopentanoids via Oxoketene Dithioacetals

B.3.   Conferences Attended

4th European Symposium on Organic Reactivity and 2nd Newcastle Meeting on Molecular Mechanisms in Bioorganic Processes, Newcastle, England, 11-16 July 1993.

3rd International Meeting of the Biology of Nitric Oxide, Cologne, Germany, 3-6 October, 1993.

       Poster presented: "Cu(II) Catalysed Nitrosothiol Decomposition"

List of Abbreviations

BH_4	tetrahydrobiopterin
BIBA	2-bromo isobutyric acid
cAMP	cyclic adenosine monophosphate
cGMP	cyclic guanosine monophosphate
CME	cysteine methyl ester
DCC	1,3-dicyclohexylcarbodiimide
DGA	2,2-dimethylglutaric acid
DMAP	4-dimethylaminopyridine
EDRF	endothelium-derived relaxation factor
EDTA	ethylene diamine tetra-acetic acid
ESR	electron spin resonance
FORCE	First-Order Rate Constant Evaluation program
GC	guanylate cyclase
GTN	glyceryl trinitrate
GTP	guanosine triphosphate
Hb	haemoglobin
HEPES	N-2-hydroxyethylpiperazine-N'-2-ethanesulphonic acid
L-NA	N^G - nitro-L-arginine
L-NAME	N^G - nitro-L-arginine methyl ester
L-NMMA	N^G - monomethyl-L-arginine
LPS	lipopolysaccharide
M4PO	3,3,5,5-tetramethyl-1-pyrroline N-oxide
MAA	mercaptoacetic acid
MetHb	methaemoglobin
MIBA	2-mercapto isobutyric acid
MMP	methyl mercaptopropionic acid
MPA	mercaptopropionic acid
MTL	methyl thiolactate
NANC	non-noradrenergic, non-cholinergic
NAP	N-acetylpenicillamine
NMA	N-methylaniline
NMANO	N-nitroso-N-methylaniline
NNED	N-(1-Naphthyl) ethylenediamine
NO	nitric oxide
OxyHb	oxyhaemoglobin

List of Abbreviations

pGC	particulate guanylate cyclase
PNP	p-nitrosophenol
SAL	salicylic acid
sGC	soluble guanylate cyclase
SNAC	S-nitroso-N-acetylcysteine
SNAP	S-nitroso-N-acetylpenicillamine
SNO	S-nitroso (group)
SNOCAP	S-nitroso-captopril
SNOG	S-nitroso-glutathione
SNP	sodium nitroprusside
SOD	superoxide dismutase
SPEN	S-nitroso-penicillamine
SUL	sulphanilamide
TLA	thiolactic acid
TRIS	tris(hydroxymethyl) methylamine
SMIBA	S-nitroso-mercaptoisobutyric acid
SMAA	S-nitroso-mercaptoacetic acid
SMMA	S-nitroso-methylmercaptoacetic acid
SMMP	S-nitroso-methylmercaptopropionic acid
SCYS	S-nitroso-cysteine
SECYS	S-nitroso-ethylcysteine
SMPA	S-nitroso-mercaptopropionic acid
STLA	S-nitroso-thiolactic acid